

THESIS

THE EFFECTS OF MANNOSE CAPPED

LIPOARABINOMANNAN ON DENDRITIC

CELL FUNCTION

Submitted by

Eric J Lee

Graduate Degree Program in Cell and Molecular Biology

In partial fulfillment of the requirements

For the Degree of Master of Science

Colorado State University

Fort Collins, Colorado

Spring 2009

COLORADO STATE UNIVERSITY

April 3rd, 2009

WE HEREBY RECOMMEND THAT THE THESIS PREPARED UNDER OUR SUPERVISION BY ERIC JOHN LEE ENTITLED “THE EFFECTS OF MANNOSE CAPPED LIPOARABINOMANNAN ON DENDRITIC CELL FUNCTION” BE ACCEPTED AS FULLFILLING IN PART REQUIREMENTS FOR THE DEGREE OF MASTER OF SCIENCE.

Committee on Graduate work

Dr Chaoping Chen

Dr Alan Schenkel

Adviser, Dr Mercedes Gonzalez-Juarrero

Department Head/Coordinator, Dr Paul Laybourn

ABSTRACT OF THESIS

THE EFFECTS OF MANNOSE CAPPED LIPOARABINOMANNAN ON DENDRITIC CELL FUNCTION

M. tuberculosis is one of the leading causes of death due to infectious disease in the world [1]. While the majority of people are capable of controlling the initial infection, many progress to a latent stage of disease where the *M. tuberculosis* bacilli persist for long periods of time within the host [2]. The *M. tuberculosis* cell wall lipoglycan mannose capped lipoarabinomannan (ManLAM) has been characterized as one of the immunomodulatory factors associated with the bacteria [3-5]. ManLAM interacts with dendritic cells (DCs) via DC-SIGN, mannose receptors and to a lesser extent TLR-2 [6-8]. Thus we set out to examine the effects that ManLAM has on DCs both *in vitro* and *in vivo*. ManLAM treatment of bone marrow derived DCs (BMDCs) prevents their phenotypic maturation reduces the expression of MHC class II and CD1d. BMDCs stimulated with ManLAM also exhibit altered phagocytic capacity and the inability to stimulate naïve CD4+ T-cell proliferation.

The anti-inflammatory cytokine IL-10 has been shown to be secreted in response to simultaneous ManLAM and LPS stimulation of DCs. Here we show that ManLAM by itself is capable of inducing high levels of intracellular IL-10 within BMDCs. Additionally, intrapulmonary delivery of ManLAM to naïve mice induced an increase in the IL-10 production from pulmonary phagocytes. ManLAM also increased the number of migratory IL-10 positive cells found within the pulmonary vessels. This increase in IL-10 expression could inhibit the ability of DCs to mature and express antimicrobial molecules such as nitric oxide (NO). Using the intracellular dye DAF-FM diacetate NO

was analyzed at the single cell level. Unlike the pro-inflammatory activation signal LPS, ManLAM showed reduced capacity to induce NO expression after treatment with purified molecules. When cells were pretreated with ManLAM then infected with live *M. tuberculosis* both the number of NO positive cells and the amount of intracellular NO were reduced in comparison to infected LPS pretreated DCs. In all ManLAM treatment of DCs leads to the production of intracellular IL-10 and a state of incomplete maturation. These cells are unable to properly function as antigen presenting cells, showing reduced CD4+ T-cell stimulatory capacity and low levels of antimicrobial NO production. This furthers the idea that ManLAM is an immunomodulatory molecule, helping the bacteria survive within the host.

Eric John Lee
Graduate Degree Program in Cell and Molecular Biology
Colorado State University
Fort Collins, CO 80523
Spring 2009

Acknowledgements

I would like to first thank my adviser Dr Mercedes Gonzalez-Juarrero for guiding my research, being an endless source of research ideas and always being available to answer questions. Additionally I would like to thank Dr Ian Orme for allowing me to work within his lab and for pushing me to learn. David Higgins, Dr Adrian Rosas-Taraco and Dr Joaquin Sanchez all provided much appreciated assistance with experiments and insight on data analysis. Dr Randall Basaraba greatly aided my understanding of pathology, helping with the analysis of *in vivo* tissue section histology and cell identification. A special thanks to all members of the Orme, Lenaerts and Izzo labs for creating a wonderful working environment and for always sharing ideas and techniques so that I could further my knowledge base.

Thanks to all of the graduate students and faculty of the “Cell and Molecular Biology” and “Microbiology, Immunology and Pathology” departments at CSU for sharing this journey with me. My parents and family were instrumental in supporting my pursuit of a graduate degree, pushing me to succeed and encouraging me to work hard. Lastly, a special thanks to all of my friends outside the lab for listening to me talk about scientific topics for which they most likely cared nothing about. My research was made possible by funding from the NIH grant AI44072.

Dedication

I would like to dedicate this thesis to my late grandmothers, Betty Pearson and Lillian Lee. Both of whom played a large part in raising me to be the individual that I am today. They both taught me to challenge myself both mentally and physically in everything that I do. By their examples I've learned that one should take pride and pleasure in everything we do and to never forget those whom have molded your life. Dedicated in loving memory to Betty Pearson and Lillian Lee, thank you for everything.

Table of Contents

Title Page: The Effects of Mannose Capped Lipoarabinomannan on Dendritic Cell Function	pg i
Signature Page	pg ii
Abstract of Thesis	pg iii-iv
Acknowledgements	pg v
Dedication	pg vi
Table of Contents	pg vii-ix
List of Figures	pg x-xi
List of Abbreviations	pg xii-xiii
Chapter 1: Literature Review	pg 1-29
1.1 History and Epidemiology of Tuberculosis	pg 1
1.2 Animal Models of Tuberculosis	pg 4
1.3 Immunology of Tuberculosis Infection	pg 6
1.4 Changes within the Immune Response	pg 13
1.5 Immune Response Dysfunctions during Infection	pg 15
1.6 The Role of ManLAM in the Immune Response to <i>M. tuberculosis</i>	pg 18
1.7 Interaction of Macrophages and Dendritic Cells with <i>M. tuberculosis</i>	pg 19
1.8 Dendritic Cell Response to <i>M. tuberculosis</i> and ManLAM	pg 24
1.9 Anti-Inflammatory Cytokines Dampen the Immune Response to <i>M. tuberculosis</i>	pg 25
1.10 Changes in Nitric Oxide and Inducible Nitric Oxide Synthase Expression	pg 27
1.11 Fight against <i>M. tuberculosis</i>	pg 28

Chapter 2: The Effects of ManLAM on the General Functions of Dendritic Cells	pg 30-48
Introduction	pg 30
Materials and Methods	pg 32
Results 2.1 Morphological Maturation of Treated BMDCs	pg 36
Results 2.2 Cell Surface Phenotype of Cultured BMDCs	pg 38
Results 2.3 ManLAM Alters BMDC Phagocytic Capacity	pg 40
Results 2.4 ManLAM Treated BMDCs are unable to Stimulate CD4+ T-cell Proliferation	pg 44
Discussion	pg 47
Chapter 3: Intracellular IL-10 Production in Response to ManLAM	pg 50-73
Introduction	pg 50
Materials and Methods	pg 52
Results 3.1 ManLAM Treated BMDCs Produce Intracellular IL-10	pg 60
Results 3.2 Intrapulmonary ManLAM Delivery	pg 62
Results 3.3 Intrapulmonary ManLAM Increases IL-10 Production <i>In Vivo</i>	pg 64
Results 3.4 ManLAM Increase the Number of IL-10 Positive Cells in the Pulmonary Vessels	pg 68
Discussion	pg 70
Chapter 4: Modulation of Dendritic Cell Nitric Oxide Production in Response to ManLAM	pg 74-95
Introduction	pg 74
Materials and Methods	pg 77
Results 4.1 DAF-FM Diacetate Single Cell Nitric Oxide Analysis	pg 81
Results 4.2 ManLAM Alters DC Nitric Oxide Expression	pg 83

Results 4.3 ManLAM Decreases BMDC Nitric Oxide Expression in Response to <i>M. tuberculosis</i>	pg 88
Discussion	pg 92
Chapter 5: Conclusion	pg 96-104
5.1 <i>M. tuberculosis</i> Infection, ManLAM, and the Dendritic Cell	pg 96
5.2 Analyzing Dendritic Cell Maturation in Response to ManLAM	pg 98
5.3 ManLAM Induced IL-10 Modulation of Dendritic Cells	pg 99
5.4 Nitric Oxide Expression of ManLAM Treated Dendritic Cells	pg 101
References	pg 104-112

List of Figures

Figure A: Worldwide Distribution of <i>M. tuberculosis</i> Cases	pg 3
Figure B: Tuberculosis Path of Infection in the Human Host	pg 7
Figure C: <i>M. tuberculosis</i> Primary Granuloma	pg 12
Figure D: Structure of the <i>M. tuberculosis</i> Cell Wall	pg 17
Figure E: ManLAM, DC-SIGN and Immunoregulation	pg 23
Figure 1: Dendritic Cell Morphology	pg 36
Figure 2: Changes in BMDC Morphology	pg 38
Figure 3: BMDC Cell Surface Phenotype	pg 40
Figure 4: Phagocytic Capacity of BMDCs	pg 42
Figure 5: Time Course of DC Bead Phagocytosis	pg 43
Figure 6: BMDC CD4+ T-cell Proliferatory Capacity	pg 46
Figure 7: ManLAM Induces Intracellular IL-10 Production	pg 62
Figure 8: Intrapulmonary ManLAM Delivery	pg 63
Figure 9: Whole Lung IL-10 in Response to ManLAM	pg 64
Figure 10: Intrapulmonary ManLAM Increases Intracellular IL-10	pg 66
Figure 11: Representative Pulmonary IL-10 Positive Cells	pg 67
Figure 12: IL-10 Positive Cells within Pulmonary Vessels	pg 69
Figure 13: DAF-FM Single Cell Nitric Oxide Analysis	pg 83
Figure 14: NO Flow Cytometry Histograms; Untreated, ManLAM , LPS	pg 85
Figure 15: Analysis of NO Production after Treatment	pg 87
Figure 16: BMDC Rate of Infection with <i>M. tuberculosis</i>	pg 89

Figure 17: NO Flow Cytometry Histograms Post-Infection	pg 90
Figure 18: Analysis of NO Production Post-Infection	pg 91
Figure 19: Summary of Results	pg 96

List of Abbreviations

AM: Arabinomannan

AMO: Alveolar Macrophage

BMDC: Bone Marrow Derived Dendritic Cell

BMMO: Bone Marrow Derived Macrophage

CMG: Chronic Granulomatous Disease

cNOS: Constitutive Nitric Oxide Synthase

ConA: Concanavalin A

CR: Complement Receptor

CRD: Carbohydrate Recognition Domain

DC: Dendritic Cell

DOTS: Directly Observed Treatment, Short Course

ELISA: Enzyme-Linked ImmunoSorbent Assay

GM-CSF: Granulocyte Macrophage Colony Stimulating Factor

HIV: Human Immunodeficiency Virus

IHC: Immunohistochemistry

IL: Interleukin

INH: Isoniazid

iNOS: Inducible Nitric Oxide Synthase

LAM: Lipoarabinomannan

LM: Lipomannan

LPS: Lipopolysaccharide

M. tuberculosis: Mycobacterium tuberculosis

ManLAM: Mannose Capped Lipoarabinomannan

MDR: Multi-drug Resistant

MFI: Mean Fluorescence Intensity

MO: Macrophage

MPI: Mannosyl-Phosphatidyl-Myo-Inositol

MR: Mannose Receptor

NIS: Nikon Image Software

NK Cell: Natural Killer Cell

NO: Nitric Oxide

PAMP: Pathogen-Associated Molecular Patterns

PIM: Phosphatidylinositol Mannoside

PRR: Pattern Recognition Receptor

qRT-PCR: Quantitative Real-time Polymerase Chain Reaction

RMP: Rifampicin

RNI: Reactive Nitrogen Intermediate

ROI: Reactive Oxygen Intermediate

TB: Tuberculosis

TCR: T-cell Receptor

Th1/Th2: Type 1 Helper T-cell/Type 2 Helper T-cell

TLR: Toll-like Receptor

Treg: Regulatory T-cell

WHO: World Health Organization

XDR: Extremely Drug Resistance

Chapter 1: Literature Review

1.1 History and Epidemiology of Tuberculosis

Mycobacterium tuberculosis (*M. tuberculosis*) is the causative agent of tuberculosis (TB), a disease whose history has been traced back as far as the Egyptians in 2400 BCE [9]. For many centuries this tiny invader killed people worldwide without any insight into its causative agent and pathogenesis. In 1720 Dr Benjamin Marten first proposed that TB could be caused by “wonderfully minute living creatures”, a truly revolutionary thought at the time. Then in 1882 Dr Robert Koch described these bacteria and developed a successful staining technique, allowing him to visualize *M. tuberculosis* for the first time [10]. In 1921 *Mycobacterium bovis* Calmette-Guerin (*M. bovis* BCG) was administered as a vaccine for the first time. By the 1940s chemotherapeutics were being developed and utilized against *M. tuberculosis*, ushering in a new era in the fight against TB [9].

Despite being an ancient disease, TB is still a worldwide infection. The *M. tuberculosis* bacteria infects nearly 2 billion people worldwide and 9 million people each year, while killing greater than 1.5 million people annually [1]. The current vaccine against TB consists of an 80 year old *M. bovis* strain developed by Calmette and Guerin in France (BCG) [11]. While the vaccine has showed up to 80% efficacy in protecting children from TB meningitis and miliary disease, it is much less effective in protecting adults and shows no benefit in those already infected with *M. tuberculosis* [12]. Even though BCG has been very beneficial to the fight against TB, the variable efficacy makes it less than perfect [13]. Current research into vaccines consisting of mycobacterial

proteins and peptides, recombinant BCG strains, and DNA are all being developed, but are not ready for worldwide distribution [13]. Due to the inability to adequately prevent *M. tuberculosis* infection, post exposure treatment of the disease becomes even more important.

Treatment of TB is achieved with a multi-drug chemotherapeutic treatment regimen to eliminate the bacteria. Isoniazid (INH) and rifampicin (RMP) are the two most common first line drugs, though pyrazinamide (PZA) and ethambutol (EMB) are also commonly used. Standard treatment for diagnosed infection with *M. tuberculosis* consists of a two month high intensity multi-drug chemotherapy regimen followed by four months of lower intensity multi-drug chemotherapy. Combination chemotherapy is at the heart of the World Health Organization's (WHO) "directly observed treatment, short course" (DOTS) strategy which has been the corner stone in the worldwide fight to treat TB since 1995. The goal of DOTS was to ensure a political commitment to treatment from each country, increase case detection, standardize treatment with supervision and patient support, maintain a constant drug supply for those in need and to improve international monitoring and epidemiology. Since 1995 DOTS has encompassed most of the endemic countries and is making great strides in detection and treatment [1].

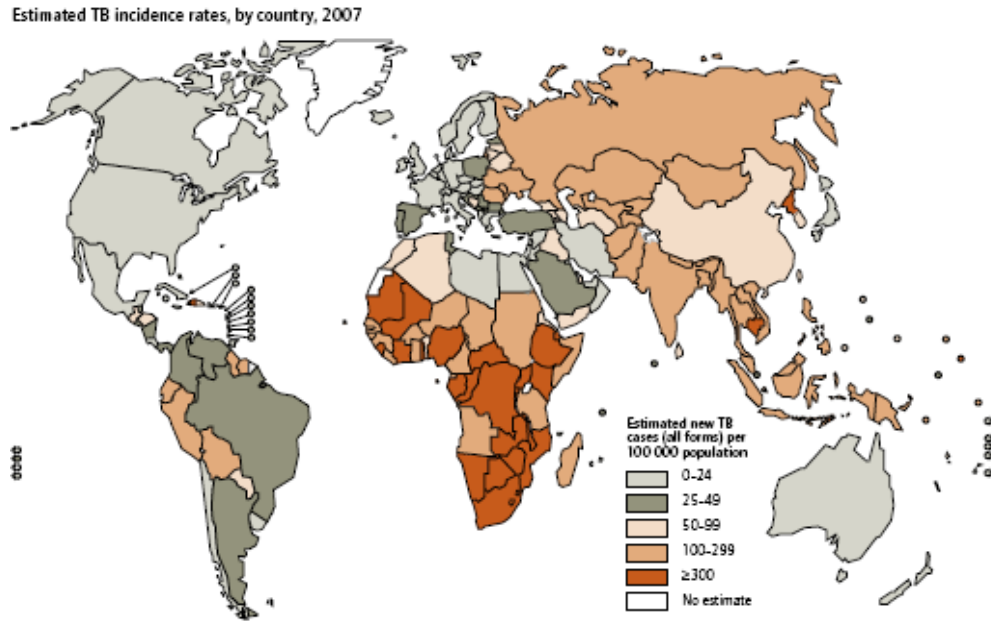


Figure A: 2007 Worldwide Distribution of New *M. tuberculosis* Cases. The map shows the regions with the highest prevalence of new *M. tuberculosis* cases to be within sub-Saharan Africa and Asia, the orange shaded areas [1].

Unfortunately, even though DOTS has been quite successful in increasing detection and treatment, some regions have seen an increase in multi-drug resistant (MDR) and extensively drug resistant (XDR) strains of *M. tuberculosis*. MDR TB is defined as TB that is resistant to INH and RMP, while XDR TB is additionally resistant to one or more fluoroquinolones and one or more injectable drugs. The fluoroquinolones; ciprofloxacin, levofloxacin, moxifloxacin and ofloxacin, and the injectables; capreomycin, kanamycin and amikacin, are known as second line drugs. These second line drugs are reserved for use when primary treatments are ineffective since they are more toxic or less efficacious. Due to natural mutations within the bacteria, incomplete chemotherapy regimens and improper use of drugs, these resistant strains have been able to spread when they should be kept in check [14]. The XDR epidemic in KwaZulu-Natal,

South Africa should serve as a reminder to how dangerous and how rapidly this disease can strike if not properly monitored and treated [15].

The disease primarily infects people in developing countries, with the most endemic regions being Africa, Southeast Asia and the Western Pacific (Figure A). Even though TB is most highly concentrated in developing countries it is becoming more of a threat to the developed world as MDR and XDR strains of *M. tuberculosis* spread. Of those who are exposed to *M. tuberculosis*, only 10-30% become infected, indicating that some humans may be capable of resolving the infection on their own. Of the population that does become infected only 10% progress to active disease with the majority entering a latent phase of infection. These latently infected individuals usually do not spread the bacteria, but if they become immunocompromised or weakened the disease can reactivate. TB is one of the first secondary infections to appear in HIV+ patients, this synergism is leading to an increase in the number of people progressing to active TB [12]. Upwards of 60-70% of those infected with HIV will develop TB during their lifetime, quite often leading to death [16]. To make matters worse current anti-TB regimens take anywhere from four to nine months and require drugs that many of those infected with *M. tuberculosis* are unable to afford. With the spread of drug resistant strains and an increase in active TB cases due to HIV+ co-infection, TB is becoming much more of a global health hazard.

1.2 Animal Models of Tuberculosis

The use of animal models of tuberculosis helps us understand disease pathogenesis, immunology and anti-tuberculosis treatments. The four most common

animal models used for studying *M. tuberculosis* infection are; the mouse, rabbit, guinea pig and non-human primate [17]. While none are perfect models, they each have their advantages and disadvantages. The murine model is by far the most commonly used within research and during early drug testing. Most mice are able to tolerate fairly high bacterial loads for an extended period of time, leading to a chronic state of infection rather than the low bacterial load latent infection seen in humans [18]. Despite this discrepancy the availability of many well characterized mouse strains, including knock-outs and overexpressors, and the wide array of immunological tools available make the murine model a great animal for research [19]. The rabbit model most often utilizes *M. bovis* BCG to study the pathogenesis of TB [17]. This model is very important due to the formation of cavitating lesions, something commonly seen in human TB that is associated with spread of the bacilli [20]. The use of guinea pigs to model TB infection is relatively new, hence the lack of immunological reagents available to researchers. Still, the guinea pig model is an excellent tool for studying the development of caseous and necrotic granulomas during infection with *M. tuberculosis* [21]. This allows researchers to study contributions of the innate and adaptive immune responses to granuloma formation and bacilli persistence within these structures [17]. The last major model is the non-human primate, commonly cynomolgus macaques. These primates exhibit disease progression very similar to humans and are a great model for latent disease and reactivation [22]. Non-human primates also allow researchers to study co-infections with SIV, the primate strain of HIV, and TB [17]. Each model described above has its advantages and disadvantages, owing to the importance of utilizing all animals to their strengths. The murine model remains one of the most important models for characterizing

specific immunological responses as we strive to better understand host infection with *M. tuberculosis*.

1.3 Immunology of Tuberculosis Infection

M. tuberculosis normally infects its host through aerosolized droplets, which are coughed up by actively shedding carriers of the bacilli. The droplets are inhaled by close contacts and taken up into the lungs where the bacillus takes up residence. Here the bacterium is able to infect some endothelial cells, but more importantly encounters alveolar macrophages (AMOs) and dendritic cells (DCs), the first lines of defense within the lungs. AMOs engulf the bacilli and attempt to destroy it via an array of antimicrobial pathways. Additionally AMOs and DCs process the bacteria for presentation to naïve T-cells (Figure B). DCs traffic the bacteria and their antigens to the draining lymph nodes in order to activate CD4+ and CD8+ T-cells. These T-cells then migrate back to the lungs to further activate AMOs, contain the bacterial replication and remove the unwanted invader. While the host is initially able to control the spread of *M. tuberculosis* through AMO antimicrobial activity and T-cell responses, somewhere along the line the bacilli escapes complete clearance and a population of the bacteria are able to remain latent within the host. These persisting bacteria remain within the host waiting for a chance to initiate disease reactivation and spread to new hosts. This inability of the host to completely clear the infection is what makes *M. tuberculosis* a very successful pathogen. While both host and bacterial factors play a role in *M. tuberculosis*'s ability to subvert immune clearance, there has been much evidence that the bacteria's cell wall

components, especially mannose capped lipoarabinomannan (ManLAM), play a key role in the ability of the bacteria to survive [23].

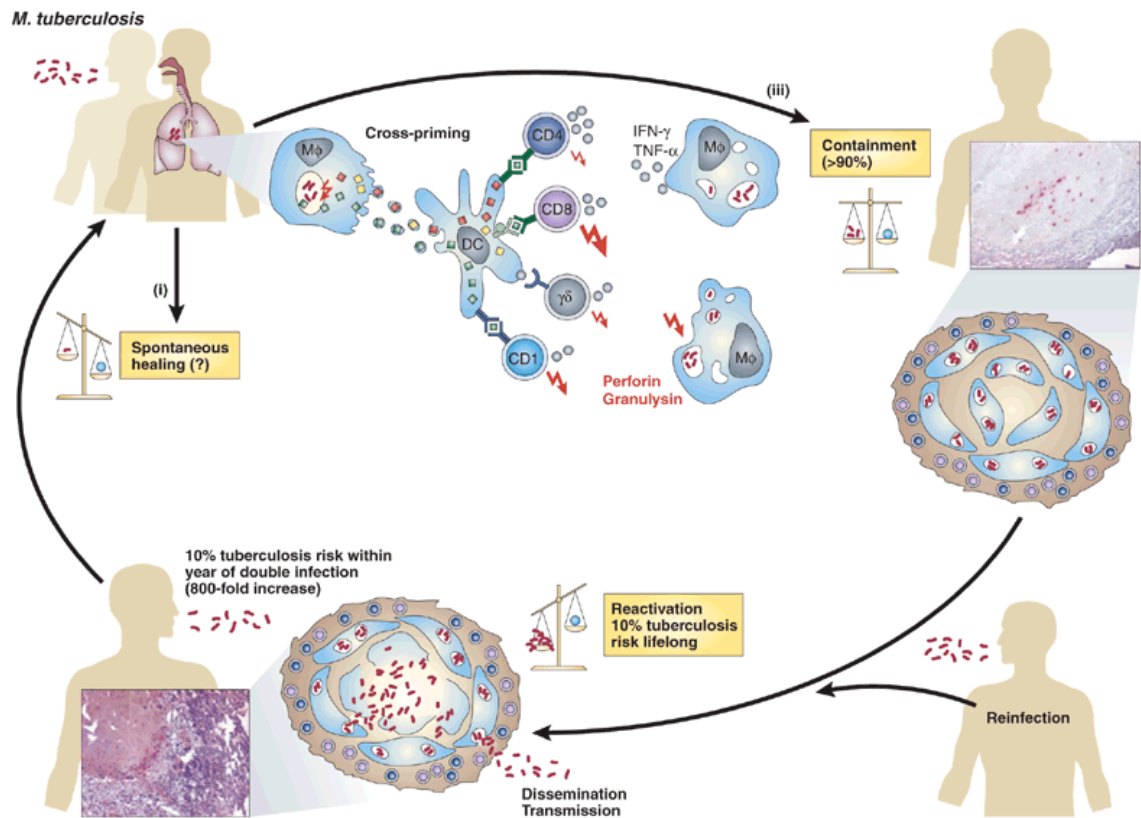


Figure B: Overview of *M. tuberculosis* Infection and the Immune Response. *M. tuberculosis* bacilli are ingested by the host and most commonly take up residence within the lungs. The host immune responses are triggered, led by MOs and DCs. In most cases the persisting immune response eventually leads to the formation of a granuloma and control of the bacilli, but not full elimination. In 10% of cases the disease reactivates, the bacilli spread and are capable of being transmitted a new host [24, 25].

M. tuberculosis is an intracellular facultative aerobic gram-positive bacterium, able to survive within aerosolized droplets coughed up by the host. It is within these droplets that the bacterium is usually transferred from an infected host to a new host individual. The bacillus then travels down the trachea of the new host and takes up residence within the lungs, infecting epithelial cells, AMOs and DCs within the airways.

During the first days of infection the AMO and DC are two of the host's first lines of defense against the bacterial invader and the two predominantly infected cell types [26]. Both of these cell types are found dispersed throughout the lungs, sampling their local environment for anything foreign. Within the lungs AMOs and DCs are commonly defined by their expression of the cell surface markers CD11b and CD11c. AMOs are characterized as CD11b⁻/CD11c^{+high} cells, while lung DCs are characterized as CD11b^{+high}/CD11c^{+high} cells. Within the uninfected mouse model AMOs constitute approximately 20% of the total pulmonary cell population, while DCs initially make up 1% of the total pulmonary cell population. As the infection progresses into the chronic state in the mouse the populations shift, with AMOs making up approximately 6% of the lung population and DCs increasing to 4%. This shift highlights the involvement of both cell types during different stages of the infection [27].

On AMOs the bacteria binds mannose receptors (MRs), complement receptors (CRs), TLR-2 and TLR-4 before it is phagocytosed into the cell [16]. Within the AMO the bacteria enters the phagosome, which traffics through the AMO in route to fusing with the lysosome, finally acidifying the new phago-lysosome and degrading the bacteria. This fusion does not always occur within infected macrophages, and will be further discussed later. These partially activated AMOs secrete tumor necrosis factor- α (TNF- α) and interleukin-12 (IL-12), helping to upregulate the initial Th1 response [24, 28]. NK cells, also present during the early stages of infection, are capable of interacting with the bacilli, and have been shown to be important during the early stages of infection [16, 28]. NK cells are able to produce interferon- γ (IFN- γ) which upregulates the antimicrobial activity of AMOs [29]. Despite IFN- γ release from NK cells early, AMOs do not reach

full functionality and antimicrobial capacity until IFN- γ secreting CD4⁺ T-cells enter the lungs around day 15 [30]. This delay may be one of the reasons that AMOs are not always fully capable of eliminating the intracellular bacilli.

M. tuberculosis also interacts with DCs within the lungs through MRs, CRs, TLR-2, TLR-4 and C-type lectins. Through these cell surface receptors the bacteria is phagocytosed into the cell, processed and trafficked to the lymph nodes for presentation to naïve T-cells. Once internalized, the bacteria are degraded within the phago-lysosomal compartment [31], and antigens are loaded onto MHC class II receptors for presentation. DCs can also present mycobacterial antigens via MHC class I and CD1 receptors to CD8⁺ T-cells, though this response is secondary to MHC class II mediated CD4⁺ T-cell activation [32]. The DCs concurrently upregulate the costimulatory surface molecules CD80, CD86 and CD40 as they mature in response to successful processing of the bacteria [26, 33].

As the DCs mature they lose their ability to phagocytose antigens [34] and begin to produce cytokines and chemokines in order to increase the host immune response to the invading pathogen [28]. DCs specifically secrete IL-12 and TNF- α , two pro-inflammatory cytokines that aid in upregulation of the immune response [8, 24]. IL-12 is a key component in activating Th1 immunity within the host, while TNF- α has been shown to be an important factor in upregulating antimicrobial activity. Mice lacking the TNF- α receptor or in which TNF- α is neutralized show an inability to control bacterial replication [35]. In addition to pro-inflammatory cytokines DCs are able to secrete a host of chemokines including; CCL2, CCL3, CCL7, CCL12, CXCL12 and CXCL10 [28].

Together these cytokines and chemokines contribute to increasing the influx of additional MOs, DCs, NK cells, neutrophils and T-cells [28].

In addition to cytokine and chemokine production, the mature DCs are able to migrate to the draining lymph nodes where they can interact with naïve T-cells. These stimulated DCs prime naïve T-cells within the lymph nodes to differentiate, proliferate and migrate to the lungs to combat *M. tuberculosis*. Antigen presentation to T-cell receptors (TCRs) by MHC class II in conjunction with costimulatory signals between CD80 or CD86 and CD28 and between CD40 and CD40L serves to activate CD4⁺ T-cells within the lymph nodes [10]. Chemokines produced by MOs and DCs in response to infection within the lungs aid in T-cell migration to the lungs [16]. While most activated DCs migrate to the lymph nodes in order to activate T-cells, it has been shown that highly infected DCs containing multiple bacilli remain within the lungs of infected mice and are less efficient CD4⁺ T-cell activators than their lymph node counterparts. This defect may be part of the reason the Th1 response malfunctions during the later stages of infection in mice [26]. These CD4⁺ T-cells are the primary responders to *M. tuberculosis* infection, entering the lungs within a week or two after the initial infection [10, 24]. CD8⁺ T-cells also play a role in TB immunity, functioning both in a cytolytic manner and by producing IFN- γ , which supplements IFN- γ produced by CD4⁺ T-cells [36, 37]. Even though other cell types are present, the activated Th1 CD4⁺ T-cells have been shown to be key to the host response to *M. tuberculosis* [10, 24]. CD4⁺ T-cells are the primary source of IFN- γ and an additional source of TNF- α further activating infected AMOs, and increasing their antimicrobial capacity in order to destroy the bacilli.

IFN- γ and TNF- α both serve to upregulate the production of reactive oxygen intermediates (ROI) and reactive nitrogen intermediates (RNI) within MOs and DCs [16]. Both ROIs and RNIs are key components of the antimicrobial capacity of the host phagocyte. Upregulation of NADPH oxidase and inducible nitric oxide synthase (iNOS) lead to an increase in ROIs and RNIs respectively during infection with *M. tuberculosis*. These reactive species can induce apoptosis, cellular toxicity, DNA damage, protein nitration and oxidative stress among other functions, leading to destruction of the invading bacilli and lysis of the infected host cell [38]. The goal of both the bactericidal activity and the cell lysis is to eliminate bacteria hiding within host cells. Cells harboring *M. tuberculosis* are also induced to undergo apoptosis by a downregulation of the expression of bcl-2. Once the bacteria are released from infected cells they are much more susceptible to host antimicrobial activity [39]. Since these initial responses are not always able to fully eliminate the *M. tuberculosis* bacilli, the continued influx of CD4+ T-cells and increased levels of TNF- α lead to formation of a granuloma.

The granuloma is a hallmark of many chronic infections within humans, especially TB (Figure C). During *M. tuberculosis* infection constant inflammation leads to an influx of MOs, DCs, CD4+ T-cells and CD8+ T-cells. These cell populations, together with high levels of TNF- α and IFN- γ mediate the coalescing of a solid mass known as a granuloma, aimed at walling off persisting bacilli within the host. Infected MOs and DCs begin to collect within the core of the granuloma, while CD4+ and CD8+ T-cells surround this core of infected phagocytes. These pro-inflammatory T-cells secrete additional TNF- α and IFN- γ to help stimulate antimicrobial activity in yet another effort to eliminate the infecting *M. tuberculosis* bacilli. As the granuloma develops, foamy

macrophages begin to accumulate outside the lymphocytic ring. These cells are highly vacuolated and filled with lipid droplets due to their ingesting of large amounts of cellular debris and bacteria from within the granuloma [40]. These highly lipidated foamy cells have also been shown to be a reservoir for persisting bacilli [41].

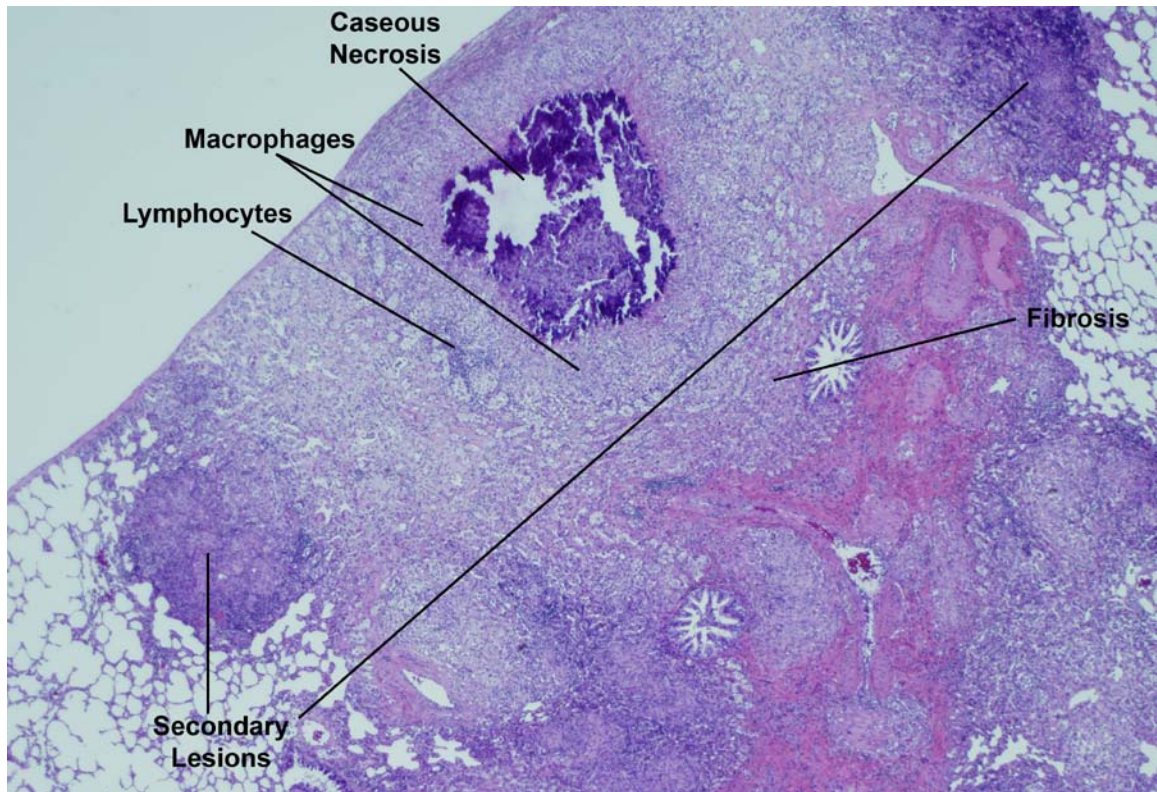


Figure C: Primary Granuloma from an Infected Guinea Pig.

Above is an image of a tuberculosis primary granuloma from an infected guinea pig. The region of central caseous necrosis is stained deep purple and is mineralized. Surrounding this is a region rich in macrophages and DCs, followed by a diffuse ring of lymphocytes and a region of fibrosis (light pink). Secondary lesions are seen developing around the periphery of the primary lesion. Image taken at 20x total magnification courtesy of Donald Hoff.

Surrounding the granuloma is a rim of fibroblasts, encasing the granuloma and producing collagen, which leads to fibrotic encapsulation of the granuloma. This common structure provides the host a method for isolating the bacilli within a specific region of the lung, in an attempt to prevent its spread. Containing the spread of the bacilli

also helps to limit large scale tissue damage, as excessive pathology can also be very detrimental to the host. The granuloma also serves to create a microenvironment within the lung for DCs, MOs, T-cells and associated cytokines to interact and further attempt to eliminate the bacteria. While some of the bacteria are eliminated through the formation of a granuloma, a population of bacteria persists within the lesion, lying dormant within MOs, DCs and foamy cells, leading to a latent stage of infection [2].

1.4 Changes within the Immune Response

It is during this latent stage of infection that *M. tuberculosis* sits within the host, not inducing severe disease, but also not being eliminated by the host response. Two hypothesis of how latency is maintained exist; the classical or “static” hypothesis and the “dynamic” hypothesis [40]. The classical model of latent infection is rooted in the bacilli’s ability to enter a dormant phase, where it is capable of remaining in a state of slow replication and low metabolic activity [42]. This model is losing favor, as it relies upon a “reactivation” factor, and does not account for the low levels of constant immune activation during the latent stage of infection [10]. The dynamic hypothesis suggests that naturally slow growing *M. tuberculosis* disseminates from the granuloma, possibly in foamy cells, at a very low level. These bacilli reach the alveolar space where they begin to multiply, but are often killed by the active immune system [40]. This theory is in line with the constant activation of the immune system and supports the data that reactivation negatively correlates with the period of time after infection [40]. While the exact response of the bacilli during the latent stage has not been fully characterized within

humans, the immunological responses have been studied within the many animal models available.

During the latent stage, expression of TNF- α is needed for maintenance of the granuloma and the continued sequestration of the bacilli. The anti-inflammatory cytokines interleukin-10 (IL-10) and transforming growth factor- β (TGF- β) have been shown to affect the ability of the host to fully eliminate the bacilli. TGF- β primarily functions to maintain T-cell tolerance to self and abundant antigens, while IL-10 performs more of a negative feedback mechanism in response to inflammatory activity [43]. TGF- β expression within the granuloma may serve to inhibit ROI and RNI production within MOs by reducing the effectiveness of IFN- γ and by reducing T-cell proliferation [44, 45]. IL-10 production does not appear to affect the initial stages of infection, though increased IL-10 production from MOs, DCs and T-cells has been shown to lead to reactivation of disease within the mouse model [46]. IL-10 is a potent inhibitor of antigen presenting cell (APC) function and CD4⁺ T-cell responses by counteracting IL-12 and IFN- γ induced activation [47]. While some expression of the anti-inflammatory cytokines is necessary to prevent excessive inflammation in the host, it appears that during *M. tuberculosis* infection the cytokines TGF- β and IL-10 are also preventing the host from continuing its response to the persisting bacilli [16, 43]. Thus the host is unable to fully eliminate the infection, leaving a small reservoir of bacteria alive for possible reactivation and dissemination later on.

1.5 Immune Response Dysfunctions during Infection

While no single reason has surfaced for the incomplete elimination of the invading *M. tuberculosis* bacilli, a host of immunological dysfunctions have been proposed as contributing to the ability of *M. tuberculosis* to persist within the lungs. One major candidate for the inability of the host to fully combat the bacteria is a deregulation of the normal functionality of DCs within the lungs. Since DCs play a role in both the innate immune response and priming of the adaptive immune response, subverting the normal functionality of the DC would provide the bacteria an avenue by which both responses could be modulated to suit its survival needs. The first dysfunction within the host response that indirectly affects the DC occurs immediately after MOs ingest live *M. tuberculosis* bacilli. Once the bacteria are phagocytosed by the host MO, *M. tuberculosis* has the ability to inhibit phago-lysosomal fusion [48]. By inhibiting the Ca^{2+} dependent recruitment of the type III PI3K hVPS34 and SapM the bacteria is able to arrest phagosomal maturation within the MO [49]. By blocking this pathway the bacteria reduces the amount of antigen available to the DC, thus reducing DC activation and priming of T-cells. In addition to this mechanism of hiding within infected MOs, the bacteria are also able to enter a non-replicating persistent state, where its growth slows and the host has trouble recognizing the invader. These non-replicating persisting *M. tuberculosis* bacilli are able to remain within the host lungs for many years, but are still able to reactivate and grow once host conditions permit. This strategy of immune evasion allows the bacteria to avoid recognition by DCs and limits their ability to activate CD4+ T-cells, which are very important steps in controlling the infection [50].

The third and most diverse field of immune evasion utilized by the *M. tuberculosis* bacilli is its complex cell envelope. The mycobacterial cell envelope consists of three layers; the inner plasma membrane, the cell wall and the outer capsule [4, 51]. The inner plasma membrane primarily consists of phosphatidylinositol mannosides (PIMs) and the polyprenols, thought to be associated with cell wall biosynthesis [52]. The outer capsule of *M. tuberculosis* consists of a loosely associated layer, primarily composed of polysaccharides with some lipids and proteins all non-covalently attached to the cell wall underneath. The main polysaccharide in the capsule is arabinomannan (AM), which is structurally similar to lipoarabinomannan (LAM), and is found in a mannose capped form in slow growing mycobacterial strains [51]. The capsule thickness has been shown to be quite variable depending on growth conditions and strains, and research has identified many secreted proteins and components of the cell wall within the capsule [4, 51]. It is still uncertain what role the capsule may play in the pathogenicity of the bacilli. Thus, the *M. tuberculosis* cell wall may be the most important structure within the envelope, as many of its components have been shown to be important factors in virulence and the pathogenicity of the bacilli [4, 52].

The cell wall of *M. tuberculosis* is composed of a complex array of proteins, lipids and carbohydrates, all intertwined into an immunomodulatory barrier around the bacilli (Figure D). The cell wall is composed of two layers, the lower and upper layer. The lower layer consists of peptidoglycans covalently attached to arabinogalactans, which are then linked to the mycolic acids. This core of the cell wall is also known as the mycolyl-arabinogalactan-peptidoglycan complex. The upper layer consists of free lipids and fatty acid chains. Interspersed among the lipids and fatty acids are the cell wall

proteins, PIMs, lipomannans (LMs) and LAMs. This complex outer portion of the cell wall, in conjunction with the capsule, serves to shield the bacteria from many of the hosts' responses [53]. The molecule LAM is of particular interest as an immunomodulatory factor due to its structural similarity to many other bacterial lipopolysaccharide (LPS) molecules, which are known to be potent activators of the immune system [54, 55]. Additionally its prevalence in the outer portion of the cell wall and its numerous binding partners on MOs and DCs make it a prime candidate for eliciting responses from these phagocytes.

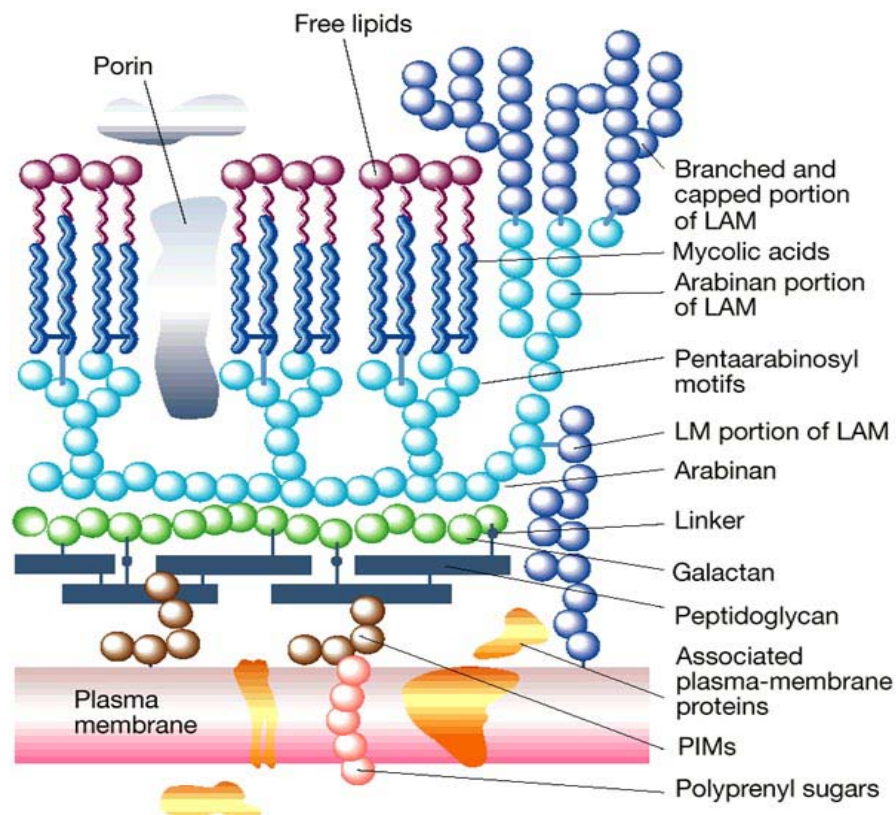


Figure D: Structure of the *M. tuberculosis* Cell Wall. The *M. tuberculosis* cell wall is a complex network of proteins, lipids and carbohydrates. While the exact structure of the *M. tuberculosis* cell wall is still being fine tuned, much work has gone into better understanding the components and how they interact. The figure above depicts the hypothesized structure of the cell wall, with its hallmark peptidoglycans, mycolic acids and LAMs [56].

1.6 The Role of ManLAM in the Immune Response to *M. tuberculosis*

LAM is a complex lipoglycan consisting of a cell wall anchor, mannan core with branched arabinan polymers and a mannose cap in the case of *M. tuberculosis*. The mannosyl-phosphatidyl-myo-inositol (MPI) is believed to be the anchor that inserts these molecules into the plasma membrane. From this anchor the mannan backbone extends, which consists of α 1,6-linked Man_p residues. The arabinan polymer extends from the mannan backbone either in a linear or branched fashion, greatly contributing to the large size of the LAM molecule. The capping of LAM molecules is species dependent and broken down into three different categories. LAM from pathogenic strains such as; *M. tuberculosis*, *M. avium*, *M. leprae* and *M. kansasii* are terminally capped with one, two or three mannose residues (ManLAM), with dimannoside capping dominating. *M. tuberculosis* ManLAM is commonly composed of 50 Man_p units, 60 Ara_f units, and a mannose cap. In fast growing strains such as; *M. smegmatis* and *M. fortuitum* the terminal arabinan are capped by inositol phosphate caps, these LAM molecules are commonly identified as PILAMs. The third group of LAMs are found within; *M. chelonae*, *M. tuberculosis* H37Ra (non-virulent) and *M. smegmatis* and are devoid of any capping residues [57]. Since LAM from virulent *M. tuberculosis* differs from that of many non-pathogenic strains due to its mannose capping, it is a prime virulence factor candidate.

As described above ManLAM is a major component of the *M. tuberculosis* cell wall and is exposed on the surface of the bacteria allowing for interaction with host immune cells. Recent research has also shown that LAMs, along with other arabinomannans, are actively trafficked out of the MO phagosome [58]. This finding that ManLAM, freed from the bacterial cell wall, is found within the host perpetuates the

notion that ManLAM could be an immunomodulatory component of *M. tuberculosis*. This abundance of both free ManLAM and cell wall associated ManLAM has spurred a copious amount of important work in regards to the interaction between ManLAM and MOs and DCs. As previously mentioned *M. tuberculosis* is able to arrest phagolysosomal fusion, recent research has shown that ManLAM is one of the bacterial factors contributing to this arrest [59]. ManLAM is also able to serve as a chemotactic agent for CD4+ and CD8+ T-cells *in vitro* [60] and to scavenge potentially cytotoxic oxygen free radicals [23]. While ManLAM plays an array of different roles in modulating the host immune response, ManLAM's immunomodulatory capacity starts with its interactions with cell surface receptors on MOs and DCs.

1.7 Interaction of Macrophages and Dendritic Cells with *M. tuberculosis*

MOs and DCs utilize a multitude of receptors to interact with extracellular molecules including; pattern recognition receptors (PRRs), C-type lectins and integrins. The Toll-like receptors (TLRs) are a widely utilized set of PRRs, with TLR-2, TLR-4 and TLR-9 all involved in *M. tuberculosis* uptake or interaction with host cells [8, 61, 62]. The TLRs are a set of protein receptors that are heavily involved in the innate immune response to pathogen-associated molecular patterns (PAMPs). Currently there have been 10 mammalian TLRs described, though more likely exist. TLRs most commonly function as homodimers, signaling through intracellular adapter molecules in order to activate specific cellular responses [63]. Each TLR has a specific set of PAMPs that commonly bind the homodimeric receptor. TLR-9, which is able to recognize bacterial DNA within

phagosomes, has been shown to be important during DC recognition of whole *M. tuberculosis*, contributing to the distinct cytokine profile of these DCs [8].

While most bacterial LPS molecules are known to be strong ligands for TLR-4, LAM and LM molecules do not show the same affinity for this PRR. Instead TLR-2 has been shown to be the more important TLR receptor on the surface of MOs and DCs for recognition of LAMs and LMs [5, 64]. Differential activation of TLR-2 and TLR-4 is able to affect the Th1/Th2 balance of the host response, with excessive TLR-2 signaling skewing the host response in the Th2 direction [65]. The coreceptor CD14 is another important receptor on the cell surface, mediating LPS and LM/LAM interactions through TLR-4 and TLR-2 respectively [55, 66]. Together with LPS-binding protein (LBP), the CD14 coreceptor can facilitate activation of TLRs within lipid rafts. It is also through the interactions of TLR-2, LBP and CD14 that LAM and LM may be able to incorporate into host cell lipid rafts via the acyl chain of the MPI anchor [67]. This direct incorporation into lipid rafts may destabilize these rafts, leading to a disturbance of the functioning of raft-associated signaling complexes on the host cell. Even though a clear role for TLR-2 in the interaction with mycobacterial cell wall components has been seen in several experiments, this interaction is most pronounced with uncapped LAMs and LMs [68]. Since it has been shown that ManLAM from virulent *M. tuberculosis* is not as strongly associated with TLR-2 as AraLAM and LM, recent research has turned to different receptors on the surface of DCs, namely the MR and the C-type lectin DC-specific intracellular adhesion molecule-3-grabbing non-integrin (DC-SIGN).

The MR is expressed on the surface of immature monocyte derived dendritic cells [6]. The MR contains eight carbohydrate recognition domains (CRDs) whose primary

duty is to bind branched sugars with terminal mannose, fucose or N-acyl-glucosamine residues. The MR is down regulated in the presence of pro-inflammatory cytokines, while anti-inflammatory cytokines such as IL-4, IL-13 and IL-10 increase its expression [69]. Binding of the highly branched *M. tuberculosis* lipoglycan ManLAM to MRs leads to cross-linking of the receptors and downregulation of IL-12 production from LPS treated DCs [6, 70]. The MR has a clear role in controlling over active Th1 immune responses through induction of IL-10, IL-1ra, IL-1RII, CCL17 and CCL22 [6], in this case *M. tuberculosis* may utilize the receptor to inhibit the bactericidal activity of the host and promote its survival.

The other C-type lectin that is widely viewed as a major binding site for ManLAM and other *M. tuberculosis* carbohydrates is DC-SIGN [4, 71]. DC-SIGN functions as an adhesion receptor by interacting with ICAM-2 on endothelial cells, is able to mediate DC clustering with naïve T-cells through ICAM-3 and functions as a PRR [69, 71-74]. DC-SIGN forms a tetramer and is able to bind carbohydrate structures such as mannose-containing glycoconjugates. Unlike most other C-type lectin receptors, the CRD of DC-SIGN is able to bind more than one mannose residue within an oligosaccharide, increasing its affinity [3, 69]. Signaling through DC-SIGN is able to modulate immunological responses through TLRs in addition to producing its own signals [75, 76]. Specifically, signaling through DC-SIGN has been shown to modulate TLR initiated NF- κ B activated pathways, leading to upregulation of IL-10 (Figure E) [7, 74, 75, 77]. The ability of DC-SIGN to modulate signals from other receptors makes it a very important component of the immune response. While blocking ManLAM binding to DC-SIGN prevents much of the ManLAM uptake into DCs, there is still some

internalization, possibly attributed to TLR-2 or the MR [7]. The actions of DC-SIGN can lead to downregulation of the inflammatory response, as has been shown for *M. tuberculosis* infection where ManLAM is able to alter the phenotype of immature DCs [75].

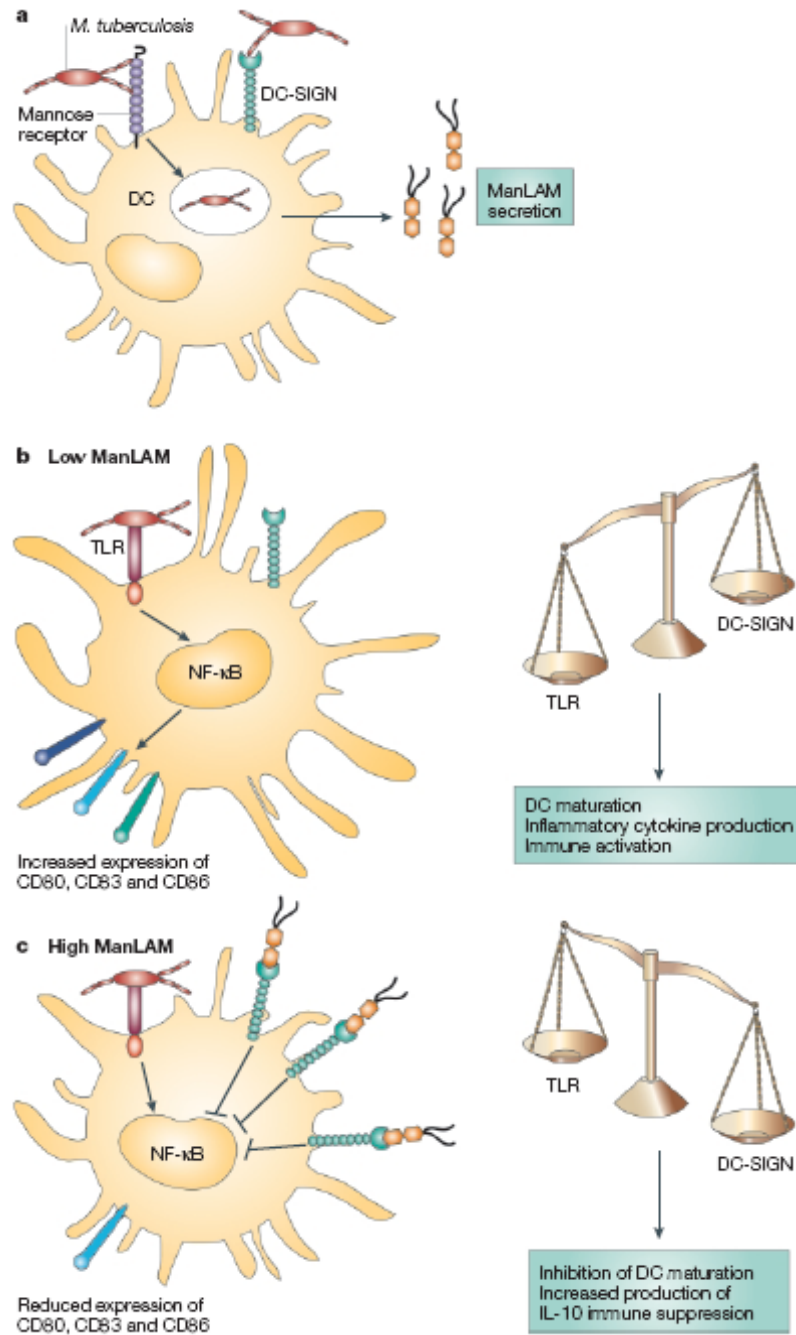


Figure E: Function of ManLAM and DC-SIGN in Immunoregulation.

A) Whole *M. tuberculosis* bacilli are ingested by DCs and MOs, and are processed within the cell leading to the release of free ManLAM to the extracellular space. B) Low concentrations of ManLAM in conjunction with higher levels of TLR stimulation leads to maturation and pro-inflammatory activation by DCs. C) Higher concentrations of ManLAM in conjunction with low level TLR stimulation leads to an inhibition of DC maturation and increased production of IL-10 by these cells [72].

1.8 Dendritic Cell Response to *M. tuberculosis* and ManLAM

After infection with *M. tuberculosis*, DCs within the lungs initially undergo maturation, expressing increased levels of MHC class II, CD86, CD80 and CD40, while migrating to the lymph nodes to initiate a CD4+ T-cell dominated Th1 response [26]. *In vitro* treatment of human monocytes with live *M. tuberculosis* also led to the upregulation of CD83 and CCR7, but expression of CD1, MHC class II and CD80 were reduced compared to fully matured DCs [78]. The inflammatory response is reduced during the later stages of infection with *M. tuberculosis*, owing to changes in the ability of DCs to continue to prime pro-inflammatory T-cell responses. The ability of free ManLAM to interact with DC cell surface receptors has come into play as a possible contributor to this immunomodulation [76]. In response to purified ManLAM alone immature DCs did not upregulate MHC class I, MHC class II, CD80, CD83, CD86 and CCR7, all commonly associated with the activation and maturation of immature DCs [7, 79]. ManLAM treated DCs also release reduced levels of the cytokines IL-6, IL-12p70, TNF- α and IL-10 in comparison to fully matured LPS treated DCs. Even though ManLAM matured DCs are able to expand CD8+ memory T-cell populations, they are unable to induce proliferation of CD8+ naïve T-cells. ManLAM treatment appears to impair the maturation and functionality of DCs, since providing a secondary signal via CD40 was able to rescue their functionality and maturation back to the same level as DCs fully activated with LPS [79]. Thus DCs that interact with ManLAM, either on live bacteria or free within the extracellular space, appear to undergo partial maturation, leading to an inability to fully respond and prime the host immune system.

1.9 Anti-Inflammatory Cytokines Dampen the Immune Response to *M. tuberculosis*

To counter-balance the inflammatory responses mediated by CD4⁺ T-cells, IFN- γ and TNF- α , the host implements numerous immunoregulatory methods, among them are the cytokines IL-10 and TGF- β . As previously mentioned these cytokines function in many ways, both constructively regulating the immune response to the host's advantage and over dampening the immune response to the pathogen's advantage. During *M. tuberculosis* infection TGF- β is most prominently found within the granulomatous lesions being produced by monocytes in response to both whole *M. tuberculosis* [80] and LAM [81]. Within these lesions TGF- β serves to prevent excessive T-cell responses, but it is also capable of deactivating DCs and MOs by down regulating RNI and ROI production [44]. The other major player in inflammatory regulation during *M. tuberculosis* infection is IL-10. While several experiments utilizing gene knockout mice have shown that a lack of IL-10 has little effect on the early stages of infection, a significant role has been seen during the later stages of chronic disease, most notably during reactivation [46, 82, 83]. Over-expression of IL-10 within resistant mouse strains leads to a decrease in CD4⁺ T-cell populations within the lungs and reactivation of disease. This is also seen with the susceptible mouse strain, CBA/J, where an abundance of IL-10 positive MOs are seen within lung lesions as early as 50 days post infection [46]. Conversely IL-10 gene disrupted mice show increased levels of Th1 mediated inflammation during *M. tuberculosis* infection, which eventually led to inflammation induced death 185 days after infection [82]. Thus, IL-10 appears to be playing two roles during infection with *M. tuberculosis*. The first function is a constructive dampening of inflammation by preventing the Th1 response from becoming over active and destroying

the host through pathology. The second function is to even further down regulate IFN- γ and TNF- α mediated inflammatory responses that are necessary to control the growth of the bacteria, leading to reactivation of the disease.

While it is clear that completely eliminating IL-10 is detrimental to the host, it also appears the bacteria is able to harness this anti-inflammatory cytokine to allow its persistence within the host. Human monocytes have been shown to produce IL-10 in response to *M. tuberculosis* infection [84]. Several groups have also shown that while ManLAM itself does not induce high levels of secreted IL-10 from murine DCs, ManLAM is able to synergistically induce increased IL-10 production from LPS treated DCs. Thus DCs that are primed with ManLAM are capable of secreting large amounts of IL-10 when the correct costimulant is provided [6, 7]. IL-10 expression within these cells is capable of counteracting pro-inflammatory IL-12, reducing IFN- γ CD4+ T-cell priming and down regulating overall DC maturation [2]. Exposure of DCs to high levels of IL-10 is also capable of creating a population of regulatory DCs. These DCs preferentially prime T-cells that induce tolerance and are aimed at counteracting pro-inflammatory responses [85, 86]. Though the importance of the Th2 response and Tregs during infection with *M. tuberculosis* is still unclear, both have been shown to contribute to inhibiting the pro-inflammatory response against the bacilli [3]. The specific cause of IL-10 expression during the later stages of TB infection is still debated, but there is a clear correlation between the levels of IL-10 within the host and the state of disease [46]. During the latent and chronic stages of the disease, IL-10 production from DCs, MOs and T-cells increases leading to inhibition of the host antimicrobial responses that are needed to keep the bacteria in check.

1.10 Changes in Nitric Oxide and Inducible Nitric Oxide Synthase Expression

Host antimicrobial responses to invading *M. tuberculosis* are primarily controlled by RNIs and ROIs. Both sets of molecules are induced by enzymatic activation within host cells in response to the invading pathogen. In mouse strains deficient in iNOS, the primary producer of RNIs, and human patients with chronic granulomatous disease (CMG), individuals incapable of making ROIs, disease progression is much more severe [87, 88]. The role of ROIs in controlling *M. tuberculosis* is still unclear, with some work in the mouse model showing H₂O₂ as an effective antimicrobial molecule against *M. tuberculosis*, while experiments by Jones et al showed ROIs to not be as important [89]. The importance of RNIs during infection with *M. tuberculosis* has a better defined role as NO has been shown to be effective at killing *M. tuberculosis* within MOs [90-93] and at low concentrations extracellularly [94]. RNI production from MOs and DCs has been shown to be a key step in regulating *M. tuberculosis* growth and dissemination. Human monocytes from patients with active TB showed increased levels of iNOS and spontaneous secretion of NO₂⁻ [95]. MO mediated killing of intracellular *M. tuberculosis* is dependent upon the upregulation of NO production by IFN- γ and TNF- α [96]. While DCs are capable of producing RNIs to the same level as MOs, the outcome is much different. Infected DCs are able to control the growth of *M. tuberculosis* in an iNOS dependent fashion, but unlike MOs they are unable to kill the bacilli harbored within [31]. This inability to kill the intracellular bacilli may be a reason for the persistence of *M. tuberculosis* within the host.

The bacteria also employ a number of defense mechanisms in order to prevent RNI and ROI induced death. LAM from virulent strains of *M. tuberculosis* has been shown to be a much less potent stimulator of TNF- α from DCs and MOs and also has the capacity to increase IL-10 production within these cells [7, 28, 64, 97]. Thus, indirectly ManLAM is capable of increasing IL-10 and decreasing TNF- α leading to inhibition of iNOS expression and a decrease in NO production. Additionally the peroxiredoxin gene *Ahpc* has been shown to provide *M. tuberculosis* with a mechanism for detoxifying ONOO⁻ and NO₂⁻ and preventing RNI induced necrosis and apoptosis within the host [98]. *In vitro* cultured *M. tuberculosis* has been shown to upregulate a series of genes associated with dormancy in response to low nontoxic levels of NO. This NO induced dormancy controlled by bacterial DosR leads to a decrease in aerobic respiration, reversibly slow replication and possibly prolonged survival of the bacteria *in vivo* [99]. *M. tuberculosis* appears capable of modulating the host's RNI and ROI responses as yet another mechanism of immune evasion.

1.11 Fight against *M. tuberculosis*

The *M. tuberculosis* bacillus is a minute infectious agent, but its ability to subvert the host immune response and persist is very complex. As has been discussed within this review, the bacilli have many mechanisms of immune evasion; from subversion of recognition by the initial innate response, to modulation of cell mediated immunity, to regulation of its own gene expression. The host DC and the bacterial cell wall lipoglycan ManLAM are proving to be critical components of the response and immunomodulation. Pinpointing a single reason for the inability of the host to incompletely eliminate the

invading bacilli may not be possible, but each dysfunction may play an equal role in the ability of the *M. tuberculosis* bacilli to persist. The worldwide fight against TB is one that needs to be attacked on all three fronts; further understanding of the roles of the host and bacterial responses, treatment of those whom are infected and prevention of the spread of TB to new hosts. Even though much has been discovered in the past 130 years since Dr Robert Koch first identified the TB bacilli, the work is far from over, as the fight against the tiny *M. tuberculosis* bacilli is just beginning.

Chapter 2: The Effects of ManLAM on the General Functions of Dendritic Cells

Introduction

The dendritic cell (DC) is the major link between the innate and adaptive immune response. DCs act as sentinels between peripheral tissues and the major sites for immune activation; the lymph nodes. The three main functions of the DCs are; phagocytosis of foreign matter, maturation and migration to draining lymph nodes, and stimulation of T-cell responses [100, 101]. All three are important steps in the ability of the host to mount an adaptive immune response and efficiently eliminate the microbe. During an infection with *M. tuberculosis*, the ability of the host to eliminate these bacilli is dependent on DC's capacity to prime CD4⁺ and CD8⁺ T-cell responses [10]. Thus DCs are known to carry *M. tuberculosis* and its antigens from the site of infection to the lymph nodes where activation of T-cells occurs [26].

Previous work has described the changes that occur on the surface of DCs in response to DC stimulation by *M. tuberculosis* and its antigens [4, 7, 26, 79, 102-105]. In most studies changes in the antigen presenting capacity and the maturation state of the DC after stimulation are monitored by changes in the cell surface expression of markers such as; CD40, CD80, CD83, CD86, DC-SIGN, MHC class I and MHC class II molecules [106]. Within many of those studies, the cell wall lipoglycan mannose capped lipoarabinomannan (ManLAM) of *M. tuberculosis* has received special attention for its capacity to downregulate DC functions and has also been characterized as a potential virulence factor in the pathogenesis of *M. tuberculosis* infection [23]. It is known that

ManLAM is capable of interacting with the host cell as a component of the whole bacilli and as a free lipoglycan [58]. It has also been shown that ManLAM mainly interacts with host cells through the mannose receptor and DC-SIGN [4, 6, 7]; although other receptors present on these cells can participate in this event [3, 8]. The interactions between ManLAM and DCs results in decreased levels of expression of DC surface markers such as MHC class II and CCR7, of which the former is important for activating CD4+ T-cells and the latter is essential for the migration of DCs from sites of infection to the draining lymph nodes [79].

The focus of this chapter is to further characterize ManLAM's interaction with DCs and to determine the functional changes occurring within the context of the three main functional aspects described above. We studied changes in the morphological features as an indicator of maturation, modulation of phagocytic capacity and T-cell priming capacity of bone marrow derived DCs (BMDCs) after stimulation with ManLAM. These studies' goal is to further the understanding of the virulence factors associated with ManLAM antigens during an infection with *M. tuberculosis*.

AIM: To analyze the capacity of ManLAM isolated from *M. tuberculosis* H37Rv to alter the function of DCs. The following studies analyzed the ability of ManLAM stimulated BMDCs to modify the morphological features of DC maturation, alter phagocytic capacity, and to induce CD4+ T-cell proliferation.

Hypothesis: ManLAM impairs full maturation of DCs and their ability to non-specifically phagocytose particles in addition to impairing the ability of DCs to induce CD4+ T-cell proliferation.

Materials and Methods

Mice: Female C57BL/6 mice and female BALB/c mice, six to eight weeks of age, were purchased from Jackson Laboratories. Mice were housed in a sterile pathogen free environment, and were given sterile water, mouse chow, bedding and enrichment for the duration of the experiments.

Bone Marrow Derived Dendritic Cells (BMDCs): Femurs were removed from C57BL/6 mice and placed into 10mL of RPMI media (Gibco #21870-076). Tissue was removed from the femurs and the bone marrow was flushed out using a 30 ½ gauge needle and 5mL of RPMI media. Cell aggregates were broken up and the cell suspension was spun at 1000xG for 10 minutes. Bone marrow cells were resuspended in cRPMI media supplemented with 20ng/mL GM-CSF (Peprotech #315-03), Streptomycin/Penicillin (Sigma #P0781), Sodium Pyruvate (Sigma #S8636), Non-essential Amino Acids 100x (Sigma #M7145), L-glutamine (Sigma C7513 Lot#73K2410), β-mercaptoethanol (Sigma #M6250), and 10% Fetal Bovine Serum (Atlas Biologicals #F-0500-A). Cells were cultured for six to eight days at 37°C/5% CO₂/85% humidity in 25cm² culture flasks (Corning #430168). cRPMI culture media was changed every two days during growth. After six to eight days cell suspensions were spun, resuspended in fresh media at 1x10⁶ cells/mL and plated into either a 24well or 96well tissue culture dish (Corning Costar #3526 and BD Falcon #353070).

Cell Culture Antigen Stimulation: After six to eight days of culture, cells were replated at 1x10⁶ cells/mL in a 24well or 96well dish. Cells were then either left untreated or treated with 20ng/mL *E. coli* LPS (Sigma #L5024) or 1µg/mL ManLAM from *M. tuberculosis* H37Rv (NIH CSU TB Vaccine Testing and Research Materials Contract #

HHSN266200400091c, 7/26/07). Twenty hours after treatment the cells were used for the various analytical assays described below. ManLAM was purified from whole mycobacteria via a series of gradient extractions. Endotoxin levels were all less than 2ng/mg of LAM.

Light and Fluorescent Microscopy: Light microscopy images were taken on an Olympus BX41 microscope with an Olympus DP70 color camera. White balance, exposure and light intensity were kept the same for all images within a single experiment. Images were collected from fluorescently stained cells and tissue using an Olympus IX71 and a Zeiss Axio Observer microscope. The Olympus fluorescent microscope was used to take still images of fluorescent micro beads while the Zeiss confocal microscope was used to capture live time courses of fluorescent bead uptake. A QImage Retiga 2000R camera was connected to the Olympus IX71 microscope, and a mercury lamp was used as a fluorescent light source. An excitation filter of 405nm and emission filter of 460nm/20nm and an excitation filter of 488nm and emission filter of 520nm/20 were used on the Olympus IX71. The Zeiss Axio Observer microscope was connected to an LSM 510 META confocal laser detector. A 405nm diode laser was used with an emission filter of 420-480nm to image DAPI and a 488nm argon laser was used with emission filters of 505LP or 505-550nm to image fluorescent beads.

Nikon Image Software (NIS)-Element AR 3.0 Morphology Analysis: Images of BMDCs treated for 20 hours with different treatments were taken at 200x total magnification with an Olympus BX41 microscope and an Olympus DP70 color camera. Using the NIS-Element program cells were analyzed for changes in shape and size. The program was set to distinguish between small round cells and larger more oblong cells containing

increased numbers of protrusions. The exact same algorithm was applied to each image. Three representative images from each treatment and two different experiments were analyzed and the total number of immature and mature DCs was compared.

Flow Cytometry: Cells were cultured for six to eight days and treated as previously described. After treatment cells were fixed and permeabilized in 4% paraformaldehyde (Electron Microscopy Sciences #15710) containing 0.05% Tween20 (JT Baker, #X251-07) in 1x PBS for 20 minutes at 4°C. Cells were then stained for 30 minutes at 4°C in 1x PBS containing 0.05% Tween20 and select monoclonal antibodies at a 1:50 dilution. Cells were then washed and data was obtained using a BD LSR II flow cytometer designed with a 488nm blue laser, a 633nm HeNe laser, a 405nm VioFlame laser and a 355nm UV laser and corresponding filters for each fluorochrome. Data was analyzed using BD FACS Diva Software. Antibodies used were; anti-CD4 APC (eBioscience #17-0041), anti-CD11b PerCP-Cy5.5 (eBioscience #45-0112), anti-CD11c PE-Cy7 (eBioscience #25-0114), anti-DC-SIGN PE (eBioscience #12-2091), anti-MHC class II labeled with Alexa350 (eBioscience #14-5321, Alexa350 Invitrogen #A-10170), anti-CD1d PE (eBioscience #12-0011), anti-CCR7 APC (eBioscience #17-1971), anti-CD80 PE (eBioscience #12-0801), anti-IL-10 FITC (eBioscience #11-7101), anti-iNOS FITC (BD #610330).

Bead Phagocytosis: BMDCs were cultured for eight days as previously described. BMDCs were mixed with fluoresbrite Carboxy 1µm fluorescent beads (YO #18449-10) at a ratio of ten beads per DC. The mixture was incubated at 37°C/5% CO₂/85% humidity overnight. The cells were then washed with fresh media to remove non-phagocytosed beads and resuspended in PBS. Live cell images were taken using a Zeiss LSM 510

META confocal microscope as previously described and population data was acquired with a BD LSR II flow cytometer as previously described.

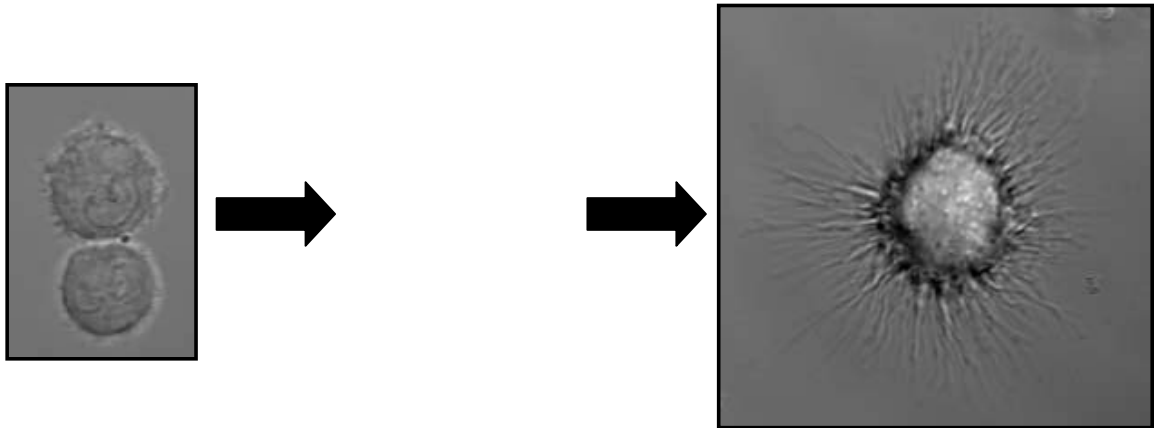
Mixed Lymphocyte Reaction: Whole spleens were harvested from naïve BALB/c mice and homogenized through a cell strainer. CD4⁺ T-cells were isolated from this cell suspension using a CD4⁺ magnetic bead kit (Miltenyi Biotech # 130-090-860). Enriched CD4⁺ T-cell suspensions were stained with 5 μ M CFSE (Molecular Probes #V12883) for 20 minutes at 37°C. CFSE labeled CD4⁺ T-cells were diluted to 1x10⁶ cells/mL in cRPMI media and mixed with BMDCs [5:1]. BMDCs were treated as previously described before coculture with CD4⁺ T-cells. Cell mixtures were incubated for four days at 37°C/5% CO₂/85% humidity in a 24 well tissue culture dish. CD4⁺ T-cells without BMDCs were treated with 10 μ g/mL Concanavalin A (Sigma #C-0412) as a positive control. Four days after BMDCs and CD4⁺ T-cells were mixed; cell suspensions were spun and stained for flow cytometry as previously described. Samples were read on a BD LSR II flow cytometer.

Statistics: The results presented in this publication are representative of two or three experiments. The data are expressed as the mean values from the duplicate or triplicate assays. A parametric method, the one-way ANOVA with a Tukey post-test was used to assess the statistical significance between groups of data. Values of $p < 0.05$ were considered statistically significant. p values for all statistically significant data are indicated on the bars above the data sets.

Results

2.1 Morphological Maturation of Treated BMDCs

Bone marrow precursor cells from C57BL/6 bone marrow were cultured in complete RPMI media containing 20ng/mL GM-CSF for six to eight days. The morphological appearance of most cells obtained by this procedure was that of immature dendritic cells. When these cell cultures were treated with activating stimuli such as; LPS, IL-12 or whole *M. tuberculosis*, the immature DCs developed morphological features associated with mature DCs [34, 107]. Figure 1 shows representative photographs of cells from the three main stages of *in vitro* BMDC maturation. According to their morphology, cells were classified as bone marrow monocyte precursors (left), immature dendritic cells (center) and mature dendritic cells (right).



After antigen stimulation DCs undergo both changes in their morphology and in the expression of cell surface markers. When DCs are activated by stimuli, they mature into cells that are larger with an increased number of protrusions. These protrusions are also known as “dendrites” and give the DC its name. *E. coli* LPS shares many structural similarities to *M. tuberculosis* ManLAM [54, 55], and has previously been described to induce activation and maturation of DCs [34]. For these reasons we used *E. coli* LPS as a positive control for DC stimulation within these experiments. To study the stimulatory capacity of ManLAM we treated BMDCs with 1µg/mL *M. tuberculosis* H37Rv ManLAM [7, 79], 20ng/mL *E. coli* LPS [positive control] or left untreated [control] for 20 hours. Thereafter cells were washed with fresh media and changes in the morphological features determined by microscopic observation and computer assisted analysis. Images of live cells from each culture were taken and analyzed using Nikon’s NIS-Element program. The software was set to distinguish between smaller round immature DCs and larger more mature DCs depicting some or many protrusions. Analysis of the data indicated that when BMDCs were treated with ManLAM cells did not undergo any changes in their morphology when compared to untreated cultures (Figure 2). On the contrary, and as expected, LPS treated DCs showed a significant increase, of nearly 40%, in the number of cells with morphological aspects of mature DCs.

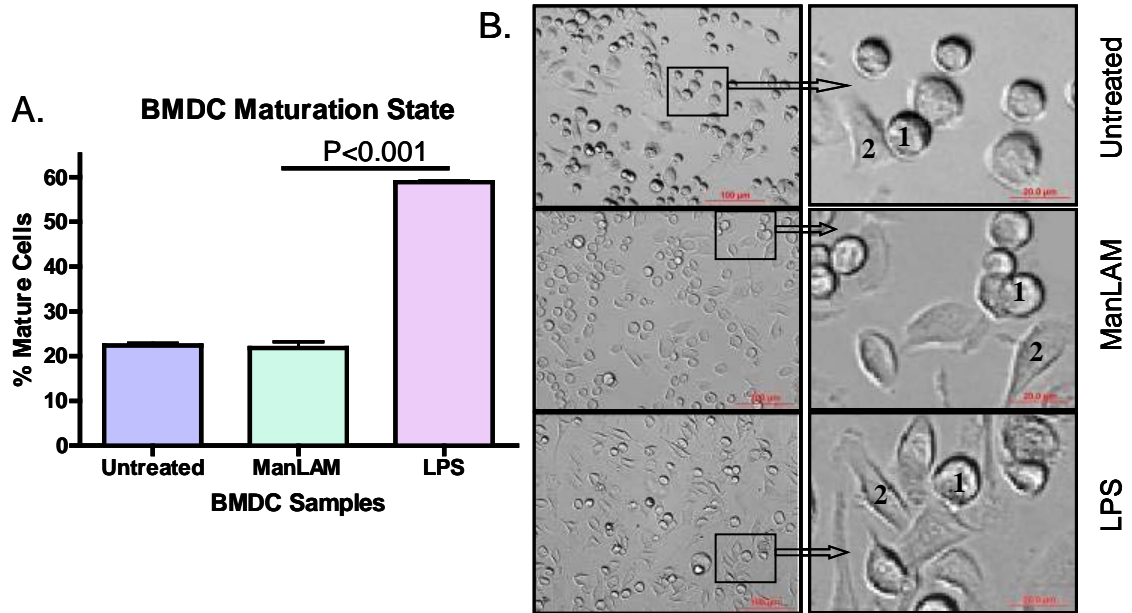


Figure 2: ManLAM Treatment Inhibits Maturation of BMDCs.

DC maturation in response to specific stimuli is a key step in the process of antigen presentation and T-cell activation. One marker of the maturation process is changes in the morphological features of the DC. As DCs mature they grow in size and show an increase in their hallmark “dendrites” or protrusions, which extend from the cell in all directions. Using NIS-Element the morphology of DCs subjected to different treatments was analyzed and compared. The number of mature cells; larger and less circular, were counted and compared to the number of immature cells; all images are taken at 200x total magnification (left column). When compared to A) untreated DCs (first panel B), ManLAM (second panel B) does not increase the number of morphologically mature DCs, while LPS (third panel B) treated BMDCs show distinct features of mature DCs. Representative images of immature DCs (#1) and mature DCs (#2) are shown in the blown up pictures on the far right.

2.2 Cell Surface Phenotype of Cultured BMDCs

Pulmonary dendritic cells have been characterized as expressors of CD11c and CD11b, two cell surface molecules that are involved in adhesion, migration and phagocytosis among other functions [102, 109]. Monocytes cultured for eight days in cRPMI media and 20ng/mL GM-CSF (as previously described) differentiate into immature dendritic cells, with a majority of the population expressing high levels of CD11b and CD11c (Figure 3A). To analyze changes in the cell surface markers of DCs,

cultures were treated with ManLAM, LPS or left untreated and thereafter we performed flow cytometry studies on each culture of DCs. While extensive characterization of ManLAM induced cell surface marker expression has already been reported, it is the purpose of this section to verify that our model system aligns with previously reported studies [7, 34, 79]. CD11b/CD11c expression did not change significantly after treatment with ManLAM or LPS (Figure 3B); though a slight, but insignificant, increase in CD11b expression was seen in LPS treated cultures.

The cell surface molecules MHC class II and CD1d are two important receptors expressed on the surface of DCs and are involved in presenting peptide and lipid antigens respectively to T-cells. In response to ManLAM stimulation MHC class II expression dropped slightly and CD1d expression slightly increased when compared to untreated BMDCs, though the change in CD1d was not significant. LPS treatment stimulated a two-fold increase in the cell surface expression of MHC class II and CD1d on BMDCs (Figure 3C and 3D). BMDCs differentiated from bone marrow precursor cells in GM-CSF produced a population of cells that primarily express high levels of CD11b and CD11c and upon activation with LPS these cells are capable of upregulating the expression of MHC class II and CD1d, a key step in the maturation of DCs in preparation for T-cell stimulation. On the other hand ManLAM was unable to upregulate MHC class II and CD1d expression.

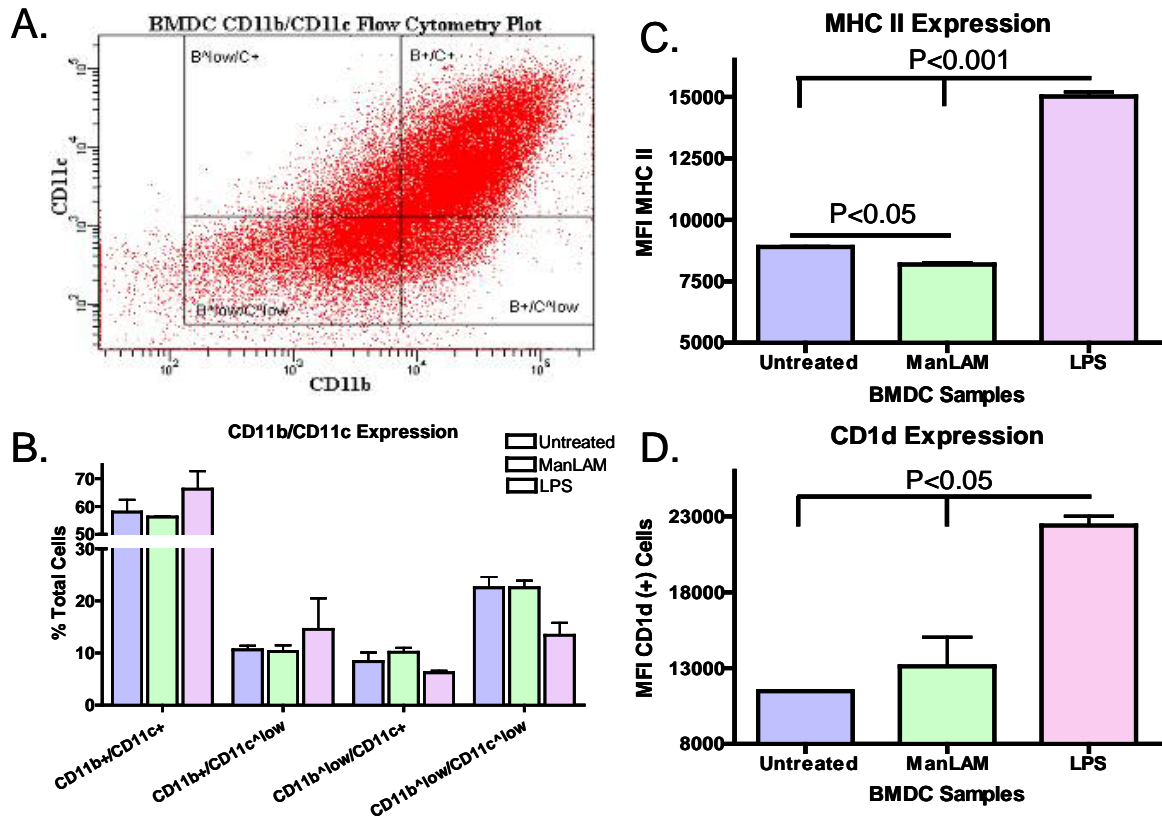


Figure 3: MHC Class II and CD1d Expression are depressed on ManLAM Stimulated BMDCs.

BMDCs cultured for six to eight days in cRPMI media and 20ng/mL GM-CSF show intermediate to high expression of A) CD11b and CD11c prior to treatment with antigens. B) After treatment there is a slight, but insignificant, increase of CD11b on LPS treated BMDCs, and no change in the expression on ManLAM treated BMDCs. C) MHC class II levels are upregulated in BMDCs stimulated with LPS, but are depressed in ManLAM stimulated BMDCs compared to untreated cells. D) CD1d expression is also upregulated in LPS treated samples, but ManLAM itself is incapable of significantly increasing the CD1d expression on BMDCs.

2.3 ManLAM Alters BMDC Phagocytic Capacity

The phagocytic capacity of BMDCs stimulated with ManLAM, LPS or left untreated was analyzed by incubating each cell culture with 1 μ m fluorescent beads. BMDCs were pretreated as previously described for 20 hours and then incubated overnight with the 1 μ m fluorescent beads at a ratio of ten beads per DC. Only a small

number of cells immediately interacted with fluorescent beads, hence why cultures were incubated overnight to allow for a greater number of cells to interact with fluorescent beads. The number of cells containing fluorescent beads was analyzed using a LSR II flow cytometer. Untreated BMDCs had a low level of autofluorescence when no beads were present (Figure 4A first panel) and a low level of non-specific phagocytosis (Figure 4A second panel). Both LPS (Figure 4A fourth panel) and ManLAM (Figure 4A third panel) activation of BMDCs led to an increase in their phagocytic capacity compared to untreated BMDCs. However, the increase seen in ManLAM treated samples was lower and not significant when compared to the phagocytic capacity of untreated BMDCs (Figure 4B). Using live cell microscopy we also tracked fluorescent bead uptake by DCs. Fluorescent bead uptake appeared to be a very rapid process, occurring in less than 10 minutes after beads interacted with DCs. After interaction with the cell surface, beads are actively trafficked inside the DC (Figure 5). While ManLAM does appear to have some effect on the ability of DCs to phagocytose foreign particles, it is at an intermediate level between fully activated LPS treated DCs and untreated immature DCs.

Figure 4: Phagocytic Capacity of BMDCs is altered after ManLAM Treatment

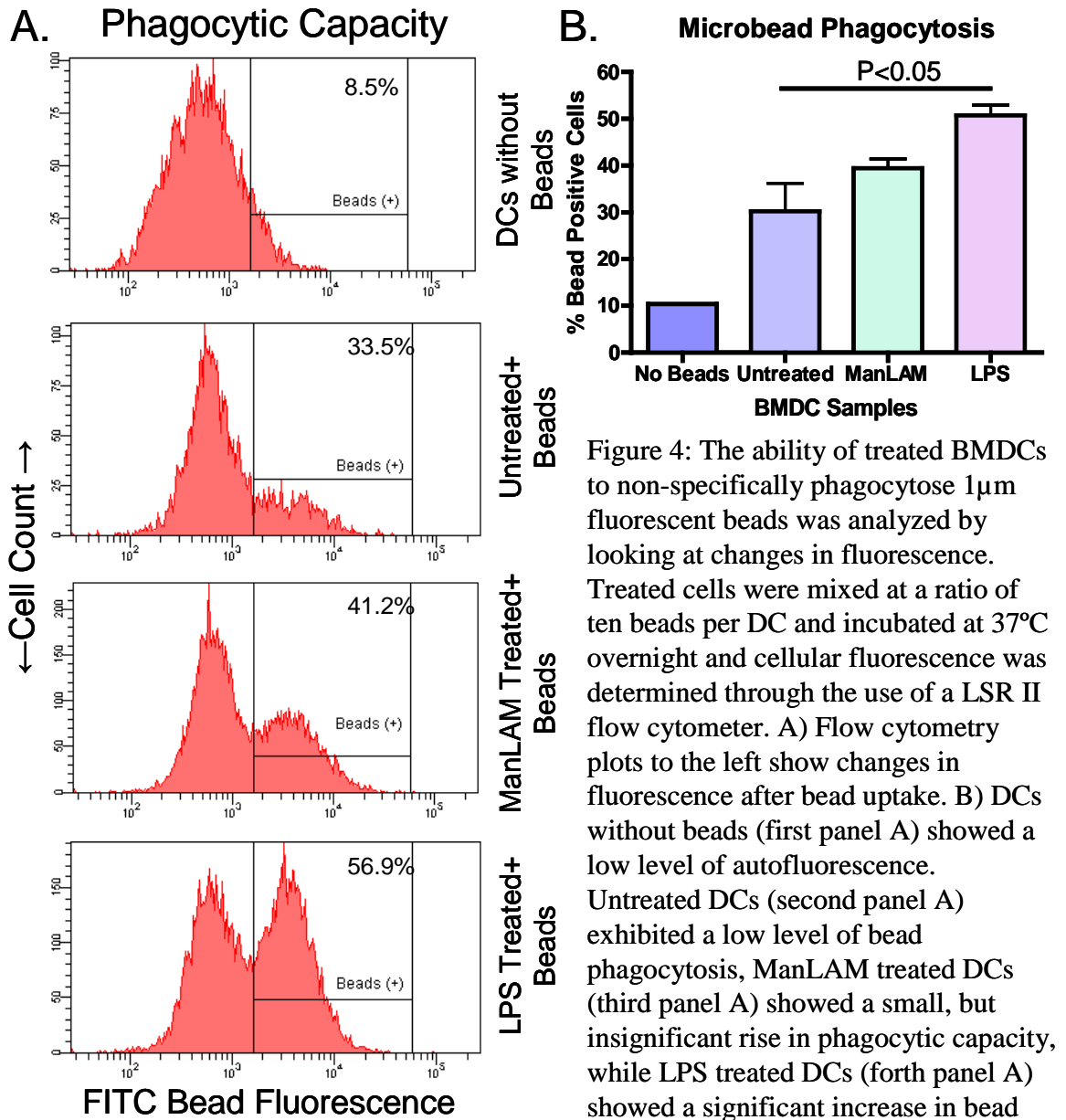


Figure 4: The ability of treated BMDCs to non-specifically phagocytose $1\mu\text{m}$ fluorescent beads was analyzed by looking at changes in fluorescence. Treated cells were mixed at a ratio of ten beads per DC and incubated at 37°C overnight and cellular fluorescence was determined through the use of a LSR II flow cytometer. A) Flow cytometry plots to the left show changes in fluorescence after bead uptake. B) DCs without beads (first panel A) showed a low level of autofluorescence. Untreated DCs (second panel A) exhibited a low level of bead phagocytosis, ManLAM treated DCs (third panel A) showed a small, but insignificant rise in phagocytic capacity, while LPS treated DCs (fourth panel A) showed a significant increase in bead phagocytosis. Percentages in A) represent the average number of bead positive cells for all experiments.

Fluorescent Bead Uptake

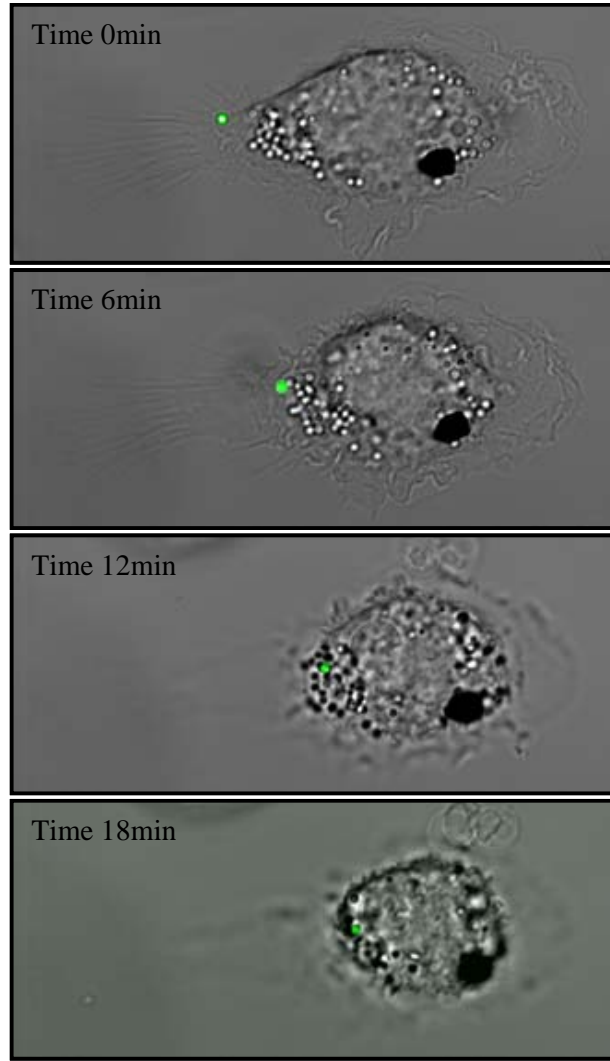


Figure 5: Time Course of BMDC Bead Phagocytosis.

From top to bottom are images illustrating a live time course of fluorescent bead uptake into a live BMDC. The time lapse was captured immediately after DCs were mixed with fluorescent beads at a ratio of ten beads per DC. DC phagocytosis of fluorescent beads occurred within 10 minutes of beads interacting with DCs. A Zeiss LSM 510 META confocal microscope was used to capture the images, and the video was taken with a total magnification of 630x over a time of 30 minutes.

2.4 ManLAM Treated DCs are unable to Stimulate CD4+ T-cell Proliferation

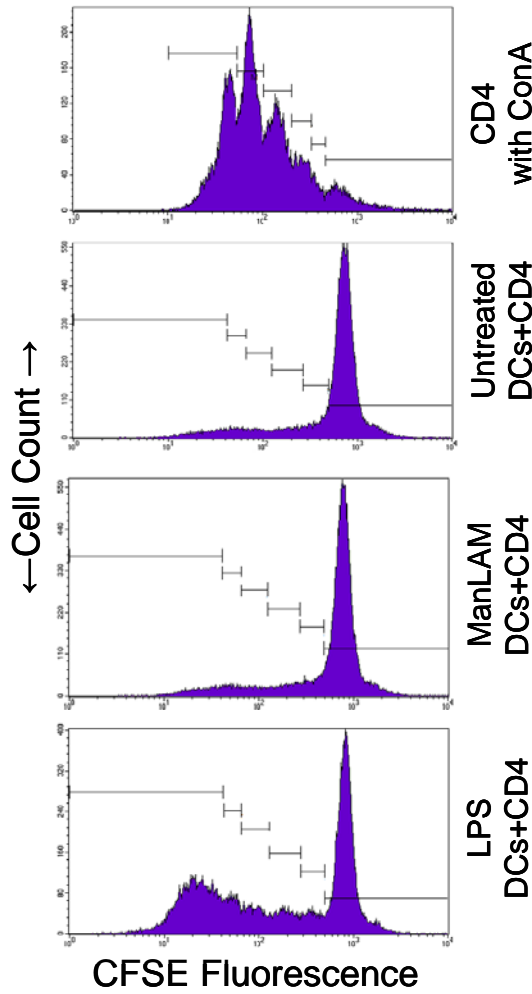
It is believed that when DCs internalize foreign particles and initiate the process of maturation they migrate to the draining lymph nodes and present antigen to naïve lymphocytes. The stimulatory ability of BMDCs to activate naïve T-cell proliferation *in vitro* can be determined by using an allogeneic mixed lymphocyte reaction. Thus, we prepared allogeneic mixed reaction cultures of ManLAM, LPS or untreated BMDCs from C57BL/6 mice and CD4+ T-cells obtained from spleens of BALB/c mice. The mixed cultures were incubated at 37°C/5% CO₂/85% humidity for four days. After four days the ability of treated BMDCs to activate naïve T-cells was determined by measuring the proliferative capacity of T-cells in the culture. Proliferation of T-cells was measured by staining naïve T-cells prior to culture with CFSE dye and flow cytometric analysis on day four using a LSR II flow cytometer. To determine the number of T-cell divisions during the four days of the mixed reaction the cellular intensity of the cytoplasmic dye CFSE was measured. CFSE is a cytoplasmic dye that couples to intracellular proteins [110], thus as the cells divide the fluorescent dye splits evenly between the two daughter cells, creating two cells each containing half the fluorescence of the parental cell. With each round of division the fluorescence is further reduced and this reduction in fluorescence can be measured and analyzed using flow cytometry.

The lymphocyte mitogen Concanavalin A (ConA) was used as a positive control in order to identify and gate each population of dividing cells (Figure 6A first panel). Cells having undergone no division are contained within the gate furthest to the right in the flow cytometry histograms, while cells undergoing the most rounds of division are found within the gate furthest to the left. As expected, untreated DCs only induced a very

low level of CD4⁺ T-cell proliferation (Figure 6A second panel), while LPS activated BMDCs induced a five fold increase in the number of CD4⁺ T-cell divisions (Figure 6A forth panel). BMDCs treated with ManLAM were unable to induce any increase in CD4⁺ T-cell proliferation above background levels (Figure 6A third panel). Even though ManLAM is able to slightly increase phagocytic capacity of BMDCs, it is unable to stimulate CD4⁺ T-cell proliferation above the level of untreated BMDCs.

Figure 6: ManLAM BMDCs are Incapable of Initiating CD4+ T-cell Proliferation

A. CD4+ T-cell Proliferation



B. BMDC Mixed Lymphocyte Reaction

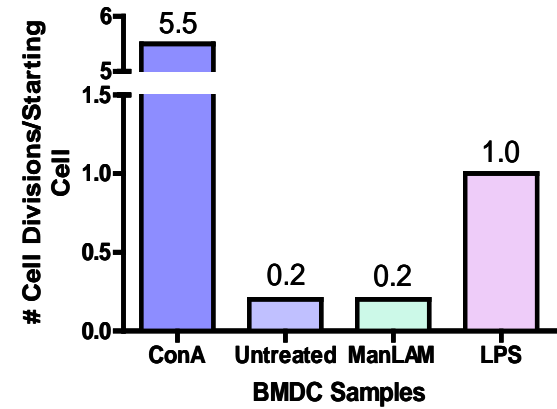


Figure 6: Analysis of the capacity of treated BMDCs to stimulate CD4+ T-cell proliferation was examined using an allogeneic mixed lymphocyte reaction. Treated C57BL/6 BMDCs were co-cultured with BALB/c CD4+ T-cells for 4 days. The dye CFSE was used to track CD4+ T-cell proliferation, as the T-cells divide the fluorescence of each subsequent daughter cell is half that of its parent. A) Flow cytometry plots on the left show proliferation, while B) the graph illustrates the average number of divisions per T-cell initially placed in the reaction. The lymphocyte mitogen concanavalin A (first panel A) was used as a positive control for CD4+ T-cell proliferation. Untreated BMDCs (second panel A) did not cause any T-cell proliferation, ManLAM treated BMDCs (third panel A) only induced background levels of T-cell proliferation, while LPS treated BMDCs (forth panel A) induced a five fold increase in T-cell proliferation.

Discussion

The results above further support the notion that treatment of DCs with ManLAM leads to an incomplete stage of maturation [79]. The initial findings that there are no morphological changes (Figure 2), a decrease in MHC class II expression (Figure 3C) and no change in CD1d expression (Figure 3D) further this notion and align with the phenotypic data that has been previously published. This includes the findings that ManLAM has shown an inability to fully upregulate DC surface markers of maturation such as; MHC class I, MHC class II, CD80, CD83, CD86 and CCR7 [7, 79]. While some may contest that the lack of change in morphology and cell surface marker expression may imply ManLAM is having no effect on DCs, further evidence proves the contrary. ManLAM treatment of DCs was shown to slightly increase the expression of CD83 and CD86, but to a much lesser degree than LPS fully matured cells [79]. ManLAM, but not AraLAM, has been shown to inhibit LPS induced upregulation of CD80, CD83 and CD86 [7]. The effects of ManLAM on the DC surface phenotype may not be drastic, but other ManLAM induced functional changes are much more noticeable.

Non-specific phagocytosis of 1 μ m fluorescent beads is impaired in ManLAM treated BMDCs 20 hours after treatment. While ManLAM treated cells do show a small increase in phagocytic capacity over untreated DCs, it is reduced compared to DCs fully activated with LPS (Figure 4). Fully mature DCs are commonly known to lose their phagocytic capacity and to increase their ability to present antigens and stimulate T-cell proliferation [79, 105], though this can take up to 48 hours for full maturation [111]. Previous reports have demonstrated that activated DCs that are in the process of maturing undergo several steps before becoming fully mature migratory antigen presenting cells.

The initial phase of DC maturation encompasses a reduction in migratory capacity, coupled with a large increase in phagocytic capacity [34]. Within my experiments LPS and ManLAM activated DCs that are in the process of maturing exhibit an increase in phagocytosis 20 hours after stimulation. While Grannuci et al reported that phagocytic capacity peaked between two to four hours after LPS stimulation, their use of high concentration LPS treatment, 10 μ g/mL, may have accelerated the maturation process of the DCs [34]. Thus it does appear that low dose ManLAM is able to cause some level of maturation of DCs, inducing a small early rise in phagocytic capacity (Figure 4), followed by an inhibition of phagocytosis after 48 hours [79].

Several groups have demonstrated that ManLAM has the ability to bind DCs in a dose dependent manner [7, 79]. Despite this binding and ManLAM's activation of intracellular pathways, the inability of these cells to upregulate costimulatory molecules may prevent further downstream functionality. It has been reported that ManLAM stimulated DCs are capable of expanding CD8⁺ memory T-cells, but they were unable to properly prime naïve CD8⁺ T-cells [79]. While CD8⁺ T-cells play a role in controlling *M. tuberculosis* infection, it has been well established that CD4⁺ T-cells are the most important cell type when it comes to controlling infection with *M. tuberculosis*. The results reported above show clearly that ManLAM treated DCs, while capable of altering their phagocytic capacity, are incapable of stimulating naïve CD4⁺ T-cell proliferation (Figure 6). Additional preliminary results have shown that if the degree of branching of the ManLAM molecule is reduced, its ability to stimulate CD4⁺ T-cell proliferation is at least partially rescued (data not shown). Thus, it appears that ManLAM in a reduced form

is capable of stimulating CD4⁺ T-cell proliferation, but that due to its extensive branching or size something is inhibiting T-cell activation.

The results reported in this chapter further support the idea that ManLAM treatment leads to a state of incomplete maturation by DCs. The three main functions of the DCs; foreign particle uptake, maturation and expression of cell surface markers and activation of naïve T-cells all appear to be impaired in ManLAM treated DCs. Without full activation of the adaptive immune response, the host's ability to clear the bacilli would be impaired. Free ManLAM excreted from *M. tuberculosis* infected MOs and released from whole bacilli may be capable of initiating this cascade. As T-cell numbers decrease during the later stages of infection [16], the inflammatory response remises, leaving a population of persisting bacilli within the host. ManLAM's capacity to modulate DC phagocytosis, maturation and T-cell activation may play a key role in inducing this latent phenotype.

Chapter 3: Intracellular IL-10 Production in Response to ManLAM

Introduction

Maturation of dendritic cells (DCs) in response to *M. tuberculosis* is a very important step in the host defense against these bacilli. Mature DCs process, transport and present antigens to T and B-cells, priming the adaptive immune response. *M. tuberculosis* infection is initially contained by the host immune response, led by DC priming of IFN- γ secreting CD4⁺ T-cells and activated macrophages (MOs). The host is able to contain the initial challenge by the bacilli, but in many instances the host immune response is incapable of completely eliminating the invading microbe, leading to a latent stage of disease [30]. The latent stage of tuberculosis is not completely understood, though there are probably several reasons for the onset of latent *M. tuberculosis* infection. Among them, the cytokine interleukin-10 (IL-10) has been shown to be involved in both downregulating the immune response to *M. tuberculosis* infection [24, 82, 83, 112] and inducing reactivation disease [46]. In the mouse model of *M. tuberculosis* infection IL-10 levels were shown to increase through day 20 post-infection and remained elevated through at least 100 days post-infection [83]. This cytokine is produced by MOs, DCs and T-cells, commonly functioning to dampen the inflammatory response activated by the bacteria and is considered an anti-inflammatory mediator of the immune response [24].

Host IL-10 expression can lead to both beneficial and detrimental dampening of the immune response. IL-10 specifically functions by modulating the expression of many cytokines, chemokines and cell surface molecules, thus altering the responses elicited by

leukocytes [47]. IL-10 is capable of inhibiting the process of DC maturation from monocytes, preventing immature DCs from upregulating MHC class II, CD1, CD80 and CD86 [47, 112-114] and has been shown to concurrently block IL-12 production [47]. The downstream effect of this inhibition of maturation and downregulation of IL-12 is the inability of DCs to stimulate T-cell associated IFN- γ production [115]. This reduction in IFN- γ further cascades into reduced antimicrobial activity of DCs and MOs and a full dampening of the immune response. While the expression of IL-10 has been shown to be beneficial during allergic responses, its expression during immune responses to *M. tuberculosis* is much more complicated due to the necessity for a balance between antimicrobial activation and the management of excessive immunopathology [47].

Complete elimination of IL-10 expression during infection with *M. tuberculosis* has shown a productive role for the cytokine, as mice deficient in IL-10 exhibit excessive pathology that leads to complete deterioration of the lungs [82]. Conversely, overexpression of IL-10 in mice leads to reactivation of the disease and an increase in the bacterial load [46]. At the cellular level both MOs and DCs produce IL-10 when cultured *in vitro* with live or heat killed *M. tuberculosis* [116, 117]. DCs are also capable of secreting IL-12 in response to *M. tuberculosis* though the simultaneous production of IL-10 may serve as a counter-balancing factor [116]. Monocyte derived IL-10 is capable of dampening the activity of CD4⁺ and CD8⁺ T-cells by reducing their ability to secrete IFN- γ , a key step in the activation of antimicrobial activity against *M. tuberculosis* [28].

Several groups have shown TLR signaling to be an important step in IL-10 production in response to *M. tuberculosis* infection of DCs [8, 72, 116, 117]. Recent studies have presented evidence that *M. tuberculosis* also binds the receptor DC-SIGN [4,

7], which is known to induce IL-10 production [72, 75]. Even though previous experiments have shown the DC-SIGN ligand ManLAM to upregulate IL-10 production, they all relied on concurrent stimulation with bacterial LPS. These same experiments showed that ManLAM alone does not increase IL-10 secretion from DCs [6, 7]. Within this chapter we aim to better understand the role of IL-10 induced by ManLAM both *in vitro* from cultured bone marrow derived DCs (BMDCs) and *in vivo* after the intrapulmonary delivery of ManLAM.

AIM: To characterize the production of the cytokine IL-10 by DCs stimulated with ManLAM *in vitro*. Additionally, we will also characterize the production of IL-10 in lung cells after intrapulmonary delivery of ManLAM directly into the lungs of C57BL/6 mice.

Hypothesis: Production of IL-10 after DC stimulation with ManLAM differs from the production of IL-10 after DCs are stimulated with LPS. *In vivo* ManLAM is capable of stimulating IL-10 expression from alveolar phagocytic cells and other cells within the lungs.

Materials and Methods

Mice: Female C57BL/6 mice, six to eight weeks of age, were purchased from Jackson Laboratories. Mice were housed in a sterile pathogen free environment, and were given sterile water, mouse chow, bedding and enrichment for the duration of the experiments.

Bone Marrow Derived Dendritic Cells (BMDCs): BMDCs were prepared as previously described in Chapter 2. Briefly, bone marrow was removed from femurs of C57BL/6 mice, and the cell aggregates were broken down into an individual cell suspension. Bone marrow cells were resuspended in cRPMI (Gibco #21870-076) media supplemented with

20ng/mL GM-CSF as previously described in Chapter 2. Cells were cultured for six to eight days at 37°C/5% CO₂/85% humidity in 25cm² culture flasks (Corning #430168). After six to eight days cell suspensions were spun, resuspended in fresh media at 1x10⁶ cells/mL and plated into either a 24well or 96well tissue culture dish (Corning Costar #3526 and BD Falcon #353070).

Bone Marrow Derived Macrophages (BMMOs): Bone marrow cells were harvested and processed as previously explained in Chapter 2 and then cultured in cDMEM media (Cellgro #15-017-CV) supplemented with L929 media as a source of M-CSF (Orme Lab 11/28/07), Streptomycin/Penicillin (Sigma #P0781), Sodium Pyruvate (Sigma #S8636), Non-essential Amino Acids 100x (Sigma #M7145), L-glutamine (Sigma #C7513), β-mercaptoethanol (Sigma #M6250), and 10% Fetal Bovine Serum (Atlas Biologicals #F-0500-A). Cells were cultured for six to eight days at 37°C/5% CO₂/85% humidity in 25cm² culture flasks (Corning #430168). cDMEM culture media was changed every two days during growth. After six to eight days cells were spun, resuspended in fresh media at 1x10⁶ cells/mL and plated into either a 24well or 96well tissue culture dish (Corning Costar #3526 and BD Falcon #353070).

Agglutination Assay and Opsonization: Sheep red blood cells (SRBCs)(Lampire Biological #7249007) were diluted to a concentration of 1x10⁸ cells/mL and mixed with a Goat anti-SRBC monoclonal antibody (Sigma #S8014-1VL) at concentrations of 1:20 to 1:20,000 in a Immulon 2HB 96well U-bottom plastic dishes (Thermo Scientific #3655). The dish was allowed to settle for one to two hours at room temperature. Non-agglutinating titers were identified by the ability of the red blood cells to settle into a solid mass or dot in the bottom of the dish.

Cell Culture Antigen Stimulation: After six to eight days of culture, cells were replated at 1×10^6 cells/mL in a 24well or 96well dish. Cells were then either left untreated or treated with 20ng/mL *E. coli* LPS (Sigma #L5024) or 1 μ g/mL ManLAM from *M. tuberculosis* H37Rv (NIH CSU TB Vaccine Testing and Research Materials Contract # HHSN266200400091c, 7/26/07). Twenty hours after treatment the cells were used for the various analytical assays described below. ManLAM was purified from whole mycobacteria via a series of gradient extractions. Endotoxin levels were all less than 2ng/mg of LAM. Some cultures were also treated concurrently with opsonized SRBCs coated with Goat anti-SRBC monoclonal antibodies (previously described). Opsonized SRBCs were mixed with DCs at a ratio of ten opsonized SRBCs per DC.

Intrapulmonary Delivery: C57BL/6 mice, six to eight weeks of age, were anesthetized by i.p. injection of 100mg/kg body weight ketamine and 10mg/kg xylazine. The mice were suspended by their upper teeth on a platform slanted at a 45° angle. The tongue was gently pulled out with a set of padded tweezers and a small laryngoscope was used to hold the tongue down and visualize the trachea. An intratracheal microsyringe (Penn-Century #FMJ-250) was inserted into the trachea and used to deliver 10 μ g ManLAM, 20 μ g ManLAM or 40 μ g ManLAM suspended in 25 μ l of sterile dH₂O. Control mice were treated via the intrapulmonary route with 25 μ l of sterile dH₂O. After each dose the microsyringe was immediately withdrawn and the mouse was removed from the platform and placed back into its cage on a heated pad. Mice were monitored until they recovered from the anesthesia. Treatments were repeated at days zero, three and five. On day seven after the initial treatment mice were asphyxiated using concentrated CO₂. Lung lobes were then harvested for histology, ELISA, qRT-PCR and western blot.

Light and Fluorescent Microscopy: Light microscopy images were taken on an Olympus BX41 microscope with an Olympus DP70 color camera. White balance, exposure and light intensity were kept the same for all images within a single experiment. Images were collected from fluorescently stained cells and tissue using a Zeiss Axio Observer microscope. The Zeiss Axio Observer microscope was connected to an LSM 510 META confocal laser source. A 405nm diode laser was used with an emission filter of 420-480nm for DAPI, a 488nm argon laser was used with emission filters of 505LP or 505-550nm for FITC and Alexa488, a 543nm HeNe laser was used with an emission filter of 590-630nm for Alexa594, and a 633nm HeNe laser was used with a META detector emission filter of 680-710nm for Alexa647.

ELISA: Secreted cytokines were measured with sandwich ELISA kits; IL-10 Ready-set-go ELISA kit (eBioscience #88-7104-88), IFN- γ Ready-set-go ELISA kit (eBioscience #88-7314-86) and TGF- β 1 Ready-set-go ELISA kit (eBioscience #88-7344-88). In short, ELISA plates were coated with the capture antibody for one hour at room temperature as suggested by the manufacturer. The rest of the plate was then blocked for one hour at room temperature and coated with unknown samples overnight at 4°C. Samples were then sandwiched with a secondary detection antibody for one hour at room temperature before being linked to an Avidin-HRP molecule for 30 minutes at room temperature. Wells were finally developed for five to forty five minutes using a TMB substrate (Dako #S1599) and read on a microplate reader (Biorad #Model 680) at 450nm. All samples were run in triplicate.

Tissue Processing: Lung lobes and whole spleens were harvested, placed into tissue cassettes (Fischer Scientific #22-272417) and fixed in BD Formalin free Zinc fixative

(BD #552658) overnight. Fixed tissue samples were embedded into paraffin blocks at the CSU Veterinary Diagnostic Lab and 5µm tissue slices were cut and baked onto microscopy slides (VWR Superfrost Plus # 48311-703). Hematoxylin and eosin staining was performed by the CSU Veterinary Diagnostic Lab for analysis of tissue histology. Tissue slices were then dewaxed and hydrated before staining and analysis. Briefly, tissue was dewaxed in EZ-DeWax (BioGenex #HK585-5K) then washed with a series of EtOH gradients; 200 proof, 180 proof, 150 proof and 60 proof. Finally tissue was rehydrated in dH₂O before being placed into capillary chambers for staining, described below.

Immunohistochemistry (IHC): Cells were plated and treated as previously described.

100µl of cells were then placed into Shandon cytofunnels (Thermo Scientific #5991040) and spun at 400rpm for 30 seconds in a Shandon Cytospin 1 (Shandon Southern #SCA0031) onto positive charged slides (VWR Superfrost Plus # 48311-703). The slides were then washed with 200 proof ethanol to adhere cells to the slides; then slides containing cells and tissue sections were set into capillary humidity chambers (Thermo Shandon Immuno Starter low volume user package #7339910). Endogenous peroxidases were blocked with 400µl of 0.5% H₂O₂ in Methanol for 10 minutes at room temperature. Between steps slides were washed three times with 750µl of 1x PBS (Cellgro #21-040-CV) with 0.05% Tween20 (JT Baker, #X251-07). Non-specific sites were blocked with a 400µl mixture of 1x PBS, 0.05% Tween20 and 3% Bovine Serum Albumin (Sera Care LS #A-4500-01) for one hour at room temperature. Slides were then washed and 300µl of the primary antibody was added to the humidity chambers and incubated overnight at 4°C. Primary antibodies used were; 1:45 goat anti-IL-10 (Santa Cruz #SC-1783), 1:75 rabbit anti-TGF-β (Santa Cruz #SC-7892), 1:50 goat anti-TNF-α (Santa Cruz #SC-1350),

1:50 goat anti-IL-12p35 (Santa Cruz #SC-9350), 1:50 goat anti-IFN- γ (Santa Cruz #SC-1377), 1:75 rabbit anti-LAM (CSU TB Contract #A193). Primary antibodies were detected using 1:2000 donkey anti-goat Alexa488 (Invitrogen #A-11055), 1:4000 goat anti-rabbit Cy5 (GE Healthcare #PE45004), 1:200 donkey anti-goat-HRP (Santa Cruz #SC-2020), 1:200 goat anti-rabbit-HRP (R&D Systems #HAF008). HRP antibodies were detected either with an AEC chromogen kit (Vector Labs #SK-4200) for 5 minutes or a 568 Tyramide Signal Amplification kit (Invitrogen #T-20934) for 3 minutes. Chromogen developed slides were mounted with Crystal Mounting medium (Santa Cruz #SC-24943), while fluorescent slides were mounted using Prolong Gold with DAPI (Invitrogen #P36931).

Nikon Image Software (NIS)-Element AR 3.0 IHC Analysis: Images of cells positive for IHC staining were taken at 400x total magnification on an Olympus BX41 microscope with an Olympus DP70 color camera. Exposure, white balance and contrast were kept the same for all samples analyzed. Images were imported into the NIS-Element program for analysis of reddish/brown AEC chromogen staining. The red, green, blue (RGB) color ratio was set such that only positive AEC staining was selected for analysis by the program. This algorithm was then applied to all images and the mean intensity of all the positively stained pixels was recorded for each image. For *in vitro* IL-10 positive DCs, three images from each of two slides were analyzed for each treatment group for a total of six images, containing two to six cells per image. For *in vivo* IL-10 positive cells, two separate slides, each containing three lung lobes, were analyzed. A minimum of thirty IL-10 positive cells per lobe were imaged and processed and lobes from similar treatment groups were compared.

Western Blot: BMDCs and BMMOs were spun at 1000rpm for 10 minutes (Beckman Allegra 6R). Cells were then resuspended in 1x RIPA buffer supplemented with 10 μ l PMSF, 10 μ l sodium orthovanadate and 10 μ l protease inhibitor per 1mL of RIPA buffer (Santa Cruz sc-24948). The suspension was allowed to incubate at 4°C for 5 minutes; then spun at 14,000xG for 15 minutes at 4°C to pellet cellular debris. The supernatant was removed to a new tube for use in a Western Blot. Samples were analyzed by spectrophotometer analysis at a wave length of 260nm to roughly determine protein concentration. 40 μ g of total protein were mixed with 6x sample buffer (NEB #B7021S) and boiled at 90°C for five minutes then allowed to cool at room temperature. Samples were then loaded into a 1mm 12% Bis-Tris 10well SDS-PAGE gel (Invitrogen #NP0342BOX) in a gel apparatus (Invitrogen Xcel SureLock #EI0001) containing 1x NuPAGE MES running buffer (Invitrogen #NP0002). Samples were run through the gel at 80v for 2.5 hours or until the sample buffer reached the bottom. The gel was then transferred into a stack containing a sponge, filter paper (Biorad #1704085), the gel, nitrocellulose (Schleicher & Schuell Bioscience #10402468), filter paper and another sponge. The stack was placed into the transfer chamber containing Tris-tricine buffer and run at 3A/40v for 1.5 hours. The nitrocellulose membrane was then rinsed with dH₂O and blocked for 1.5 hours at 37°C in 1x PBS containing 5% BSA and 0.05% Tween20. The nitrocellulose membrane was then placed into a 15mL conical tube (Corning #420052) containing 5mL of 1x PBS, 1% BSA and 1:45 goat anti-IL-10 antibody (Santa Cruz SC-1783) and incubated overnight at 4°C on a rotating rack (Miltenyi MacsMix #130-090-753). The following morning the nitrocellulose membrane was washed and placed into a 50mL conical tube (Corning #430291) containing 30mL of 1x PBS, 1% BSA and 1:7500

rabbit anti-goat-HRP for one hour at room temperature on a shaker table. The nitrocellulose membrane was then rinsed and bands were developed using either 10mL of AEC (Vector Labs #SK-4200) for 30 minutes or 10mL of a 568 Tyramide Signal Amplification kit (Invitrogen #T-20934) for 5 minutes at room temperature. 568 TSA membranes were imaged using a Typhoon Imaging system (GE Healthcare Typhoon Trio) with a Cy3 filter.

RT-PCR: For RNA extractions, whole lungs were homogenized or cell cultures were resuspended in 1mL of Trizol reagent (Invitrogen #15596-018) for 5 minutes at room temperature. Samples were then frozen at -80°C for later processing. Samples were later thawed and 200µl of chloroform (Fischer Scientific #574-1) was added. Samples were spun and crude RNA extracts were removed to a new tube and washed with 700µl of 2-propanol (Fischer Scientific #A416-1). Samples were again spun to pellet the RNA which was again washed with 750µl of 200 proof ethanol (Sigma #E7023). RNA pellets were treated with a RQ1 DNase kit (Promega #M610A) for 60 minutes at 37°C and 10 minutes at 65°C and were then extracted and rewashed via the Trizol method explained above. RNA was resuspended in nuclease free dH₂O and concentrations were taken using an UV spec (Eppendorf Biophotometer). 0.5µg of total RNA per reaction was mixed with MMuLV Reverse Transcriptase (New England Biosciences M0253L) and cDNA was reverse transcribed in an MJ thermal cycler (MJ Research DNA Engine PTC-200) with the protocol; 10 minutes at 25°C, 60 minutes at 40°C and 15 minutes at 70°C. cDNA was then mixed with primers and SYBR Greener SuperMix (Invitrogen #1171-100) and run in a Biorad Thermal Cycler (Biorad iQ5). Primers used were; mature IL-10 For: GGTTGCCAAGCCTTATCGGA Rev: AGCAAGGCAGTGGAGCAGGT, immature IL-

10 For: CATTCCAGTAAGTCACACCCA Rev: TTTGAATTCCCTGGGTGAGA, IL-12p35 For: CATCGATGAGCTGATGCAGT Rev: AGGTAGCTGTGCCACCTTTG, GAPDH For: TCACCACCATGGAGAAGGC Rev: GCTAAGCAGTTGGTGGTGCA, iNOS2 For: ACAGGAGAAGGGGACGAACT Rev: TGAGGGCTCTGTTGAGGTCT.

Each sample was normalized to GAPDH levels from the same sample in order to standardize total cDNA used in each reaction.

Statistics: The results presented in this publication are representative of two or three experiments. The data are expressed as the mean values from the duplicate or triplicate assays. A parametric method, the one-way ANOVA with a Tukey post-test was used to assess the statistical significance between groups of data. Values of $p < 0.05$ were considered statistically significant. p values for all statistically significant data are indicated on the bars above the data sets.

Results

3.1 ManLAM Treated BMDCs Produce Intracellular IL-10

M. tuberculosis induced IL-10 has been shown to play a role in inhibiting the ability of immature DCs and monocytes to mature and activate pro-inflammatory T-cells [28, 118]. Previous reports have shown ManLAM stimulated DCs to secrete very low levels of IL-10 [6, 7], leading researchers to believe that ManLAM alone does not initiate the production of IL-10. Here we show that even though ManLAM treated DCs do not secrete high levels of IL-10, they stain very intensely for intracellular IL-10 by immunohistochemistry (IHC). BMDCs were cultured for six to eight days in cRPMI media and GM-CSF then stimulated for 20 hours with 1 μ g/mL ManLAM, 20ng/mL LPS

or left untreated. Secreted cytokines from culture supernatants were measured by ELISA, while intracellular protein was analyzed by IHC and western blot.

As reported by other groups, ManLAM treatment of BMDCs induces a very low level of IL-10 secretion when measured by ELISA, while LPS stimulated BMDCs show a significant increase in secreted IL-10 (Figure 7A). Despite only secreting a small amount of IL-10 after ManLAM stimulation, BMDCs stained very intensely for intracellular IL-10 by IHC (Figure 7B second panel). LPS stimulated BMDCs also exhibited positive intracellular staining for IL-10 (Figure 7B third panel), while untreated BMDCs showed only a low level of background staining within the cells (Figure 7B first panel). We quantified and compared the average intensity of intracellular IHC staining between each set of samples using the Nikon Image Software (NIS)-Element. Within NIS-Element an algorithm was created such that only positive intracellular chromogen staining was highlighted for intensity analysis, and this algorithm was applied to all images. The intensity of intracellular IL-10 staining was compared for six different images from two experiments for each of the treatments. Using this method ManLAM treated BMDCs showed a significant increase in the intensity of intracellular IL-10 staining when compared to both untreated BMDCs and LPS treated BMDCs (Figure 7C). IL-10 was also found in both LPS treated samples and ManLAM treated samples when whole cell lysates were processed and run on a western blot gel (data not shown). Thus, ManLAM stimulation of BMDCs leads to a significant increase of intracellular IL-10 that does not appear to be secreted.

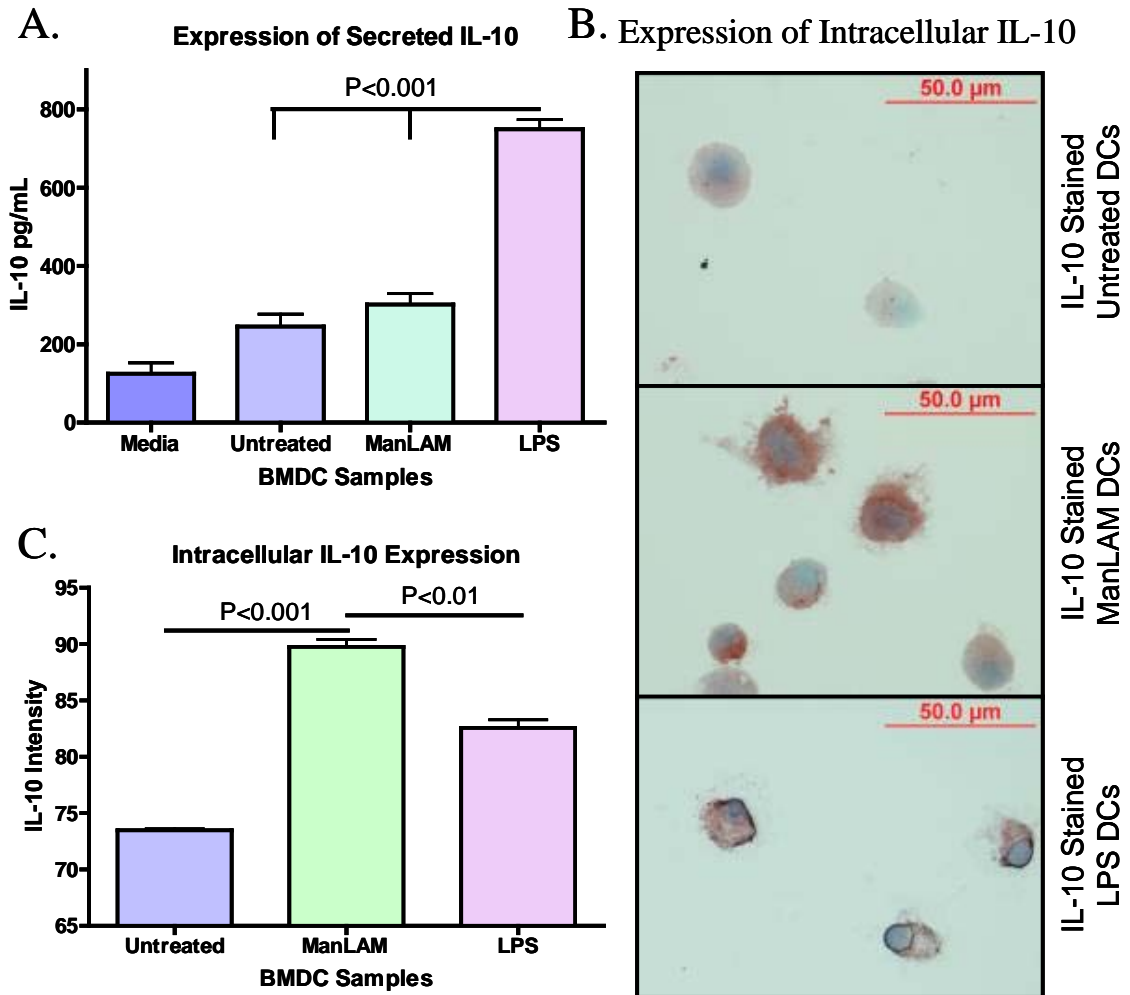


Figure 7: ManLAM Induced Intracellular IL-10 Production. IL-10 has been shown to have a regulatory effect on DCs. IL-10 production was measured by ELISA for the presence of secreted protein or IHC for intracellular protein. A) When secreted IL-10 is measured by ELISA, ManLAM treated BMDCs show no increase in the amount of the extracellular cytokine. C) Intracellular IHC tells a different tale, as ManLAM stimulated BMDCs (second panel B) stain intensely for intracellular IL-10, much higher than background staining in untreated BMDCs (first panel B) and even more intensely than LPS treated BMDCs (third panel B). Images are of representative cells taken at 400x total magnification.

3.2 Intrapulmonary ManLAM Delivery

M. tuberculosis is predominantly a disease of the lungs, infecting its host via the respiratory tract and taking up residence within the pulmonary environment. Thus we sought to analyze how the *M. tuberculosis* cell wall lipoglycan ManLAM affects the

lungs *in vivo*. C57BL/6 mice were treated via intrapulmonary delivery with various concentrations of ManLAM or sterile dH₂O three times over the course of a week. Two days after the third and final treatment mice were sacrificed and lungs were collected for analysis (Figure 8). Whole lung homogenate was analyzed for cytokine production by ELISA, qRT-PCR and western blot, while tissue sections were cut for histological analysis and IHC.

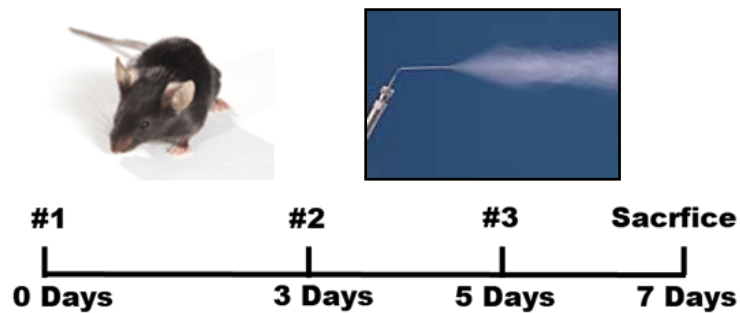


Figure 8: Intrapulmonary Delivery of ManLAM.

Using a microsprayer, mice were treated via the intrapulmonary route with 25 μ l dH₂O, 10 μ g ManLAM, 20 μ g ManLAM or 40 μ g ManLAM three times over the course of a week. Two days after the final treatment mice were sacrificed and lung lobes were collected for ELISA, qRT-PCR, western blot and histology. Three mice per treatment group were analyzed.

The right apical lobe from each mouse was placed into 3mL of sterile PBS for ELISA, while the cardiac lobe from each mouse was placed into Trizol for qRT-PCR analysis. Samples in PBS were homogenized using a tissue homogenizer, and briefly allowed to settle before being applied to cytokine ELISAs for IL-10, TGF- β and IFN- γ . Lobes in Trizol were homogenized using the tissue homogenizer, RNA was then purified from these samples, and reverse transcribed into cDNA for qRT-PCR analysis of IL-10 and IL-12p35. ELISAs of whole lung homogenate showed no significant change in IL-10 expression within the lungs (Figure 9A). Additionally there were no significant changes

in the expression of secreted TGF- β 1 or IFN- γ (Data not shown). qRT-PCR results for IL-10 showed similar results, no significant change in IL-10 mRNA levels within the whole lung (Figure 9B). Since there was no gross change in pathology for all the treated groups these results was not unexpected. Even though no global changes are seen by ELISA and qRT-PCR, this does not necessarily illustrate what is occurring at the single cell level, as significant changes in small populations of cells can be drowned out by the remaining lung tissue.

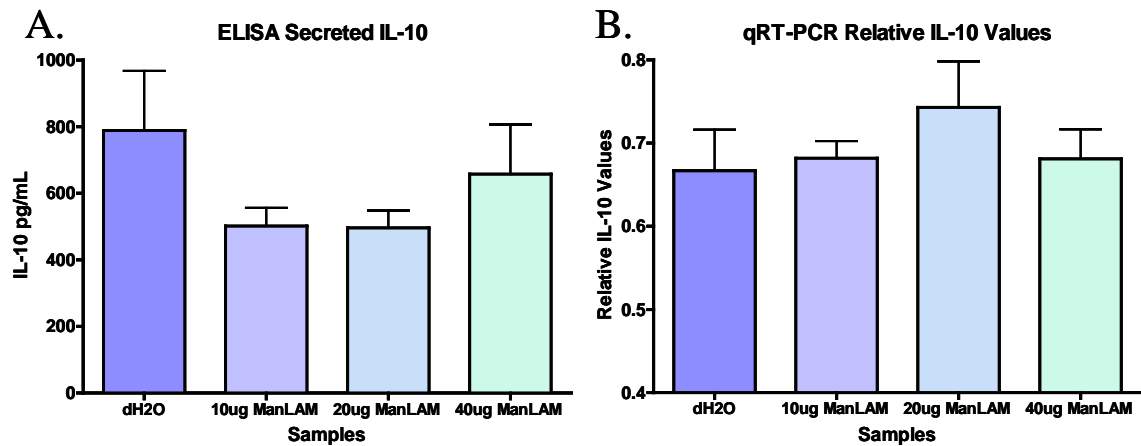


Figure 9: Whole Lung IL-10 Analysis.

The lungs of treated mice were harvested into PBS or Trizol and the whole lung homogenate was analyzed for IL-10 production by A) ELISA and B) qRT-PCR. By both methods no significant changes were seen in IL-10 protein and mRNA levels. Though analysis of the whole lung tissue can mask changes to specific cell populations within the lung.

3.3 Intrapulmonary ManLAM Increases IL-10 Production *In Vivo*

DCs comprise approximately 1% of the total lung population. To further analyze changes occurring at the single cell level hematoxylin and eosin staining for histology and IHC staining were utilized. While there were no drastic changes in the pathology of the lung sections from each treatment group, IL-10 positive cells were found scattered through out the lungs. IL-10 positive cells were found in the alveoli, parenchyma and

vessels of the lungs and had MO or DC like morphology. Even though there was no significant increase in the total number of IL-10 producing cells after ManLAM treatment (data not shown); we sought to analyze the amount of IL-10 being produced by this positively stained population.

To analyze the intensity of intracellular IL-10 staining within each lung section the NIS-Element program was once again utilized. Images of every IL-10 positive cell within each lung lobe were captured at 400x total magnification utilizing the same exposure, white balance and contrast. The software was setup to only select the chromogen staining for analysis, and the same algorithm was applied to all images in order to compare staining intensities across samples. Figure 10B shows a representative IL-10 positive cell before analysis (first image) then after analysis (second image), with the region highlighted in red representing the pixels selected for analysis. When the intracellular IL-10 intensity from different treatments was analyzed, all three ManLAM treated groups showed an increase in the average intracellular IL-10 intensity compared to the dH₂O treated group (Figure 10A). Representative cells from each treatment group are shown in Figure 11, both before analysis with the NIS-Element program (left column) and after analysis, with the red highlighted regions showing the positive staining the program selected for analysis (right column). Pulmonary cells express a steady state level of IL-10; however ManLAM treatment led to an increase in the IL-10 production within these IL-10 positive pulmonary cells.

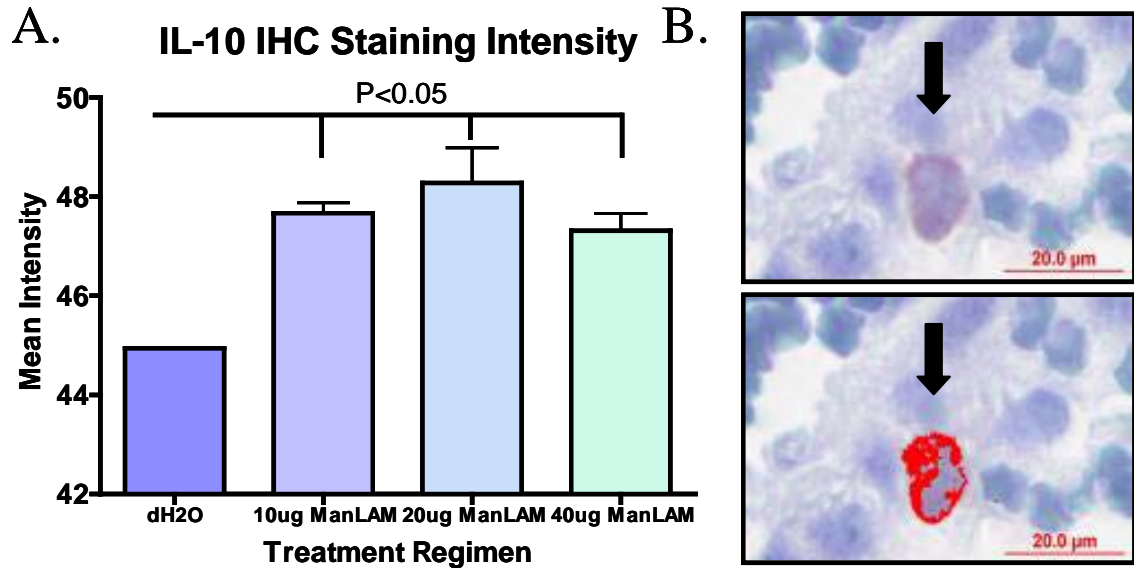


Figure 10: Intrapulmonary ManLAM Increases IL-10 Production. Analysis of intracellular IL-10 staining within positive cells was performed using the NIS-Element program. A) Mice treated with ManLAM showed more intense staining for IL-10 within the cells when compared to dH₂O treated controls. B) Images are of an IL-10 positive cell taken at 1000x total magnification and cropped, before analysis (first image) and after analysis (second image) with the NIS-Element program.

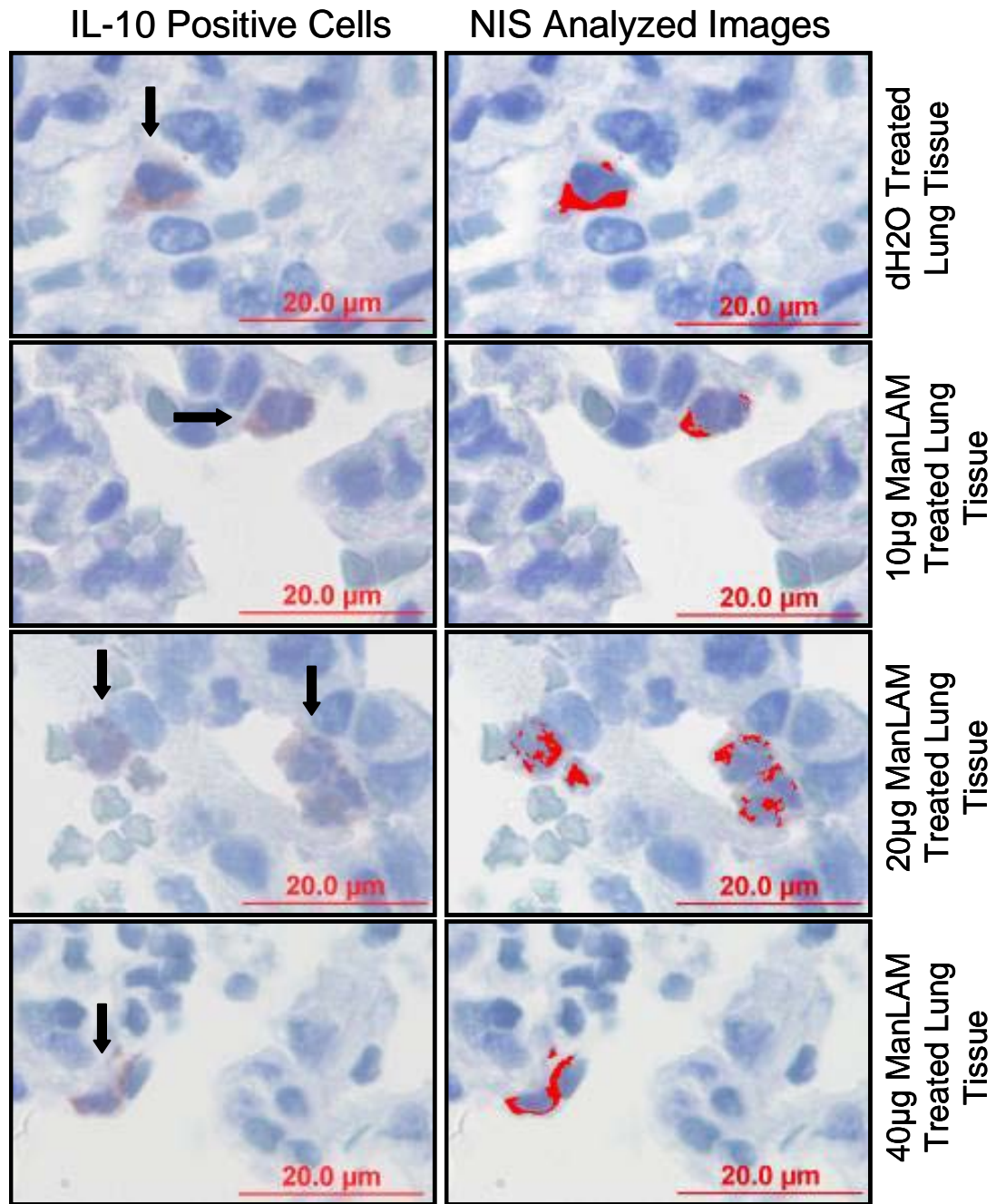


Figure 11: Representative IL-10 Positive Cells. Representative images of IL-10 positive cells within the lungs of treated mice are shown in the pictures above. In the first column reddish-brown staining for IL-10 is marked with a black arrow. In the right hand column these IL-10 positive cells are shown post analysis with the NIS-Element program. The red marks regions that are being analyzed by the program. The IL-10 positive cells analyzed exhibit MO or DC like morphology and localization within the lungs. Images are of representative cells, taken at 1000x total magnification and cropped.

3.4 ManLAM Increases the Number of IL-10 Positive Cells in the Pulmonary Vessels

While IL-10 positive cells were found within all regions of the lungs in all treatment groups, the mice treated with 20 μ g ManLAM and 40 μ g ManLAM showed a noticeable increase in the number of IL-10 positive cells found within the pulmonary vessels. Representative cells from within pulmonary vessels are shown in the images taken at 400x and 1000x total magnification (Figure 12A). When compared to dH₂O treated control mice the 20 μ g ManLAM treated group showed a four fold increase while the 40 μ g ManLAM treated group showed a five fold increase in the number of IL-10 positive cells within the pulmonary vessels (Figure 12B). Thus, not only did intrapulmonary ManLAM treatment increase the amount of IL-10 within the positive cells, it increased the population of IL-10 positive cells migrating within the blood vessels. Since this observation is based off histological analysis of fixed tissue, it does not speak toward whether the cells are entering or exiting the pulmonary compartment, simply that they are present within the pulmonary vessels. This increase in migratory IL-10 positive cells could point to the ability of ManLAM induced IL-10 to modulate responses in other organs.

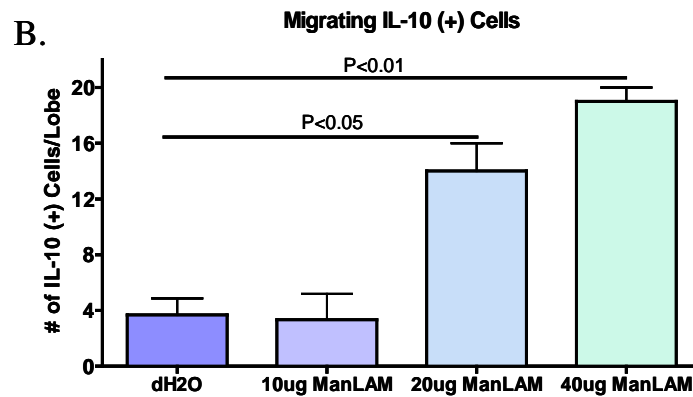
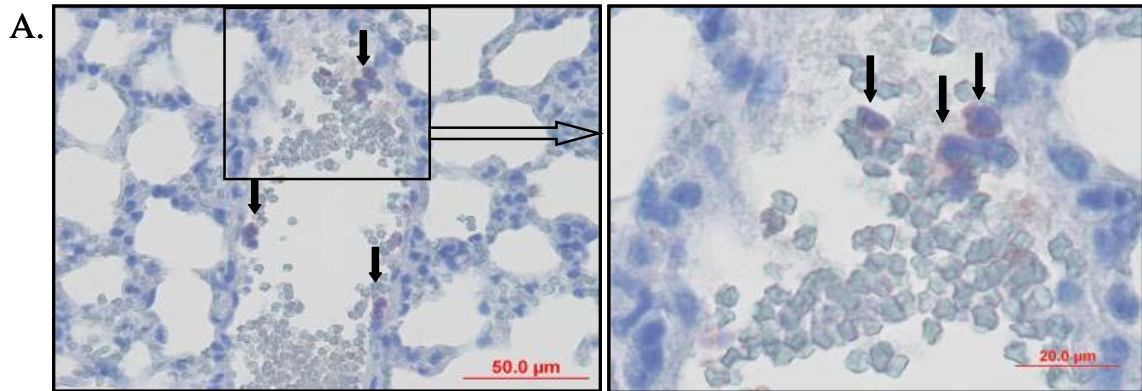


Figure 12: IL-10 Positive Cells within the Pulmonary Vessels.

The number of IL-10 positive cells migrating within the vessels of the lung was also analyzed. B) Within the lungs of mice treated with 20 μ g or 40 μ g ManLAM there was a significant increase in the number of migrating IL-10 positive cells found within the pulmonary vessels. A) Representative image of IL-10 positive cells migrating within the pulmonary vessels from a mouse treated with 40 μ g ManLAM, taken at a total magnification of 400x (left) and an enlargement of the framed section (right). IL-10 positive cells are marked with black arrows in both images.

Discussion

The immunosuppressive cytokine IL-10 plays a role in modulating the host response to *M. tuberculosis* infection. While DCs, MOs and T-cells produce IL-10 during *M. tuberculosis* infection, here we demonstrate that DCs stimulated with the *M. tuberculosis* cell wall lipoglycan ManLAM are capable of producing intracellular IL-10. ManLAM interacts with several different receptors on the surface of DCs including; mannose receptors, TLR-2 and DC-SIGN [6-8]. After interaction with any of these receptors, activation of downstream events occurs, leading to the production of many different cell products, among those the expression of IL-10. Of the three, DC-SIGN has been shown to be an important binding partner for ManLAM on DCs [7]. Several previous reports have indicated that signaling through DC-SIGN is capable of biasing TLR signaling in the direction of increased IL-10 production (Figure E) [7, 77]. All of these previous studies relied upon LPS as a costimulant and TLR-2 agonist in order to induce high levels of IL-10 from DC-SIGN ligands.

While previous studies only saw IL-10 expression from ManLAM treated DCs when LPS was used as a costimulant, here we report that ManLAM alone is capable of inducing the expression of high levels of intracellular IL-10. Our results agree with previous reports that ManLAM treatment of BMDCs does not stimulate the secretion of IL-10 when measured by ELISA (Figure 7A), but in our studies we see a dramatic increase in the levels of intracellular cytokine when stained by IHC. The intracellular IL-10 levels within ManLAM treated BMDCs were even higher than that of LPS treated BMDCs (Figure 7C). This production of intracellular IL-10 by ManLAM stimulation of DCs may be what primes the cells to secrete high levels of IL-10 when they are

concurrently stimulated with LPS. During the course of infection with *M. tuberculosis* free ManLAM within the lungs may prime DCs to produce high levels of intracellular IL-10. Upon receiving a second signal through TLRs, these primed DCs may secrete high levels of IL-10, suppressing the host immune response. The finding that ManLAM alone, without LPS, is capable of stimulating high levels of intracellular IL-10 show that this highly abundant *M. tuberculosis* cell wall molecule may play a role in downregulating the ability of DCs to mature and activate the host immune response. The production of IL-10 may also be capable of functioning in an autocrine fashion, inhibiting maturation of DCs from within.

In vitro experiments can teach us much about specific cell interactions and reactions within a very controlled environment, but these test tube results do not always translate to *in vivo* systems. Thus to examine whether the effects of ManLAM on *in vitro* BMDCs translates to the mouse model, we set up an experiment to look at the effects of the intrapulmonary delivery of ManLAM directly into the mouse lung. Only two previous reports have utilized direct pulmonary administration of LAM into the lungs and both focused on acute changes within 24 hours of LAM administration [5, 119]. While LAM from avirulent and fast growing strains was shown to induce neutrophilic influx into the bronchoalveolar lavage fluid (BAL), ManLAM did not exhibit this same capacity [5]. Additionally LAM from fast growing strains also caused an increase in the chemokines macrophage inflammatory protein-2 (MIP-2) and keratinocyte (KC) and the cytokine TNF- α 24 hour after intranasal treatment [119]. Our goal was to analyze how prolonged exposure to ManLAM affects the lung environment *in vivo* by administering 10 μ g, 20 μ g or 40 μ g ManLAM via the intratracheal route three times over the course of a week.

Histological analysis of the lungs of mice treated with ManLAM three times over the course of a week showed minor thickening of the bronchial walls, but no major inflammation or pathological changes were seen after seven days (Images not shown). Since ManLAM has been shown to function in an immunosuppressive manner this was not surprising [7, 57, 75, 79]. Analysis of whole lung homogenate cytokine levels aligned with the absence of pathology, showing no large scale increases in IFN- γ , TGF- β or IL-10 (Data not shown and Figure 9). To examine whether any changes were occurring at the cellular level, IHC was performed on tissue sections using antibodies against IL-10, TGF- β and TNF- α . IHC of tissue sections revealed very little TGF- β and TNF- α in the lungs, however IL-10 positive cells were seen scattered throughout the lungs and IL-10 expression was significantly increased in tissue sections from ManLAM treated mice.

To analyze intracellular IL-10 staining we utilized the NIS-Element program. This program allows one to measure the intensity of intracellular staining and to compare IL-10 expression between different samples. Mice treated with 10 μ g, 20 μ g or 40 μ g ManLAM showed a significant increase in intracellular IL-10 production when compared to dH₂O treated mice (Figure 10A). IL-10 positive cells also exhibited the morphological appearance of monocytes, MOs and DCs (Figure 11), and were also found in increasing numbers in the pulmonary vessels of 20 μ g and 40 μ g ManLAM treated mice (Figure 12). Since LAM is capable of acting as a monocyte chemoattractant this is not surprising [5], though by the nature of this analysis we are unable to determine whether these IL-10 positive cells are entering or leaving the tissue. This does imply a possible role for these IL-10 positive cells in affecting other organs such as; the peripheral blood, draining lymph nodes and spleen.

Within these experiments ManLAM stimulation alone has been shown to increase intracellular IL-10 production from BMDCs *in vitro* and monocyte, MO and DC like cells *in vivo*. Here we demonstrate for the first time the effects of prolonged exposure of purified ManLAM on the murine lung *in vivo*. These results provide a possible mechanism by which exposure to ManLAM during infection with *M. tuberculosis* may contribute to the downregulation of the host immune response during the latter stages of infection. While IL-10 is involved in the onset of latency [118, 120] and in reactivation [46], future work will need to further examine whether ManLAM induced IL-10 is involved in these two processes.

Chapter 4: Modulation of Dendritic Cell Nitric Oxide Production in Response to ManLAM

Introduction

Nitric oxide (NO) is a free radical produced by many different cell types within the body. It functions as a signaling molecule between neurons, in regulating smooth muscle cell contractions and as an antimicrobial agent within phagocytes [121, 122]. The ability to analyze intracellular NO production at the single cell level using a fluorescent probe allows researchers to better understand how different populations of cells are responding to the stimuli, and allows concurrent flow cytometry analysis of other cellular markers. Among the new reagents available, DAF-FM diacetate (Invitrogen #D-23842) in the green channel and DAR-4M (Kamiya Biomedical Co #BC-039) in the red channel, provide researchers with the capacity to analyze intracellular NO levels. The dyes are not specific for just NO, but react with many of the reactive nitrogen intermediates (RNIs) within the cell to become fluorescent [123]. The ability of these dyes to measure intracellular NO expression makes them an especially powerful tool for analyzing intracellular antimicrobial RNI production.

Host control of *M. tuberculosis* infection relies upon a number of different cell types and bioactive molecules [10, 16, 24, 28, 30]. Among those, the antimicrobial reactive oxygen intermediates (ROIs) and RNIs are of particular interest due to their potent capacity to kill or inhibit the growth of many different microbial agents [38, 124, 125]. *M. tuberculosis* infection results in the production of ROIs, but some studies have shown that this bacillus is able to evade ROI mediated killing [23, 89, 96]. On the other

hand the role of RNIs in *M. tuberculosis* infection is better understood, though most of the work has been done in the mouse model. RNIs include nitric oxide (NO), nitrite (NO_2^-) and nitrate (NO_3^-) [38], with NO being the most prominent antimicrobial RNI produced by MOs and DCs. *In vitro* 90 ppm of NO gas can effectively kill *M. tuberculosis* bacilli [94]. The effectiveness of *M. tuberculosis* stimulated NO at limiting the growth of the bacilli within MOs and DCs has been demonstrated in many model systems [31, 38, 126].

MOs and DCs rely upon intracellular NO as one of the mechanisms by which bacteria are destroyed. This happens via bacterial DNA, protein and lipid modification, disruption of bacterial signaling and induction of apoptosis of infected cells [38]. The cytokines TNF- α and IFN- γ , both produced during infection with *M. tuberculosis*, synergize in activating inducible nitric oxide synthase (iNOS) expression and NO production by MOs and DCs [16]. The capacity of activated MOs to kill intracellular *M. tuberculosis* via NO production is much greater than that of DCs. The study by Bodnar et al showed that *M. tuberculosis* infected DCs produced similar levels of NO to activated MOs, however the bacteria in these cells were not killed, but exhibited limited intracellular growth [31]. The impairment of NO mediated killing of *M. tuberculosis* within DCs implicates a role for DCs in the persistence of the bacilli within the host.

The specific reason for the decreased bactericidal activity of NO within DCs is not known, however the work performed in MOs may provide some insight. The mycobacterial cell wall lipoglycan LAM has many immunomodulatory functions and also appears to play a role in modulating iNOS expression and NO production [38]. Several reports agree that AraLAM from avirulent strains of mycobacteria is a more

potent inducer of NO production than ManLAM from virulent strains [127, 128].

Although ManLAM from *M. tuberculosis* has the ability to enhance NO₂⁻ production from peritoneal and RAW 264.7 MOs primed with IFN- γ [87, 129, 130], other studies have shown that *M. bovis* BCG infected RAW 264.7 cells produced lower levels of NO when they were pretreated with ManLAM in the absence of IFN- γ [131].

IL-10 is known as a potent inhibitor of TNF- α and IFN- γ production within DCs and MOs [47], and these two cytokines are key contributors to the activation of iNOS and NO as previously described. In the previous chapter we demonstrated that stimulation of DCs with ManLAM induced intracellular IL-10 production (Figures 7-10). Altogether this allows us to speculate that ManLAM stimulation may interfere with NO production by DCs via stimulation of IL-10. In the studies presented below we first evaluated the capacity of BMDCs stimulated with ManLAM + IFN- γ to produce intracellular NO in comparison to BMDCs stimulated with LPS + IFN- γ . We then looked at how pretreatment of BMDCs with either ManLAM or LPS affected the ability of BMDCs to produce intracellular NO in response to infection with *M. tuberculosis*.

Previous studies by other groups determined the extracellular expression of NO by measuring the levels of nitrite using the Griess reagent [127, 129, 130]. Thus, those studies were unable to determine NO production at the single cell level. Our interest was to study the ability of the cells to kill intracellular bacteria. In order to examine this, we believed it was very important to measure the levels of intracellular NO expression at the single cell level. We utilized an intracellular dye, DAF-FM diacetate, to measure the levels of expression of intracellular NO at the single cell level. Our experiments show that ManLAM impairs the ability of BMDCs to produce NO, even in the presence of the

NO activating cytokine IFN- γ . Additionally, pretreatment of BMDCs with ManLAM leads to a reduction in NO production after BMDCs are infected with live *M.*

tuberculosis. By reducing the ability of DCs to produce high levels of antimicrobial NO, ManLAM may be assisting the bacilli in its quest to evade intracellular killing.

AIM: Using the cell permeable NO indicator dye DAF-FM diacetate, develop an assay to measure intracellular NO at the single cell level. Then utilize this technique to study the kinetics of NO production in response to ManLAM treatment of BMDCs. Furthermore we aim to study the effect of BMDC ManLAM pretreatment on the cell's ability to respond to infection with live *M. tuberculosis*.

Hypothesis: ManLAM treatment of BMDCs will inhibit high levels of NO expression in response to stimulation with this lipoglycan and after infection with live *M. tuberculosis*.

Materials and Methods

Mice: Female C57BL/6 mice, six to eight weeks of age, were purchased from Jackson Laboratories. Mice were housed in a sterile pathogen free environment, and were given sterile water, mouse chow, bedding and enrichment for the duration of the experiments.

Bone Marrow Derived Dendritic Cells (BMDCs): BMDCs were prepared as previously described in Chapter 2. Briefly, bone marrow was removed from femurs of C57BL/6 mice, and the cell aggregates were broken down into an individual cell suspension. Bone marrow cells were resuspended in cRPMI (Gibco #21870-076) media supplemented with 20ng/mL GM-CSF as previously described in Chapter 2. Cells were cultured for six to eight days at 37°C/5% CO₂/85% humidity in 25cm² culture flasks (Corning #430168).

After six to eight days cell suspensions were spun, resuspended in fresh media at 1x10⁶

cells/mL and plated into either a 24well or 96well tissue culture dish (Corning Costar #3526 and BD Falcon #353070).

Bone Marrow Derived Macrophages (BMMOs): Bone marrow cells were harvested and processed as previously explained in Chapter 2 and then cultured in cDMEM media (Cellgro #15-017-CV) supplemented with L929 media as a source of M-CSF as previously described in Chapter 3. Cells were cultured for six to eight days at 37°C/5% CO₂/85% humidity in 25cm² culture flasks (Corning #430168). After six to eight days cell suspensions were spun, resuspended in fresh media at 1x10⁶ cells/mL and plated into either a 24well or 96well tissue culture dish (Corning Costar #3526 and BD Falcon #353070).

Cell Culture Antigen Stimulation: After six to eight days of culture, cells were replated at 1x10⁶ cells/mL in a 24well or 96well dish. Cells were then either left untreated or treated with 20ng/mL *E. coli* LPS (Sigma #L5024) or 1µg/mL ManLAM from *M. tuberculosis* H37Rv (NIH CSU TB Vaccine Testing and Research Materials Contract # HHSN266200400091c, 7/26/07). For experiments in sections 4.1, 4.2 and 4.3 cells were also simultaneously stimulated with 50 units/mL IFN-γ. Cells were analyzed at specified time points as indicated. ManLAM was purified from whole mycobacteria via a series of gradient extractions. Endotoxin levels were all less than 2ng/mg of LAM.

Mycobacterial Infections: BMDCs and BMMOs (described above) were infected with *M. tuberculosis* Erdman strain grown in Middlebrook 7H9 media (BD #271310) and frozen at -70°C. Frozen stocks were thawed and gently broken apart using a 30 ½ gauge needle and DCs were infected at a ratio of one bacterium per one DC and treated with 50 units/mL IFN-γ. Infected cells were incubated at 37°C/5% CO₂/85% humidity for up to

48 hours before analysis. *M. bovis* BCG GFP was also used to examine BMDC and BMMO infections (Courtesy of Dr David Russell, Cornell University 10/20/2000).

Auramine/Rhodamine T Staining: Cells were plated and treated as previously described. 100µl of cells were then placed into Shandon cytofunnels (Thermo Scientific #5991040) and spun at 400rpm for 30 seconds in a Shandon Cytospin 1 (Shandon Southern #SCA0031) onto positive charged slides (VWR Superfrost Plus # 48311-703). The slides were then washed with 200 proof ethanol to adhere cells to the slides. Slides were then covered in TB auramine-rhodamine T solution (BD TB kit # 212519) for 25 minutes at room temperature, washed three times with TB decolorizer and allowed to soak for 5 minutes with the final wash. Following this step the slides were washed with dH₂O and counter-stained with potassium permanganate for two minutes at room temperature. Finally the slides were again washed with dH₂O and mounted with Prolong Gold with DAPI (Invitrogen #P36931) and analyzed on a Zeiss LSM 510 META confocal microscope.

M. tuberculosis Infection Rate: BMDCs infected with *M. tuberculosis* were stained with auramine-rhodamine T as previously described. Images were captured using a Zeiss LSM 510 META confocal, HeNe 543nm excitation laser and 560-615nm emission filter at a total magnification of 400x. Five images from each of three different experiments were analyzed. The total number of cells and the number of cells in each time point containing intracellular bacteria were counted and the data was expressed as the percentage of cells positive for *M. tuberculosis*.

Single Cell Nitric Oxide (NO) Analysis: BMDCs and BMMOs were treated with LPS, ManLAM, left untreated or infected with *M. tuberculosis* as previously described. Upon

treatment or infection cells were concurrently treated with 50units/mL IFN- γ to further stimulate NO production. At specific time points cells were washed and resuspended in phenol free cRPMI media (Cellgro #90-022-PB) containing 10 μ M DAF-FM diacetate (Molecular Probes D23842). Cells were incubated for 30 minutes at 37°C, and then incubated for an additional 30 minutes at 37°C in dye free cRPMI media. Cells were then resuspended in PBS and analyzed with a BD LSR II flow cytometer or Zeiss Confocal microscope using a 488nm laser and a 505-550nm emission filter as described below.

Light and Fluorescent Microscopy: The Zeiss Axio Observer microscope was connected to a LSM 510 META confocal laser source. This system was used to take both live time course images as well as images from fixed cells. The fluorescence emitted by excitation with the 488nm laser on cells containing DAF-FM demonstrated positive expression of intracellular nitric oxide. A 405nm diode laser was used with an emission filter of 420-480nm for DAPI, a 543nm HeNe laser was used with an emission filter of 560-600nm for auramine-rhodamine T and a 488nm argon laser was used with emission filters of 505LP or 505-550nm for DAF-FM=NO staining. All images were taken at 630x total magnification on a Zeiss LSM 510 META confocal microscope.

Flow Cytometry: Cells were cultured for six to eight days and treated as previously described. After treatment cells were fixed and permeabilized in 4% paraformaldehyde (Electron Microscopy Sciences #15710) containing 0.05% Tween20 (JT Baker, #X251-07) in 1x PBS for 20 minutes at 4°C. Cells were then stained for 30 minutes at 4°C in 1x PBS containing 0.05% Tween20 and select monoclonal antibodies at a 1:50 dilution. Cells were then washed and data was obtained using a BD LSR II flow cytometer designed with a 488nm blue laser, a 633nm HeNe laser, a 405nm VioFlame laser and a

355nm UV laser and corresponding filters for each fluorochrome. Data was analyzed using BD FACS Diva Software. Antibodies used were; anti-CD4 APC (eBioscience #17-0041), anti-CD11b PerCP-Cy5.5 (eBioscience #45-0112), anti-CD11c PE-Cy7 (eBioscience #25-0114), anti-DC-SIGN PE (eBioscience #12-2091), anti-MHC II labeled with Alexa350 (eBioscience #14-5321, Alexa350 Invitrogen #A-10170), anti-CD1d PE (eBioscience #12-0011), anti-CCR7 APC (eBioscience #17-1971), anti-CD80 PE (eBioscience #12-0801), anti-IL-10 FITC (eBioscience #11-7101), anti-iNOS FITC (BD #610330).

Statistics: The results presented in this study are representative of two or three experiments. The data are expressed as the mean values from the duplicate or triplicate assays. A parametric method, the one-way ANOVA with a Tukey post-test was used to assess the statistical significance between groups of data. Values of $p < 0.05$ were considered statistically significant. p values for all statistically significant data are indicated on the bars above the data sets.

Results

4.1 DAF-FM Diacetate Single Cell Nitric Oxide Analysis

We utilized DAF-FM diacetate to investigate NO production in response to ManLAM + IFN- γ , LPS + IFN- γ and IFN- γ treatment alone. The DAF-FM diacetate dye is cell permeable, becoming trapped within the cell once cleaved by non-specific esterases. The DAF-FM diacetate dye is virtually non-fluorescent until it reacts with RNIs, upon which it will become up to 160 times more fluorescent [132]. In bone marrow derived macrophages (BMMOs) 20ng/mL LPS stimulation in conjunction with

50 units/mL IFN- γ produces a noticeable increase in NO production within two hours of treatment (Figure 13B). Figure 13B shows the reaction of the dye with intracellular NO, tracking the reaction starting at time 5 minutes (Figure 13B left) after the DAF-FM diacetate dye was added to the LPS + IFN- γ pretreated BMMOs. At 30 minutes (Figure 13B middle) post staining cells begin to show green fluorescence from the interaction between NO and the DAF-FM diacetate dye, and at time 45 minutes (Figure 13B right panel) post addition of the DAF-FM diacetate dye NO positive cells are clearly seen in green. The use of DAF-FM diacetate to examine intracellular NO production along with fluorescent microscopy and flow cytometry allows for the analysis of the intracellular NO kinetics of cells in response to various stimuli.

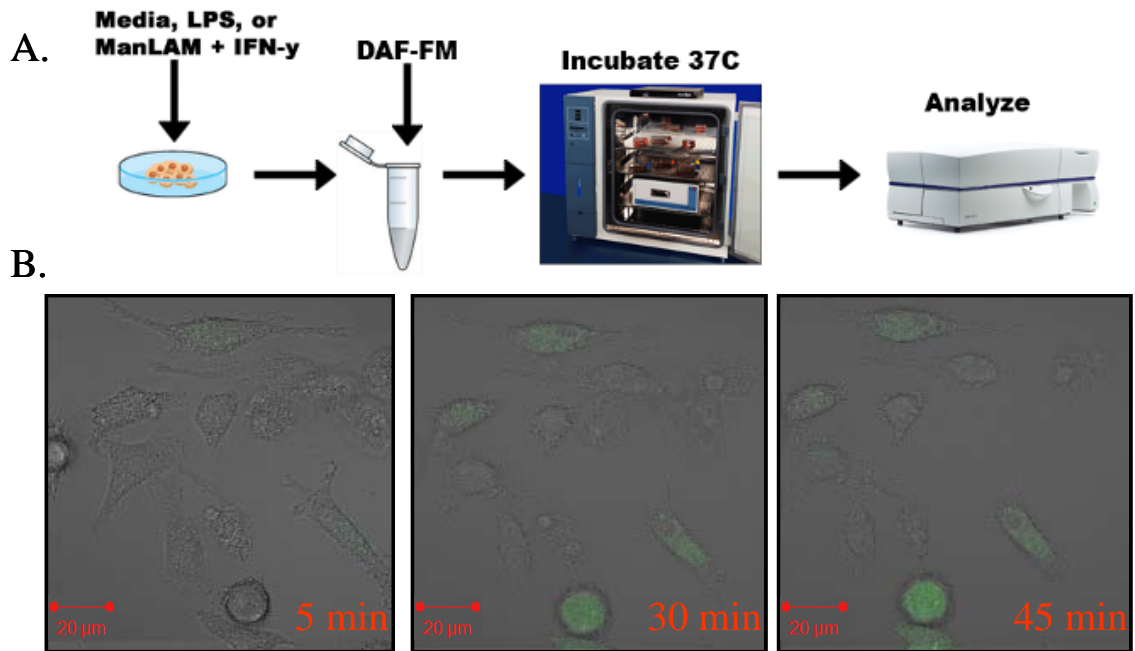


Figure 13: DAF-FM Diacetate Intracellular Nitric Oxide Staining. The cell permeable DAF-FM diacetate dye was used to analyze intracellular NO production at the single cell level. A) Cells were treated as described and then incubated with the dye for one hour at 37°C. Population data was acquired on a BD LSR II flow cytometer and images were captured using a Zeiss LSM 510 META confocal microscope. B) Representative images show DAF-FM stained macrophages treated with 20ng/mL LPS and 50 units/mL IFN- γ for one hour then imaged for one hour at 630x total magnification.

4.2 ManLAM Alters DC Nitric Oxide Expression

Previous reports have demonstrated that ManLAM modulates extracellular NO production from various MO cell types [129-131]. However, the capacity of ManLAM to alter NO production within DCs is still not fully understood. We studied the kinetics of NO production in response to ManLAM using the intracellular dye DAF-FM diacetate as a reporter for RNI production, and tracked changes in RNI levels over time using flow cytometry. BMDCs were treated simultaneously with 20ng/mL LPS, 1 μ g/mL ManLAM or left untreated and 50 units/mL IFN- γ , then at specified time points the cells were washed, stained and read with a LSR II flow cytometer. The time (in hours) indicated in

Figure 14 is the time that samples were removed from culture, washed and stained. The actual time between stimulation and analysis on the LSR II flow cytometer is approximately 90 minutes more than the initial time of removal from culture. Thus cells that had been stimulated had an additional 90 minutes to produce NO while samples were being processed.

In response to DAF-FM dye staining for NO, treated BMDCs exhibited two populations of NO production based on the mean fluorescence intensity (MFI) of emitted DAF-FM fluorescence. The DAF-FM negative population was gated out based on the cellular autofluorescence in the absence of the dye (Figure 14 ungated region to the left), as BMDCs show a moderate level of autofluorescence in the 488nm excitation 520nm emission region. Gates for NO positive cells, identified by an increase in the fluorescence emitted by the DAF-FM dye, were gated within each histogram [Figure 14, NO (+) Cells]. Unstained BMDC autofluorescence had a very small amount of carry over into the NO positive population, less than 1% of the total population (Data not shown). Quantifications for each gated region are listed at the top of each flow cytometry panel, with percentages indicating the number of cells gated within that region, and the MFI representing the average intensity of fluorescence emitted by the DAF-FM stained cells within the gated region. BMDCs appear to have a steady state level of intracellular RNIs prior to stimulation (Figure 14 first row), which is initially reduced upon stimulation with IFN- γ and the other stimulants (Figure 14 second and third row).

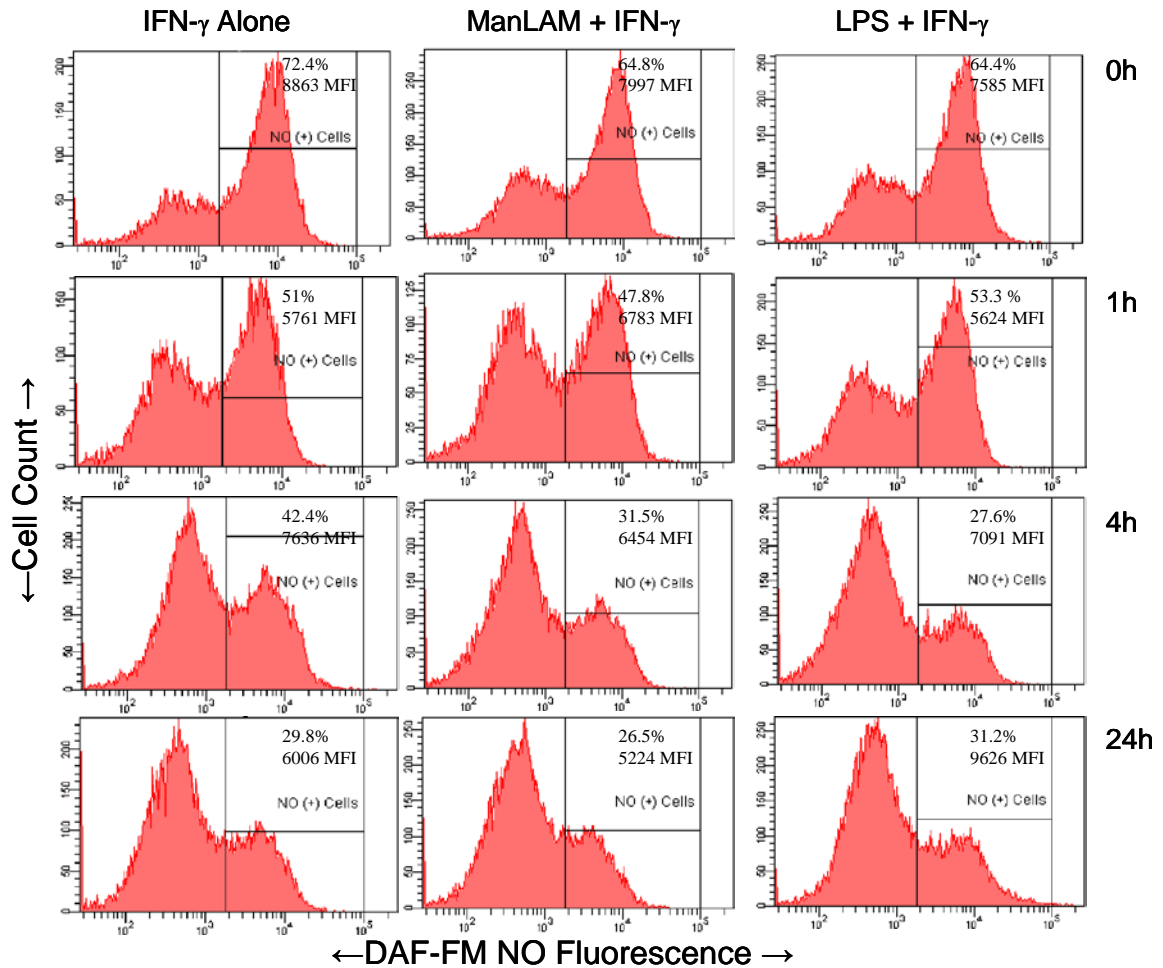


Figure 14: NO Flow Cytometry Time Course.

In response to bacterial invaders host DCs can utilize NO as an antimicrobial agent. To analyze the ability of treated DCs to produce NO, the intracellular dye DAF-FM diacetate was utilized to look at the expression of intracellular RNIs. The flow cytometry histograms above show single cell NO production for each culture and population data for each gated group is shown at the top of the region. Forward scatter and side scatter were used to gate out debris and cell aggregates, while NO gates were set based on cellular autofluorescence levels. The Mean Fluorescence Intensity (MFI) represents the average NO expression within the cells. Only LPS + IFN-γ treated DCs show the ability to increase NO expression after 24 hours of treatment (third column, fourth panel).

Stimulation of BMDCs and subsequent staining with DAF-FM dye showed similar staining kinetics, thus RNI induced fluorescence of the DAF-FM dye readily appeared 30 minutes after staining for all samples (Figure 15A). When the induction of NO after treatment was examined in each of the samples; LPS + IFN-γ, ManLAM + IFN-

γ and IFN- γ alone all had a general downward trend in the DAF-FM MFI [NO production] within positive cells for the first couple hours. After 4 hours LPS + IFN- γ treated BMDCs and IFN- γ alone treated BMDCs showed a slight increase in intracellular NO production, though this increase was sustained after 24 hours only in the presence of LPS. ManLAM + IFN- γ treated cultures showed decreasing levels of intracellular NO throughout the time course (Figure 15B). Thus, even in the presence of the activating factor IFN- γ , BMDCs do not appear capable of sustaining NO production without an additional activation signal and even exhibit a decreased capacity to produce NO in the presence of ManLAM. Representative time course data from one of two experiments is shown in Figure 15B. Additionally, the percentage of ManLAM + IFN- γ and LPS + IFN- γ treated NO positive cells were slightly increased after 24 hours, though these changes were not significant (Figure 15C). However, when the BMDCs were treated for 24 hours with LPS + IFN- γ there was a significant increase in the DAF-FM MFI when compared to ManLAM + IFN- γ treated samples and IFN- γ alone treated samples. While a small decrease in the MFI is seen after 24 hours in ManLAM + IFN- γ treated BMDCs, this change is insignificant when compared to samples treated for 24 hours with IFN- γ alone (Figure 15D).

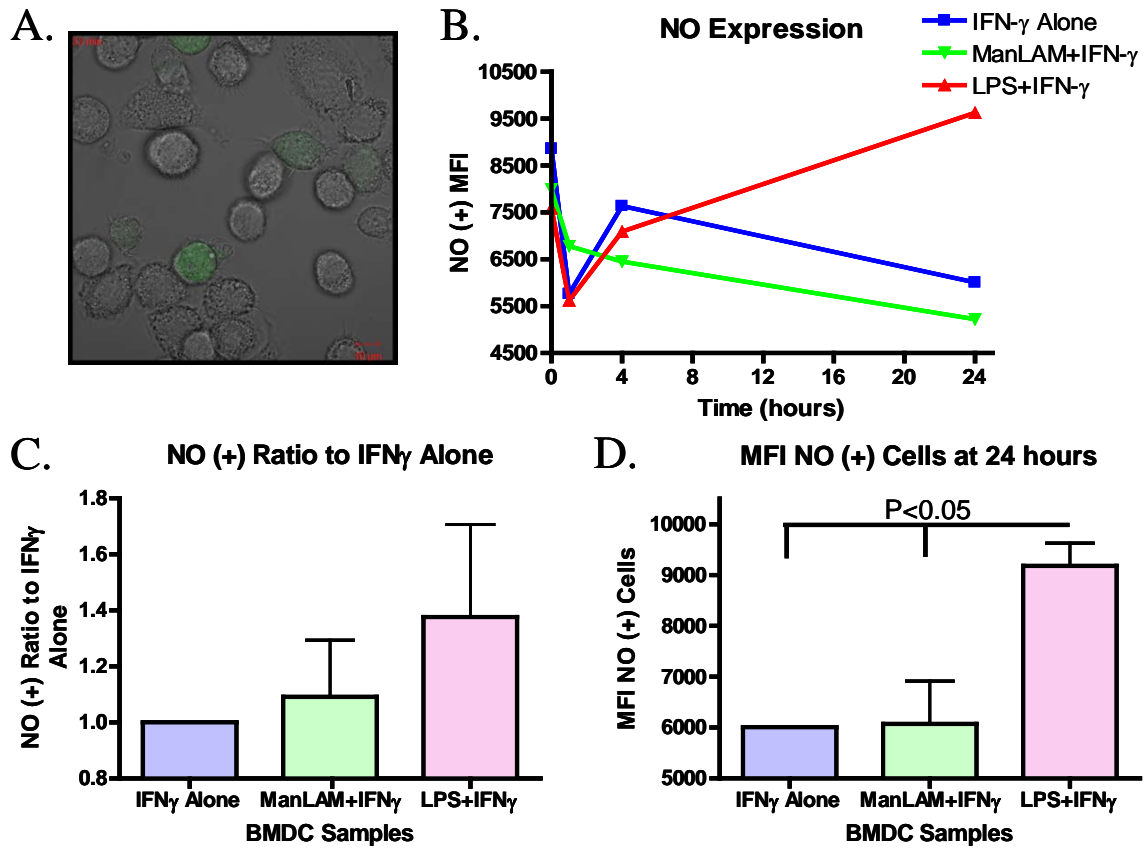


Figure 15: ManLAM Stimulation Fails to Increase NO Production.

A) Representative image of NO positive BMDCs taken on a Zeiss LSM 510 META confocal microscope at 630x total magnification, DAF-FM fluorescence is seen in green.

B) After 24 hours LPS + IFN- γ treated samples show an increase in NO production, while ManLAM + IFN- γ treatment and IFN- γ alone show an inability to sustain NO production. C) At 24 hours post treatment there is a small but insignificant increase in the number of NO positive BMDCs in LPS and ManLAM treated samples. While the total number of NO positive BMDCs is not significantly different, D) the average NO production from NO positive LPS treated BMDCs is significantly higher. Additionally no significant change is seen in the NO expression from ManLAM treated BMDCs. B) The graph shows a representative data set from one experiment, while data in C) and D) represent the mean \pm SD.

4.3 ManLAM Decreases BMDC Nitric Oxide Expression in Response to *M. tuberculosis*

As demonstrated above, the ability of purified ManLAM to prevent NO expression within BMDCs was significant. Thereafter we studied whether ManLAM pretreatment of BMDCs also alters NO production when these cells encounter the *M. tuberculosis* bacilli. To examine this, BMDCs preconditioned with ManLAM, LPS or in media as explained above were exposed to live *M. tuberculosis* + 50 units/mL IFN- γ and then the expression of intracellular NO was determined at the single cell level. BMDCs were cultured and treated with LPS, ManLAM or left untreated for 20 hours, and then mixed at a ratio of one *M. tuberculosis* bacilli per one BMDC. At the same time the cells were infected they were stimulated with 50 units/mL IFN- γ and then stained with DAF-FM for NO analysis at specific time points. To determine the number of cells infected within each culture we prepared cytopspins from each culture, and then stained the cells using the acid fast fluorescent dye auramine-rhodamine T. Cells were then analyzed by confocal microscopy, cells positive for acid fast bacilli were counted and the data was analyzed to determine the percentage of infected cells within each culture (Figure 16A). While the percentage of BMDC infection was low between one to four hours post-infection ($25\% \pm SD$, $26\% \pm SD$), at 24 hours post-infection approximately 60% of BMDCs were found to contain one or more bacilli (Figure 16B). Furthermore there were no differences in the percentages of infection seen between the different culture groups. Many of the infected BMDCs contained multiple bacilli, a phenomenon that is also seen in DCs during *in vivo* infection [26].

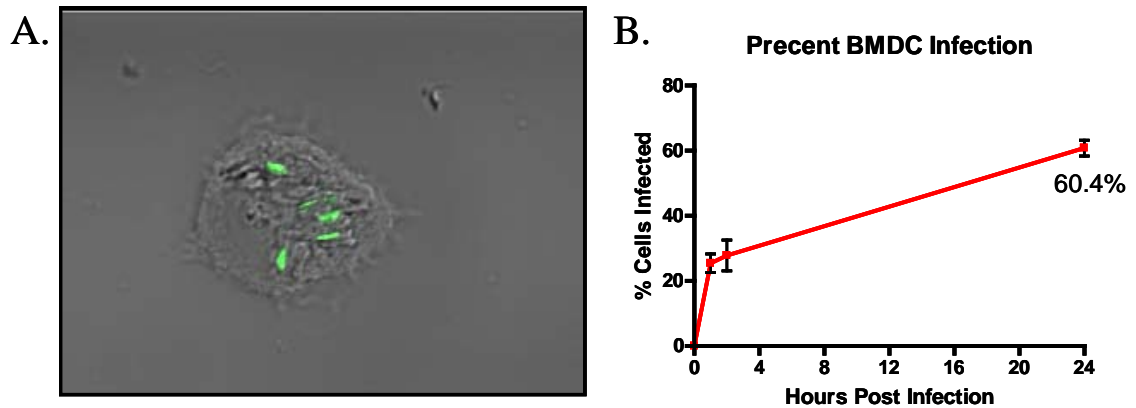


Figure 16: *In vitro M. tuberculosis* Infection Rate within BMDCs. DCs pretreated with ManLAM, LPS or media were infected with *M. tuberculosis* strain Erdman at a ratio of one to one for up to 24 hours. A) A representative fluorescent image showing an infected BMDC with *M. tuberculosis* stained by auramine-rhodamine T and imaged with a fluorescent filter for rhodamine. B) After one hour approximately 25% of DCs were infected, after two hours 26% and after 24 hours 60% of DCs were found to be infected. For each time point at least four different slides from three different experiments were analyzed. Infected cells were identified by positive *M. tuberculosis* staining with auramine-rhodamine T within the cell. Data represents the mean \pm SE.

These experiments demonstrated that the kinetics of NO production varied greatly depending on the stimulant applied prior to infection. The graphs in Figure 17 show raw data obtained from this experiment. As previously defined, flow cytometry histograms are divided into two regions; NO negative, based on cellular autofluorescence, and the NO positive gated region (Figure 17 right gated population). The MFI, which represents the cellular NO concentration and the percentage of positive cells within each gate are listed at the top of the gated regions. Flow cytometry histograms from the selected time points [0, 1, 4, 24 hours] show that untreated BMDC cultures (Figure 17 first column) and ManLAM pretreated BMDC cultures (Figure 17 middle column) exhibit a quick burst in the number of NO producing cells upon infection, while LPS pretreated BMDCs (Figure 17 right column) show a slower steady increase in the number of NO producing cells upon infection.

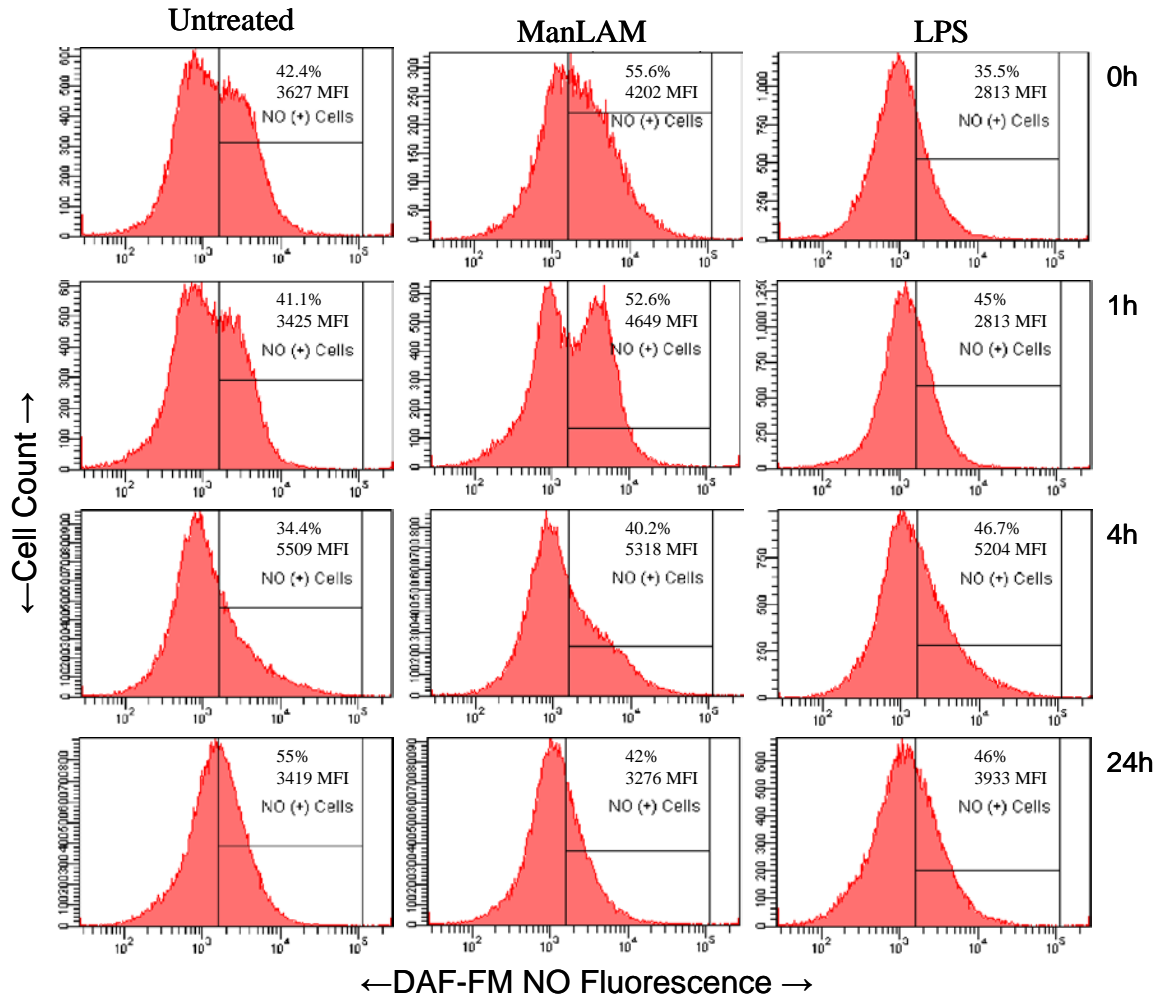


Figure 17: NO Flow Cytometry Plots Post-Infection.

BMDCs were pretreated with ManLAM, LPS or left untreated for 20 hours then infected with live *M. tuberculosis* strain Erdman to analyze how pretreatment with the listed antigens effects the DC NO expression in response to *M. tuberculosis*. Samples were analyzed at 0 hours, 1 hour, 4 hours and 24 hours post-infection for intracellular NO production at the single cell level. The flow cytometry histograms show gates and quantifications for the NO positive population. The MFI and percent of the total cells for each gate are shown at the top of each region.

The changes seen in the number of NO producing cells is different for each pretreatment group. Both ManLAM pretreated and untreated BMDCs responded with an initial drop in the total number of NO positive cells upon infection, but after 24 hours the total number of responding cells within the untreated group had rebounded and increased

by 10%, while the number of responding cells in the ManLAM pretreated culture remained lower than the earlier time points. Unlike the other two groups, LPS pretreated BMDCs showed a slow increase in the number of NO positive cells over the 24 hour period (Figure 18A). ManLAM pretreatment not only reduces the total number of NO positive cells 24 hours after infection, but also decreased the intracellular expression of NO. Twenty four hours after infection, LPS pretreated BMDCs show elevated levels of intracellular NO, while the amount of NO within untreated and ManLAM pretreated BMDCs is depressed by comparison (Figure 18B).

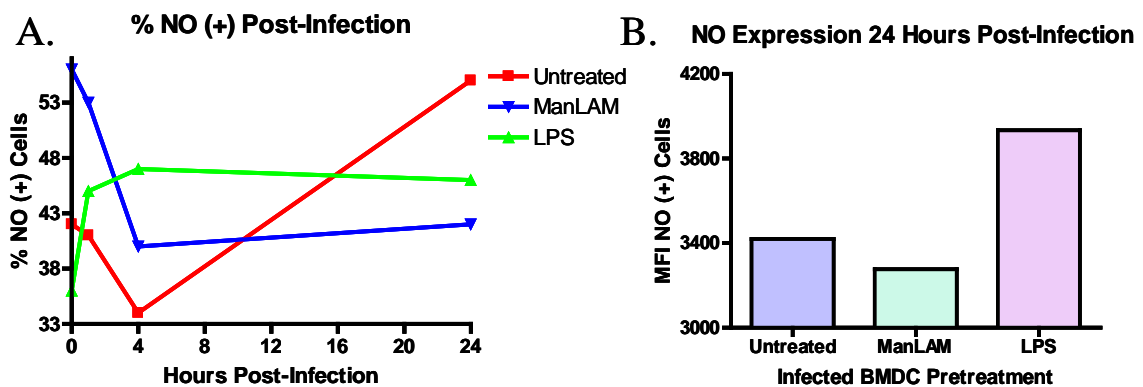


Figure 18: BMDCs Treated with ManLAM Show Reduced NO Expression Post-Infection.

Pretreated BMDCs were infected with *M. tuberculosis* Erdman at a ratio of one to one for up to 24 hours. A) After infection BMDCs pretreated with ManLAM or no pretreatment initially show a steady decrease in the number of NO producing cells. After 24 hours, untreated infected BMDCs show a sharp increase in the number of NO positive cells, while ManLAM pretreated cultures do not show this rejuvenation of NO. LPS pretreated BMDCs, which are activated as previously described, show a steady increase in the number of NO producing cells over the 24 hour period of infection. B) Infected ManLAM pretreated BMDCs also have a lower MFI than infected LPS treated and untreated DCs. Thus ManLAM pretreatment impairs the ability of BMDC cultures to upregulate NO production after infection, and leads to reduced levels of intracellular NO.

Discussion

The host employs many different defense mechanisms against intracellular bacteria such as *M. tuberculosis*, among them the production of the antimicrobial molecule nitric oxide (NO). Much is known about how NO production is stimulated and how the molecule functions in general, both within signaling pathways and in host defenses against foreign pathogens [121, 122], though the exact role during *M. tuberculosis* infection is not as clear. While previous reports have shown low levels of NO to be microbicidal against *M. tuberculosis*, how the molecule functions within the context of the phagocyte and within the host itself is the topic of on going research [38, 96, 133]. Within this study the cell wall lipoglycan ManLAM is shown to modulate NO production from BMDCs both alone and in the context of *M. tuberculosis* infection.

In order to analyze changes in intracellular NO production we utilized a novel fluorescent dye, DAF-FM diacetate, as an indicator of the presence of RNI within live BMDCs. Most studies that have examined ManLAM's capacity to affect NO production have used the Griess Reagent [127, 129, 130]. The Griess reaction is a very easy to use colorimetric assay that detects the presence of nitrite within the extracellular supernatant down to concentrations of 100nM [132]. The main draw back of this assay is it does not give information on the intracellular concentration of RNIs, which is where bacilli such as *M. tuberculosis* reside. Thus, the Griess reagent may be measuring NO that is functioning both in an antimicrobial manner and as a signaling molecule, activating other cells and inducing apoptosis. On the other hand the DAF-FM and DAR-4M dyes are cell permeable dyes that become fluorescent upon binding of RNIs within cells, allowing for the direct detection of intracellular NO [132]. By using the dye DAF-FM diacetate we

were able to track changes in RNI production in response to various treatments both by flow cytometry and fluorescent microscopy (Figures 14 and 17). Another advantage of utilizing an intracellular dye such as DAF-FM diacetate in conjunction with flow cytometry is that different populations of NO producing cells can be separated and analyzed.

Since previous work had shown that ManLAM has the ability to modify NO production by MOs, we sought to examine whether this held true for BMDCs. LPS + IFN- γ and ManLAM + IFN- γ treatments exhibit a slight capacity to increase the total number of NO producing cells, though these changes are insignificant when compared to untreated control BMDCs (Figure 15C). The effect that the specific stimulant does have is to alter the amount of NO being produced within these cells. While LPS + IFN- γ stimulation showed the ability to increase the amount of NO within BMDCs, treatment with ManLAM + IFN- γ did not have the same effect. This difference was most notable at 4 hours and 24 hours after treatment when LPS + IFN- γ induced NO production increased while ManLAM + IFN- γ treatment led to a steady decline in NO expression (Figure 15). Even though several groups reported that ManLAM + IFN- γ treatment was able to induce NO production from MOs [127, 129, 130], we have shown that ManLAM is incapable of eliciting the same response from BMDCs, while LPS + IFN- γ retains its capacity to increase NO production within BMDCs.

When BMDCs were pretreated with either; ManLAM, LPS or no treatment then infected with *M. tuberculosis* + IFN- γ , very different NO kinetics were seen for each culture. ManLAM pretreatment of BMDCs caused an impairment of NO production in response to *M. tuberculosis* infection, leading to a reduction in the total number of cells

producing NO and low levels of intracellular NO. Conversely infection of BMDCs activated by LPS pretreatment led to an increase in both the total number of NO producing cells and the MFI [mean NO expression] (Figure 18). These results show that DCs preconditioned with ManLAM are unable to fully respond to live bacilli, while immature DCs and LPS activated DCs are more capable of producing NO in response to infection with live *M. tuberculosis*.

NO production has been shown to be regulated by the nitric oxide synthase (NOS) enzymes, with constitutive NOS (cNOS) and inducible NOS (iNOS) playing roles in the ability of host phagocytes to produce NO [108]. cNOS's role is to maintain a steady state production of NO, to depress iNOS production and to produce NO for use in cell signaling. Upon cell stimulation with pro-inflammatory signals such as LPS + IFN- γ , cNOS is downregulated and iNOS levels increase as the cell gets set to increase NO production [134]. This lag between cNOS downregulation and increase in iNOS expression is evident in the uninfected LPS + IFN- γ treated BMDCs, where NO production does not begin to increase until 4 hours post treatment when iNOS levels should be increasing (Figure 15). This lag is also seen after infection of immature DCs with live *M. tuberculosis* + IFN- γ , where some untreated BMDCs initially lose their capacity to respond to the bacilli, but after 24 hours their capacity to produce NO returns. The ability of pretreatment with ManLAM to prevent this rebound in NO production in response to infection implies a role for the lipoglycan in modulating iNOS expression or function within *M. tuberculosis* infected BMDCs.

Since ManLAM has been shown to be secreted from *M. tuberculosis* infected MOs and is present within the extracellular regions of the lung, it can interact with

migrating host DCs, pushing them into this modified state of responsiveness [58, 135]. These DCs may then be unable to produce a full NO burst in response to the bacilli, further limiting their antimicrobial capacity after infection. DCs have been shown to be a reservoir for persisting bacilli, unable to fully eliminate the intracellular pathogen [38]. ManLAM induced reduction in NO expression may be a key factor, as low levels of NO have been shown to induce the DosR regulon, which activates genes that lead *M. tuberculosis* into a state of anaerobic slow replication [99]. It is within this slowly metabolic “dormant” state that they can remain within the host, avoiding the antimicrobial machinery, but still capable of reactivating and spreading when the conditions are right [50]. Much work still needs to be done in regards to bacterial growth inhibition, survival and persistence, but the ManLAM induced depression of NO within BMDCs may be a contributing factor to the inability of the host to maintain an effective immune response and clear the invading *M. tuberculosis* bacilli.

Chapter 5: Conclusion

	Untreated	ManLAM	LPS
Morphology	-	-	++
Phagocytic Capacity	-	+	++
CD4+ T-cell Stimulation	-	-	++
IL-10 Secretion	-	-	+
Intracellular IL-10	-	++	+
<i>In Vivo</i> IL-10	+	++	NA
NO Production Pre-Infection	+ (with IFN- γ)	-	++
NO Production Post-Infection	+ (with IFN- γ)	-	++

Figure 19: Summary of Results

In the table above (-) signs indicate no change or no increase, (+) signs indicate a small increase or a slight change and (++) signs indicate a large increase or change. LPS treatment of BMDCs is able to activate the cells leading to upregulation of MHC class II and CD1d, CD4+ T-cell proliferation, the release of moderate amounts of IL-10 and an increase in NO production both pre and post-infection with *M. tuberculosis*. By comparison ManLAM treated BMDCs are unable to fully mature, exhibit impaired phagocytic capacity, do not stimulate CD4+ T-cell proliferation, produce high levels of intracellular IL-10 *in vitro* and increase IL-10 production within the lungs *in vivo*. Additionally ManLAM treated BMDCs show an impaired NO response, both pre and post-infection with *M. tuberculosis*.

5.1 *M. tuberculosis* Infection, ManLAM and the Dendritic Cell

The *M. tuberculosis* bacterium is the causative agent of tuberculosis disease. At present *M. tuberculosis* infects nearly a third of the world's population and kills more than 1.5 million people a year. This scenario underscores the importance for a better understanding of the immunopathogenesis of the infection and how to prevent the disease [1]. Despite the fact that many people are capable of controlling the infection to a point where the number of bacilli are reduced to very low levels, the ability of these few bacilli to persist and await an opportune moment to reactivate and spread is a major issue [24, 135]. Previously the young and elderly were the most susceptible to the disease, but with

the recent emergence of HIV infections and its ability to suppress the immune response, the prevalence of tuberculosis cases within all age groups has risen [1]. While newer and better drugs and vaccines are needed to help fight the disease, understanding why the host is unable to eliminate the remaining few bacilli is a necessary step in creating better treatments against the disease. The bacilli persists within macrophages (MOs), dendritic cells (DCs) and epithelial cells [2], thus analyzing how the persisting bacilli evade clearance within these cells is key to understanding how to target the low numbers of latent bacilli within the host.

The DC is the major link between the innate and adaptive immune responses. DCs process pathogens and associated antigens for presentation to T and B-cells [101]. *M. tuberculosis* also infects DCs at a high rate [26] and it is known that the bacterium has the capacity to modulate the maturation process of DCs [26, 33, 78, 105]. Thus it is believed that DCs may play a key role in the inability of the host to completely eliminate the *M. tuberculosis* infection. Previous work reported that the prominent cell wall lipoglycan ManLAM has various immunomodulatory functions [3, 5, 23, 53] and may interfere with DC function. Additionally, it is also known that ManLAM shares many structural similarities with bacterial LPS [55], a well characterized potent activator of the immune response. Altogether this allows us to hypothesize that ManLAM plays a role in the immune response against *M. tuberculosis*. This study aimed to understand the ability of ManLAM to alter immune functions associated with bone marrow derived DCs (BMDCs). Furthermore we also studied how ManLAM was able to modulate expression of the cytokine IL-10 within specific cells within the lungs of mice.

5.2 Analyzing Dendritic Cell Maturation in Response to ManLAM

The ability of ManLAM to modulate the expression of many activation markers on DCs has been studied and previously discussed within this manuscript (Chapter 1.8: Dendritic Cell Response to *M. tuberculosis* and ManLAM). We show that in our model system ManLAM is unable to induce the phenotypic changes associated with the maturation process BMDCs (Figure 2), including upregulation of expression of both MHC class II and CD1d molecules on these cells (Figure 3). These two cell surface molecules are crucial in the presentation of antigens to CD4⁺ and CD8⁺ T-cells respectively, although MHC class II presentation to CD4⁺ T-cells represents the most important immune event against infection with *M. tuberculosis* [16]. Even though ManLAM treated DCs show changes in their phagocytic capacity (Figure 4) and the capacity to respond to certain costimuli, they do not appear to fully mature into DCs capable of presenting antigen and stimulating T-cell responses necessary for complete activation of the adaptive immune response.

Here we have shown that ManLAM stimulated BMDCs are unable to induce the proliferation of naïve CD4⁺ T-cells (Figure 6). This downstream effect of BMDC stimulation with ManLAM could be a major dysfunction in the host's response to infection, as many reports have shown that the depletion of CD4⁺ T-cells leads to survival and spread of the bacilli [136]. A previous report demonstrated that ManLAM stimulated DCs were capable of expanding memory CD8⁺ T-cells, but were incapable of inducing naïve CD8⁺ T-cell proliferation [79]. While CD8⁺ T-cells play a role in the response to *M. tuberculosis*, the IFN- γ producing CD4⁺ T-cell response is essential for controlling the infection. The *in vivo* application of these *in vitro* functional changes still

needs to be evaluated, though the ability of purified ManLAM in the absence of additional costimulants or cytokine factors to modulate DC functionality highlights the need for further examination within this field.

5.3 ManLAM Induced IL-10 Modulation of Dendritic Cells

The anti-inflammatory cytokine IL-10 is a common inhibitor of DC responses, and has been shown to skew DCs toward a Th2 phenotype [115]. IL-10 production within alveolar phagocytes has been reported during infection with *M. tuberculosis* [46]; leading to the hypothesis that IL-10 production within DCs during infection may serve to downregulate DC functions. Several studies have provided evidence that ManLAM stimulation of DCs is capable of synergizing with a TLR-4 signal provided by LPS and that this interaction significantly upregulates IL-10 secretion [6, 7]. Within Chapter 3 of this study we further extended this idea, showing that immature BMDCs stimulated with ManLAM alone are capable of producing high levels of intracellular IL-10, but without the additional costimuli present in the previous papers secreted only a small amount of IL-10 (Figure 7). The increased amount of intracellular IL-10 and concurrent low level of IL-12 [79, 137] produced from BMDCs stimulated with ManLAM could contribute to the inability of these cells to fully mature and activate naïve T-cells.

Several groups have examined the effects of intrapulmonary delivery of LPS on lung pathology and the immunological response; however very few studies have looked at the direct effects of ManLAM on the lungs [5, 119]. Thus, the next question in our studies was to determine if ManLAM was also able to stimulate intracellular IL-10 in the lungs. To demonstrate this we utilized an intrapulmonary delivery system to specifically

target ManLAM into the lungs of naïve mice. When we examined the lungs of mice treated three times over the course of a week with different concentrations of ManLAM very little pathology was seen. There was only a slight thickening of the bronchial walls and no significant influx of cells seven days after the start of treatment. In line with these observations, no global changes were seen in the total production of the cytokines IFN- γ , TGF- β and IL-10 (Figure 9 and unpublished data).

Despite these other observations, there were IL-10 positive cells scattered throughout the tissue. Mice treated three times with 10 μ g, 20 μ g or 40 μ g of ManLAM had the highest expression of intracellular IL-10 within positive cells in the lung parenchyma (Figure 10). IL-10 is also found in alveolar phagocytes within the steady state lung environment, though at a lower level. A majority of these intensely IL-10 positive cells exhibited MO or DC like morphology and localization (Figure 11). IL-10 positive cells resided throughout the lungs in all treatment groups being found within the alveoli, parenchyma and vessels. In mice treated with 20 μ g or 40 μ g of ManLAM a significant increase was also seen in the number of IL-10 positive cells found within the pulmonary vessels indicating these cells were in the process of migrating (Figure 12).

Many reports have shown a role for IL-10 in the creation of DCs with regulatory properties [86, 106, 115, 138]. In addition to the ability of IL-10 to downregulate MHC class II expression [115] and to block IFN- γ and TNF- α expression [47], IL-10 is capable of pushing DCs into a state where they preferentially prime T-cells exhibiting anti-inflammatory properties. It has even been shown that once DCs possess this regulatory phenotype, normal pro-inflammatory activation signals such as LPS and CpG oligonucleotides are also affected [86]. Thus, free ManLAM secreted from infected MOs

and shed from dying bacilli may be capable of interacting with DCs *in vivo* and stimulating intracellular IL-10 production. These IL-10 producing DCs become a population of cells with an immature regulatory phenotype, incapable of priming the inflammatory response, but capable of priming Th2 and Treg cells, which further suppresses the host's immune response to the bacilli before the bacteria are completely eliminated. Additional studies are needed to better understand the role of ManLAM modulation of DCs and the ability of IL-10 to modify infection with *M. tuberculosis*.

Future research will aim to gain a better understanding of how the intrapulmonary delivery of ManLAM modifies the host immune response *in vivo*. Specifically, looking at the effect of ManLAM on IL-10 expression within the lungs beyond the one week treatment regimen analyzed within the experiments reported in Chapter 3. Extending these studies further into the examination of whether intrapulmonary ManLAM treatment modulates cell populations and cytokine production within the draining lymph nodes and the spleen. The next step would be to determine if intrapulmonary ManLAM delivery affects the host's ability to respond to an aerosol challenge with live *M. tuberculosis*.

5.4 Nitric Oxide Expression of ManLAM Treated Dendritic Cells

One of the affects that IL-10 has on DCs is downregulation of the expression of or sensitivity to IFN- γ and TNF- α [47], two cytokines essential to activating pro-inflammatory and antimicrobial functions during the host response to *M. tuberculosis* infection [10, 16, 24, 30]. IFN- γ and TNF- α are both activators of iNOS expression within MOs and DCs, leading to increased production of antimicrobial NO, a free radical

with potent capacity to inhibit the growth of *M. tuberculosis* [16, 24, 44]. Thus we examined whether the treatment of BMDCs with ManLAM and subsequent expression of IL-10 affected the ability of BMDCs to upregulate NO production both in response to purified lipoglycan molecules and in response to live *M. tuberculosis*. To analyze the production of reactive nitrogen intermediates (RNIs) we used the intracellular dye DAF-FM diacetate. The dye offered the advantages of single cell analysis and the ability to measure intracellular RNI production, where the standard method of analyzing NO levels, the Griess Reagent, measures soluble NO levels in the supernatant. It is believed that most latent *M. tuberculosis* bacilli remain as an intracellular bacterium, therefore the intracellular levels of NO are critical to the ability of phagocytes to regulate intracellular growth of the bacilli.

As hypothesized, stimulation of BMDCs with ManLAM led to depressed amounts of intracellular NO even in the presence of IFN- γ , while LPS + IFN- γ led to an increase in intracellular NO production (Figure 15). This result differs from what has been reported for ManLAM + IFN- γ stimulation of MOs *in vitro*. Papers by Adams et al and Chan et al reported that ManLAM was capable of inducing a slight increase in NO production from MOs, though they both measured NO₂⁻ levels in the culture supernatants [127, 129], not intracellular expression. The inability of ManLAM to upregulate intracellular NO also applied when BMDCs pretreated with ManLAM were infected with live *M. tuberculosis*. BMDCs that were not pretreated showed a slight increase in NO production 24 hours after infection, while LPS activated BMDC samples showed a much larger increase in the intracellular amount of NO in response to live *M. tuberculosis*. ManLAM pretreated BMDCs showed both a reduced number of cells expressing NO and

a reduction in the amount of intracellular NO produced in response to infection, further showing that ManLAM is capable of modulating the ability of the DC to respond to *M. tuberculosis* infection (Figure 18).

Previous reports have shown that NO produced by DCs infected with *M. tuberculosis* is more bacteriostatic than bactericidal, meaning the bacilli are not killed, but their intracellular growth is inhibited [31]. Low levels of NO have also been shown to upregulate dormancy genes within the bacilli, causing the bacteria to slow its growth and enter a reversible state of dormancy within its environment [99]. This induced dormancy coupled with the downregulation of the host's antimicrobial capacity could contribute to the onset of latent infection and incomplete clearance. We found that ManLAM stimulation of BMDC cultures leads to decreased expression of NO within BMDCs. Reduced NO expression by host DCs in response to ManLAM may be brought on by the simultaneous expression of IL-10 within these cells. The results published within this manuscript only scratch the surface of what needs to be examined in regards to ManLAM's capacity to modulate NO production and whether IL-10 is the key factor in this inhibition.

Future experiments will concentrate on examining the NO kinetics at extended time points after treatment and infection, focusing on the changes in both intracellular and extracellular NO expression, and looking at bacterial survival within the different treatment groups. While the analysis of intracellular NO at the single cell level is a very important tool, examination of extracellular levels of NO is also an important piece of information to understanding the functions of NO expression in response to the various stimuli. Another important experiment would be to utilize BMDCs from IL-10 knockout

mice and IL-10 overexpressing mice to analyze whether the removal or drastic increase in IL-10 is capable of further manipulating the NO expression in response to ManLAM. These experiments would further tie together the role of ManLAM in producing IL-10 and its ability to regulate NO expression within DCs.

References

1. WHO. *World Health Organization*. 2009 [cited 2009; Available from: <http://www.who.int/topics/tuberculosis/en/>.
2. Tufariello, J.M., J. Chan, and J.L. Flynn, *Latent tuberculosis: mechanisms of host and bacillus that contribute to persistent infection*. *Lancet Infect Dis*, 2003. **3**(9): p. 578-90.
3. Jozefowski, S., A. Sobota, and K. Kwiatkowska, *How Mycobacterium tuberculosis subverts host immune responses*. *Bioessays*, 2008. **30**(10): p. 943-54.
4. Pitarque, S., et al., *Deciphering the molecular bases of Mycobacterium tuberculosis binding to the lectin DC-SIGN reveals an underestimated complexity*. *Biochem J*, 2005. **392**(Pt 3): p. 615-24.
5. Strohmeier, G.R. and M.J. Fenton, *Roles of lipoarabinomannan in the pathogenesis of tuberculosis*. *Microbes Infect*, 1999. **1**(9): p. 709-17.
6. Chieppa, M., et al., *Cross-linking of the mannose receptor on monocyte-derived dendritic cells activates an anti-inflammatory immunosuppressive program*. *J Immunol*, 2003. **171**(9): p. 4552-60.
7. Geijtenbeek, T.B., et al., *Mycobacteria target DC-SIGN to suppress dendritic cell function*. *J Exp Med*, 2003. **197**(1): p. 7-17.
8. Pompei, L., et al., *Disparity in IL-12 release in dendritic cells and macrophages in response to Mycobacterium tuberculosis is due to use of distinct TLRs*. *J Immunol*, 2007. **178**(8): p. 5192-9.
9. NJMS, N.T.C. *A Brief History of Tuberculosis*. 1996 [cited 2009; Available from: <http://www.umdj.edu/~ntbcweb/history.htm>.
10. Orme, I.M., *Immunity to Mycobacteria*. 1995, Austin, TX: Landes Company.
11. Wang, J. and Z. Xing, *Tuberculosis vaccines: the past, present and future*. *Expert Rev Vaccines*, 2002. **1**(3): p. 341-54.
12. Rook, G.A., G. Seah, and A. Ustianowski, *M. tuberculosis: immunology and vaccination*. *Eur Respir J*, 2001. **17**(3): p. 537-57.
13. Mitsuyama, M. and D.N. McMurray, *Tuberculosis: vaccine and drug development*. *Tuberculosis (Edinb)*, 2007. **87 Suppl 1**: p. S10-3.
14. Dye, C., *Doomsday postponed? Preventing and reversing epidemics of drug-resistant tuberculosis*. *Nat Rev Microbiol*, 2009. **7**(1): p. 81-7.
15. Singh, J.A., R. Upshur, and N. Padayatchi, *XDR-TB in South Africa: no time for denial or complacency*. *PLoS Med*, 2007. **4**(1): p. e50.
16. Raja, A., *Immunology of tuberculosis*. *Indian J Med Res*, 2004. **120**(4): p. 213-32.
17. Dharmadhikari, A.S. and E.A. Nardell, *What animal models teach humans about tuberculosis*. *Am J Respir Cell Mol Biol*, 2008. **39**(5): p. 503-8.
18. Rhoades, E.R., A.A. Frank, and I.M. Orme, *Progression of chronic pulmonary tuberculosis in mice aerogenically infected with virulent Mycobacterium tuberculosis*. *Tuber Lung Dis*, 1997. **78**(1): p. 57-66.
19. Orme, I.M., *The mouse as a useful model of tuberculosis*. *Tuberculosis (Edinb)*, 2003. **83**(1-3): p. 112-5.
20. Dannenberg, A.M., *Pathogenesis of human pulmonary tuberculosis. Insight from the rabbit model*. 2006, ASM Press: Washington DC.

21. Turner, O.C., R.J. Basaraba, and I.M. Orme, *Immunopathogenesis of pulmonary granulomas in the guinea pig after infection with Mycobacterium tuberculosis*. Infect Immun, 2003. **71**(2): p. 864-71.
22. Walsh, G.P., et al., *The Philippine cynomolgus monkey (Macaca fascicularis) provides a new nonhuman primate model of tuberculosis that resembles human disease*. Nat Med, 1996. **2**(4): p. 430-6.
23. Chan, J., et al., *Lipoarabinomannan, a possible virulence factor involved in persistence of Mycobacterium tuberculosis within macrophages*. Infect Immun, 1991. **59**(5): p. 1755-61.
24. Flynn, J.L. and J. Chan, *Immunology of tuberculosis*. Annu Rev Immunol, 2001. **19**: p. 93-129.
25. Kaufmann, S.H. and A.J. McMichael, *Annulling a dangerous liaison: vaccination strategies against AIDS and tuberculosis*. Nat Med, 2005. **11**(4 Suppl): p. S33-44.
26. Wolf, A.J., et al., *Mycobacterium tuberculosis infects dendritic cells with high frequency and impairs their function in vivo*. J Immunol, 2007. **179**(4): p. 2509-19.
27. Gonzalez-Juarrero, M., et al., *Dynamics of macrophage cell populations during murine pulmonary tuberculosis*. J Immunol, 2003. **171**(6): p. 3128-35.
28. Bhatt, K. and P. Salgame, *Host innate immune response to Mycobacterium tuberculosis*. J Clin Immunol, 2007. **27**(4): p. 347-62.
29. Bermudez, L.E. and L.S. Young, *Natural killer cell-dependent mycobacteriostatic and mycobactericidal activity in human macrophages*. J Immunol, 1991. **146**(1): p. 265-70.
30. North, R.J. and Y.J. Jung, *Immunity to tuberculosis*. Annu Rev Immunol, 2004. **22**: p. 599-623.
31. Bodnar, K.A., N.V. Serbina, and J.L. Flynn, *Fate of Mycobacterium tuberculosis within murine dendritic cells*. Infect Immun, 2001. **69**(2): p. 800-9.
32. Mogues, T., et al., *The relative importance of T cell subsets in immunity and immunopathology of airborne Mycobacterium tuberculosis infection in mice*. J Exp Med, 2001. **193**(3): p. 271-80.
33. Henderson, R.A., S.C. Watkins, and J.L. Flynn, *Activation of human dendritic cells following infection with Mycobacterium tuberculosis*. J Immunol, 1997. **159**(2): p. 635-43.
34. Granucci, F., et al., *Early events in dendritic cell maturation induced by LPS*. Microbes Infect, 1999. **1**(13): p. 1079-84.
35. Flynn, J.L., et al., *Tumor necrosis factor-alpha is required in the protective immune response against Mycobacterium tuberculosis in mice*. Immunity, 1995. **2**(6): p. 561-72.
36. Feng, C.G., et al., *Increase in gamma interferon-secreting CD8(+), as well as CD4(+), T cells in lungs following aerosol infection with Mycobacterium tuberculosis*. Infect Immun, 1999. **67**(7): p. 3242-7.
37. Serbina, N.V., et al., *CD8+ CTL from lungs of Mycobacterium tuberculosis-infected mice express perforin in vivo and lyse infected macrophages*. J Immunol, 2000. **165**(1): p. 353-63.

38. Chan ED, C.J., Schluger NW, *What is the Role of Nitric Oxide in Murine and Human Host Defense against Mycobacterium tuberculosis?* American Journal of Respiratory Cell and Molecular Biology, 2001. **25**: p. 606-612.
39. Klingler, K., et al., *Effects of mycobacteria on regulation of apoptosis in mononuclear phagocytes.* Infect Immun, 1997. **65**(12): p. 5272-8.
40. Cardona, P.J., *New insights on the nature of latent tuberculosis infection and its treatment.* Inflamm Allergy Drug Targets, 2007. **6**(1): p. 27-39.
41. Peyron, P., et al., *Foamy macrophages from tuberculous patients' granulomas constitute a nutrient-rich reservoir for M. tuberculosis persistence.* PLoS Pathog, 2008. **4**(11): p. e1000204.
42. Cunningham, A.F. and C.L. Spreadbury, *Mycobacterial stationary phase induced by low oxygen tension: cell wall thickening and localization of the 16-kilodalton alpha-crystallin homolog.* J Bacteriol, 1998. **180**(4): p. 801-8.
43. Li, M.O. and R.A. Flavell, *Contextual regulation of inflammation: a duet by transforming growth factor-beta and interleukin-10.* Immunity, 2008. **28**(4): p. 468-76.
44. Ding, A., et al., *Macrophage deactivating factor and transforming growth factors-beta 1 -beta 2 and -beta 3 inhibit induction of macrophage nitrogen oxide synthesis by IFN-gamma.* J Immunol, 1990. **145**(3): p. 940-4.
45. Rojas, R.E., et al., *Regulation of human CD4(+) alphabeta T-cell-receptor-positive (TCR(+)) and gammadelta TCR(+) T-cell responses to Mycobacterium tuberculosis by interleukin-10 and transforming growth factor beta.* Infect Immun, 1999. **67**(12): p. 6461-72.
46. Turner, J., et al., *In vivo IL-10 production reactivates chronic pulmonary tuberculosis in C57BL/6 mice.* J Immunol, 2002. **169**(11): p. 6343-51.
47. Moore, K.W., et al., *Interleukin-10 and the interleukin-10 receptor.* Annu Rev Immunol, 2001. **19**: p. 683-765.
48. Russell, D.G., et al., *Why intracellular parasitism need not be a degrading experience for Mycobacterium.* Philos Trans R Soc Lond B Biol Sci, 1997. **352**(1359): p. 1303-10.
49. Deretic, V., et al., *Mycobacterium tuberculosis inhibition of phagolysosome biogenesis and autophagy as a host defence mechanism.* Cell Microbiol, 2006. **8**(5): p. 719-27.
50. Wayne, L.G. and C.D. Sohaskey, *Nonreplicating persistence of mycobacterium tuberculosis.* Annu Rev Microbiol, 2001. **55**: p. 139-63.
51. Daffe, M. and G. Etienne, *The capsule of Mycobacterium tuberculosis and its implications for pathogenicity.* Tuber Lung Dis, 1999. **79**(3): p. 153-69.
52. Brennan, P.J. and H. Nikaido, *The envelope of mycobacteria.* Annu Rev Biochem, 1995. **64**: p. 29-63.
53. Brennan, P.J., *Structure, function, and biogenesis of the cell wall of Mycobacterium tuberculosis.* Tuberculosis (Edinb), 2003. **83**(1-3): p. 91-7.
54. Haeffner-Cavaillon, N., et al., *Molecular aspects of endotoxins relevant to their biological functions.* Nephrol Dial Transplant, 1999. **14**(4): p. 853-60.
55. Savedra, R., Jr., et al., *Mycobacterial lipoarabinomannan recognition requires a receptor that shares components of the endotoxin signaling system.* J Immunol, 1996. **157**(6): p. 2549-54.

56. Park, S.H. and A. Bendelac, *CD1-restricted T-cell responses and microbial infection*. *Nature*, 2000. **406**(6797): p. 788-92.
57. Briken, V., et al., *Mycobacterial lipoarabinomannan and related lipoglycans: from biogenesis to modulation of the immune response*. *Mol Microbiol*, 2004. **53**(2): p. 391-403.
58. Beatty, W.L., et al., *Trafficking and release of mycobacterial lipids from infected macrophages*. *Traffic*, 2000. **1**(3): p. 235-47.
59. Fratti, R.A., et al., *Mycobacterium tuberculosis glycosylated phosphatidylinositol causes phagosome maturation arrest*. *Proc Natl Acad Sci U S A*, 2003. **100**(9): p. 5437-42.
60. Berman, J.S., et al., *Chemotactic activity of mycobacterial lipoarabinomannans for human blood T lymphocytes in vitro*. *J Immunol*, 1996. **156**(10): p. 3828-35.
61. Abel, B., et al., *Toll-like receptor 4 expression is required to control chronic Mycobacterium tuberculosis infection in mice*. *J Immunol*, 2002. **169**(6): p. 3155-62.
62. Drennan, M.B., et al., *Toll-like receptor 2-deficient mice succumb to Mycobacterium tuberculosis infection*. *Am J Pathol*, 2004. **164**(1): p. 49-57.
63. Takeda, K., T. Kaisho, and S. Akira, *Toll-like receptors*. *Annu Rev Immunol*, 2003. **21**: p. 335-76.
64. Quesniaux, V.J., et al., *Toll-like receptor 2 (TLR2)-dependent-positive and TLR2-independent-negative regulation of proinflammatory cytokines by mycobacterial lipomannans*. *J Immunol*, 2004. **172**(7): p. 4425-34.
65. Dillon, S., et al., *A Toll-like receptor 2 ligand stimulates Th2 responses in vivo, via induction of extracellular signal-regulated kinase mitogen-activated protein kinase and c-Fos in dendritic cells*. *J Immunol*, 2004. **172**(8): p. 4733-43.
66. Yu, W., et al., *Soluble CD14(1-152) confers responsiveness to both lipoarabinomannan and lipopolysaccharide in a novel HL-60 cell bioassay*. *J Immunol*, 1998. **161**(8): p. 4244-51.
67. Ilangumaran, S., et al., *Integration of mycobacterial lipoarabinomannans into glycosylphosphatidylinositol-rich domains of lymphomonocytic cell plasma membranes*. *J Immunol*, 1995. **155**(3): p. 1334-42.
68. Heldwein, K.A. and M.J. Fenton, *The role of Toll-like receptors in immunity against mycobacterial infection*. *Microbes Infect*, 2002. **4**(9): p. 937-44.
69. Figdor, C.G., Y. van Kooyk, and G.J. Adema, *C-type lectin receptors on dendritic cells and Langerhans cells*. *Nat Rev Immunol*, 2002. **2**(2): p. 77-84.
70. East, L. and C.M. Isacke, *The mannose receptor family*. *Biochim Biophys Acta*, 2002. **1572**(2-3): p. 364-86.
71. Geijtenbeek, T.B., et al., *Identification of DC-SIGN, a novel dendritic cell-specific ICAM-3 receptor that supports primary immune responses*. *Cell*, 2000. **100**(5): p. 575-85.
72. van Kooyk, Y. and T.B. Geijtenbeek, *DC-SIGN: escape mechanism for pathogens*. *Nat Rev Immunol*, 2003. **3**(9): p. 697-709.
73. Geijtenbeek, T.B., et al., *DC-SIGN-ICAM-2 interaction mediates dendritic cell trafficking*. *Nat Immunol*, 2000. **1**(4): p. 353-7.

74. van Vliet, S.J., J.J. Garcia-Vallejo, and Y. van Kooyk, *Dendritic cells and C-type lectin receptors: coupling innate to adaptive immune responses*. Immunol Cell Biol, 2008. **86**(7): p. 580-7.
75. den Dunnen J, G.S., Geijtenbeek TB, *Innate signaling by the C-type lectin DC-SIGN dictates immune responses*. Cancer Immunology, Immunotherapy, 2008.
76. Zhou, T., et al., *DC-SIGN and immunoregulation*. Cell Mol Immunol, 2006. **3**(4): p. 279-83.
77. Gringhuis, S.I., et al., *C-type lectin DC-SIGN modulates Toll-like receptor signaling via Raf-1 kinase-dependent acetylation of transcription factor NF-kappaB*. Immunity, 2007. **26**(5): p. 605-16.
78. Mariotti, S., et al., *Mycobacterium tuberculosis subverts the differentiation of human monocytes into dendritic cells*. Eur J Immunol, 2002. **32**(11): p. 3050-8.
79. Dulphy, N., et al., *Intermediate maturation of Mycobacterium tuberculosis LAM-activated human dendritic cells*. Cell Microbiol, 2007. **9**(6): p. 1412-25.
80. Toossi, Z., et al., *Enhanced production of TGF-beta by blood monocytes from patients with active tuberculosis and presence of TGF-beta in tuberculous granulomatous lung lesions*. J Immunol, 1995. **154**(1): p. 465-73.
81. Dahl, K.E., et al., *Selective induction of transforming growth factor beta in human monocytes by lipoarabinomannan of Mycobacterium tuberculosis*. Infect Immun, 1996. **64**(2): p. 399-405.
82. Higgins, D.M., et al., *Lack of IL-10 alters inflammatory and immune responses during pulmonary Mycobacterium tuberculosis infection*. Tuberculosis (Edinb), 2009.
83. Jung, Y.J., et al., *Increased interleukin-10 expression is not responsible for failure of T helper 1 immunity to resolve airborne Mycobacterium tuberculosis infection in mice*. Immunology, 2003. **109**(2): p. 295-9.
84. Shaw, T.C., L.H. Thomas, and J.S. Friedland, *Regulation of IL-10 secretion after phagocytosis of Mycobacterium tuberculosis by human monocytic cells*. Cytokine, 2000. **12**(5): p. 483-6.
85. Ureta, G., et al., *Generation of dendritic cells with regulatory properties*. Transplant Proc, 2007. **39**(3): p. 633-7.
86. Wakkach, A., et al., *Characterization of dendritic cells that induce tolerance and T regulatory 1 cell differentiation in vivo*. Immunity, 2003. **18**(5): p. 605-17.
87. Adams, L.B., et al., *Comparison of the roles of reactive oxygen and nitrogen intermediates in the host response to Mycobacterium tuberculosis using transgenic mice*. Tuber Lung Dis, 1997. **78**(5-6): p. 237-46.
88. Lau, Y.L., et al., *The role of phagocytic respiratory burst in host defense against Mycobacterium tuberculosis*. Clin Infect Dis, 1998. **26**(1): p. 226-7.
89. Jones, G.S., H.J. Amirault, and B.R. Andersen, *Killing of Mycobacterium tuberculosis by neutrophils: a nonoxidative process*. J Infect Dis, 1990. **162**(3): p. 700-4.
90. Nicholson, S., et al., *Inducible nitric oxide synthase in pulmonary alveolar macrophages from patients with tuberculosis*. J Exp Med, 1996. **183**(5): p. 2293-302.
91. Rich, E.A., et al., *Mycobacterium tuberculosis (MTB)-stimulated production of nitric oxide by human alveolar macrophages and relationship of nitric oxide*

- production to growth inhibition of MTB. Tuber Lung Dis, 1997. 78(5-6): p. 247-55.*
92. Roach, T.I., et al., *Opposing effects of interferon-gamma on iNOS and interleukin-10 expression in lipopolysaccharide- and mycobacterial lipoarabinomannan-stimulated macrophages.* Immunology, 1995. **85**(1): p. 106-13.
 93. Rockett, K.A., et al., *1,25-Dihydroxyvitamin D3 induces nitric oxide synthase and suppresses growth of Mycobacterium tuberculosis in a human macrophage-like cell line.* Infect Immun, 1998. **66**(11): p. 5314-21.
 94. Long, R., B. Light, and J.A. Talbot, *Mycobacteriocidal action of exogenous nitric oxide.* Antimicrob Agents Chemother, 1999. **43**(2): p. 403-5.
 95. Wang, C.H., et al., *Upregulation of inducible nitric oxide synthase and cytokine secretion in peripheral blood monocytes from pulmonary tuberculosis patients.* Int J Tuberc Lung Dis, 2001. **5**(3): p. 283-91.
 96. Chan, J., et al., *Killing of virulent Mycobacterium tuberculosis by reactive nitrogen intermediates produced by activated murine macrophages.* J Exp Med, 1992. **175**(4): p. 1111-22.
 97. Chatterjee, D., et al., *Structural basis of capacity of lipoarabinomannan to induce secretion of tumor necrosis factor.* Infect Immun, 1992. **60**(3): p. 1249-53.
 98. Chen, L., Q.W. Xie, and C. Nathan, *Alkyl hydroperoxide reductase subunit C (AhpC) protects bacterial and human cells against reactive nitrogen intermediates.* Mol Cell, 1998. **1**(6): p. 795-805.
 99. Voskuil, M.I., et al., *Inhibition of respiration by nitric oxide induces a Mycobacterium tuberculosis dormancy program.* J Exp Med, 2003. **198**(5): p. 705-13.
 100. Vermaelen, K. and R. Pauwels, *Pulmonary dendritic cells.* Am J Respir Crit Care Med, 2005. **172**(5): p. 530-51.
 101. Wan, H. and M. Dupasquier, *Dendritic cells in vivo and in vitro.* Cell Mol Immunol, 2005. **2**(1): p. 28-35.
 102. Gonzalez-Juarrero, M. and I.M. Orme, *Characterization of murine lung dendritic cells infected with Mycobacterium tuberculosis.* Infect Immun, 2001. **69**(2): p. 1127-33.
 103. Latchumanan, V.K., et al., *Mycobacterium tuberculosis antigens induce the differentiation of dendritic cells from bone marrow.* J Immunol, 2002. **169**(12): p. 6856-64.
 104. Rajashree, P. and S.D. Das, *Infection with prevalent clinical strains of Mycobacterium tuberculosis leads to differential maturation of monocyte derived dendritic cells.* Immunol Lett, 2008. **117**(2): p. 174-80.
 105. Rajashree, P., G. Krishnan, and S.D. Das, *Impaired phenotype and function of monocyte derived dendritic cells in pulmonary tuberculosis.* Tuberculosis (Edinb), 2009. **89**(1): p. 77-83.
 106. Steinbrink, K., et al., *Induction of tolerance by IL-10-treated dendritic cells.* J Immunol, 1997. **159**(10): p. 4772-80.
 107. Buettner, M., et al., *Inverse correlation of maturity and antibacterial activity in human dendritic cells.* J Immunol, 2005. **174**(7): p. 4203-9.

108. Conti, L. and S. Gessani, *GM-CSF in the generation of dendritic cells from human blood monocyte precursors: recent advances*. Immunobiology, 2008. **213**(9-10): p. 859-70.
109. Kindt TJ, G.R., Osborne BA, Kuby J, *Immunology*. 5th ed. 2006: WH Freeman.
110. Chen, J.C., M.L. Chang, and M.O. Muench, *A kinetic study of the murine mixed lymphocyte reaction by 5,6-carboxyfluorescein diacetate succinimidyl ester labeling*. J Immunol Methods, 2003. **279**(1-2): p. 123-33.
111. Satthaporn, S. and O. Eremin, *Dendritic cells (I): Biological functions*. J R Coll Surg Edinb, 2001. **46**(1): p. 9-19.
112. Fortsch, D., M. Rollinghoff, and S. Stenger, *IL-10 converts human dendritic cells into macrophage-like cells with increased antibacterial activity against virulent Mycobacterium tuberculosis*. J Immunol, 2000. **165**(2): p. 978-87.
113. de Waal Malefyt, R., et al., *Interleukin 10 (IL-10) and viral IL-10 strongly reduce antigen-specific human T cell proliferation by diminishing the antigen-presenting capacity of monocytes via downregulation of class II major histocompatibility complex expression*. J Exp Med, 1991. **174**(4): p. 915-24.
114. Ding, L., et al., *IL-10 inhibits macrophage costimulatory activity by selectively inhibiting the up-regulation of B7 expression*. J Immunol, 1993. **151**(3): p. 1224-34.
115. De Smedt, T., et al., *Effect of interleukin-10 on dendritic cell maturation and function*. Eur J Immunol, 1997. **27**(5): p. 1229-35.
116. Hickman, S.P., J. Chan, and P. Salgame, *Mycobacterium tuberculosis induces differential cytokine production from dendritic cells and macrophages with divergent effects on naive T cell polarization*. J Immunol, 2002. **168**(9): p. 4636-42.
117. Jang, S., et al., *IL-6 and IL-10 induction from dendritic cells in response to Mycobacterium tuberculosis is predominantly dependent on TLR2-mediated recognition*. J Immunol, 2004. **173**(5): p. 3392-7.
118. Hirsch, C.S., et al., *Depressed T-cell interferon-gamma responses in pulmonary tuberculosis: analysis of underlying mechanisms and modulation with therapy*. J Infect Dis, 1999. **180**(6): p. 2069-73.
119. Juffermans, N.P., et al., *Mycobacterial lipoarabinomannan induces an inflammatory response in the mouse lung. A role for interleukin-1*. Am J Respir Crit Care Med, 2000. **162**(2 Pt 1): p. 486-9.
120. Feng, C.G., et al., *Transgenic mice expressing human interleukin-10 in the antigen-presenting cell compartment show increased susceptibility to infection with Mycobacterium avium associated with decreased macrophage effector function and apoptosis*. Infect Immun, 2002. **70**(12): p. 6672-9.
121. Bogdan, C., *Nitric oxide and the immune response*. Nat Immunol, 2001. **2**(10): p. 907-16.
122. Rettori, V., et al., *Nitric oxide at the crossroad of immunoneuroendocrine interactions*. Ann N Y Acad Sci, 2009. **1153**: p. 35-47.
123. Lacza, Z., et al., *The novel red-fluorescent probe DAR-4M measures reactive nitrogen species rather than NO*. J Pharmacol Toxicol Methods, 2005. **52**(3): p. 335-40.

124. Mannick, J.B., *Immunoregulatory and antimicrobial effects of nitrogen oxides*. Proc Am Thorac Soc, 2006. **3**(2): p. 161-5.
125. Selvaraj, P., et al., *Hydrogen peroxide producing potential of alveolar macrophages & blood monocytes in pulmonary tuberculosis*. Indian J Med Res, 1988. **88**: p. 124-9.
126. MacMicking, J., Q.W. Xie, and C. Nathan, *Nitric oxide and macrophage function*. Annu Rev Immunol, 1997. **15**: p. 323-50.
127. Adams, L.B., Y. Fukutomi, and J.L. Krahenbuhl, *Regulation of murine macrophage effector functions by lipoarabinomannan from mycobacterial strains with different degrees of virulence*. Infect Immun, 1993. **61**(10): p. 4173-81.
128. Anthony, L.S., et al., *Lipoarabinomannan from Mycobacterium tuberculosis modulates the generation of reactive nitrogen intermediates by gamma interferon-activated macrophages*. FEMS Immunol Med Microbiol, 1994. **8**(4): p. 299-305.
129. Chan, E.D., et al., *Induction of inducible nitric oxide synthase-NO* by lipoarabinomannan of Mycobacterium tuberculosis is mediated by MEK1-ERK, MKK7-JNK, and NF-kappaB signaling pathways*. Infect Immun, 2001. **69**(4): p. 2001-10.
130. Park, E., et al., *Regulation of nitric oxide induced by mycobacterial lipoarabinomannan in murine macrophages: effects of interferon-beta and taurine-chloramine*. Int J Lepr Other Mycobact Dis, 2000. **68**(4): p. 444-51.
131. Krzyzowska, M., et al., *Lipoarabinomannan as a regulator of the monocyte apoptotic response to Mycobacterium bovis BCG Danish strain 1331 infection*. Pol J Microbiol, 2007. **56**(2): p. 89-96.
132. Invitrogen, C. *Probes for Nitric Oxide Research*. 2009 [cited; Available from: <http://www.invitrogen.com>].
133. Flesch, I.E. and S.H. Kaufmann, *Mechanisms involved in mycobacterial growth inhibition by gamma interferon-activated bone marrow macrophages: role of reactive nitrogen intermediates*. Infect Immun, 1991. **59**(9): p. 3213-8.
134. Persichini, T., et al., *Cross-talk between constitutive and inducible NO synthase: an update*. Antioxid Redox Signal, 2006. **8**(5-6): p. 949-54.
135. Kaufmann, S.H., *How can immunology contribute to the control of tuberculosis?* Nat Rev Immunol, 2001. **1**(1): p. 20-30.
136. Scanga, C.A., et al., *Depletion of CD4(+) T cells causes reactivation of murine persistent tuberculosis despite continued expression of interferon gamma and nitric oxide synthase 2*. J Exp Med, 2000. **192**(3): p. 347-58.
137. Nigou, J., et al., *Mannosylated lipoarabinomannans inhibit IL-12 production by human dendritic cells: evidence for a negative signal delivered through the mannose receptor*. J Immunol, 2001. **166**(12): p. 7477-85.
138. Rissoan, M.C., et al., *Reciprocal control of T helper cell and dendritic cell differentiation*. Science, 1999. **283**(5405): p. 1183-6.